Washington University in St. Louis
Washington University Open Scholarship

All Theses and Dissertations (ETDs)

January 2009

Connections between Floer-type invariants and Morse-type invariants of Legendrian knots.

Michael Henry
Washington University in St. Louis

Follow this and additional works at: https://openscholarship.wustl.edu/etd

Recommended Citation
Henry, Michael, "Connections between Floer-type invariants and Morse-type invariants of Legendrian knots." (2009). *All Theses and Dissertations (ETDs)*. 147.
https://openscholarship.wustl.edu/etd/147

This Dissertation is brought to you for free and open access by Washington University Open Scholarship. It has been accepted for inclusion in All Theses and Dissertations (ETDs) by an authorized administrator of Washington University Open Scholarship. For more information, please contact digital@wumail.wustl.edu.

WASHINGTON UNIVERSITY IN ST. LOUIS

Department of Mathematics

Dissertation Examination Committee:
Rachel Roberts, Co-Chair
Joshua Sabloff, Co-Chair
Renato Feres
Cindy Grimm
Gary Jensen
Xiang Tang

Connections between Floer-type invariants and Morse-type invariants of Legendrian knots.

by

Michael B. Henry

A dissertation presented to the
Graduate School of Arts and Sciences
of Washington University in
partial fulfillment of the
requirements for the degree
of Doctor of Philosophy

August 2009

Saint Louis, Missouri

ABSTRACT

Connections between Floer-type invariants
and Morse-type invariants of Legendrian knots.

by

Michael B. Henry

Doctor of Philosophy in Mathematics
Washington University in Saint Louis, August 2009
Professor Rachel Roberts, Chairperson

We investigate existing Legendrian knot invariants and discover new connections between the theory of generating families, normal rulings and the Chekanov-Eliashberg differential graded algebra (CE-DGA). Given a Legendrian knot K with generic front projection Σ, we define a combinatorial/algebraic object on Σ called a *Morse complex sequence*, abbreviated MCS. An MCS encodes a finite sequence of Morse homology complexes. Every suitably generic generating family for Σ admits an MCS and every MCS has a naturally associated graded normal ruling. In addition, every MCS has a naturally associated augmentation of the CE-DGA of the Ng resolution L_Σ of the front Σ. In this manner, an MCS connects generating families, normal rulings and augmentations. We place an equivalence relation on the set $MCS(\Sigma)$ of MCSs on Σ and prove that there exists a natural surjection from the equivalence classes of $MCS(\Sigma)$, denoted $\widehat{MCS}(\Sigma)$, to the set of

chain homotopy classes of augmentations of L_Σ, denoted $Aug^{ch}(L_\Sigma)$. In the case of Legendrian isotopy classes admitting representatives with two-bridge front projections, $\widehat{MCS}(\Sigma)$ and $Aug^{ch}(L_\Sigma)$ are in bijection.

ACKNOWLEDGEMENTS

Mathematicians are a wonderfully welcoming group of people. I thank the many mathematicians who gave me support and counsel throughout my graduate studies. My advisors, Rachel Roberts and Joshua Sabloff, provided guidance and introduced me to the culture of mathematics. Thank you both for your patience and generosity. Thank you to the faculty and staff of Washington University and the University of Texas for the excellent instruction, advice, and support. Thank you to Sergei Chmutov, Dmitry Fuchs, Victor Goryunov, Paul Melvin, Dan Rutherford, and Lisa Traynor for the many fruitful discussions and continued collaborations.

Throughout my graduate studies I have received funding from the National Science Foundation. I thank the taxpayers of America for their dedication to the advancement of science and mathematics. I also thank the American Institute of Mathematics (AIM), which held the September 2008 workshop conference that led to new collaborations and new math.

Where would any of us be without our family and friends? I thank my family for the love and support that kept me focused during my graduate career. I also thank my parents for the work ethic they instilled in me as a child and that has led to so much of my success. Thank you to my many friends from Augustana College, Washington University and the University of Texas for helping me keep my feet on the ground and moving forward. Finally, I thank my dear wife Meghana from whom I draw faith, love, and inspiration.

Contents

Abstract **ii**

Acknowledgements **iv**

List of Figures **ix**

List of Symbols **xiv**

1 Introduction **1**

1.1 Legendrian knot theory 1

1.2 Results 9

1.3 Outline of the rest of the thesis 11

1.4 Origins of the MCS 13

1.5 Future directions 16

2 Background **18**

2.1 Legendrian knots in $\mathbb{R}^3$ 18

2.1.1 The front projection 21

2.1.2 The Lagrangian projection 23
2.1.3 The Ng resolution 25
2.2 Classical Legendrian knot invariants 30
2.2.1 A Word of Caution 34
2.3 The Chekanov-Eliashberg DGA 34
2.3.1 The Algebra 35
2.3.2 The Grading 35
2.3.3 The Differential 38
2.3.4 Legendrian Invariance of the CE-DGA 41
2.4 Augmentations 43
2.5 Generating families 44
2.6 Normal rulings 48

3 Defining Morse Complex Sequences 53
3.1 Ordered chain complexes 55
3.1.1 Useful Matrix Notation 57
3.2 Morse complex sequences on Σ 58
3.3 An Equivalence Relation on $MCS(\Sigma)$ 67
3.4 Associating a Normal Ruling to an MCS 82

4 Chain Homotopy Classes of Augmentations 88
4.1 Chain homotopy equivalence 88
4.2 Stable tame isomorphism classes of CE-DGAs 92

5 Dipped Resolution Diagrams **99**

5.1 Adding dips to a Ng resolution diagram 99

5.2 The CE-DGA on a sufficiently dipped diagram 104

5.3 The stable tame isomorphism of a type II move 114

5.3.1 Extending augmentations across a type II move 116

5.4 Extending an augmentation across a dip 119

5.4.1 Extending $\epsilon \in Aug(L^d_\Sigma)$ by 0. 121

5.4.2 Extending $\epsilon \in Aug(L^d_\Sigma)$ by $\delta_{i+1,i}$. 127

6 Relating MCSs and Augmentations **132**

6.1 Augmentations on sufficiently dipped diagrams 133

6.1.1 Notation for keeping track of singularities. 139

6.1.2 Assigning $\epsilon_{\mathcal{C}} \in Aug(L^d_\Sigma)$ to an MCS $\mathcal{C}$ 140

6.2 Defining $\Psi : MCS(\Sigma) \to Aug^{ch}(L_\Sigma)$ 145

6.2.1 Dipping/undipping paths for L^d_Σ 149

6.3 Algorithm 1: Associating an MCS to $\epsilon \in Aug(L_\Sigma)$ 152

6.4 Defining $\widehat{\Psi} : \widehat{MCS}(\Sigma) \to Aug^{ch}(L_\Sigma)$ 156

6.4.1 Chain homotopies on sufficiently dipped diagrams . . . 156

6.4.2 $\mathcal{C}_1 \sim \mathcal{C}_2$ implies $\Psi(\mathcal{C}_1) = \Psi(\mathcal{C}_2)$ 160

6.5 Algorithm 2: Two standard forms for MCSs 169

6.5.1 The $S\bar{R}$-form of an MCS 170

6.5.2 The C-form of an MCS. 186

7 Two-Bridge Legendrian Knots **194**

7.1 Two-Bridge Front Projections 194

7.2 Injectivity of $\widehat{\Psi} : \widehat{MCS}(\Sigma) \to Aug^{ch}(L_\Sigma)$ 195

Bibliography **205**

List of Figures

1.1 The standard contact structure on $\mathbb{R}^3$ and a Legendrian curve. 2

1.2 Generating family example. 5

1.3 Graded normal rulings of a Legendrian trefoil. 6

1.4 An MCS on a Legendrian trefoil. 8

1.5 A MCS as a decorated front projection. 8

1.6 Two MCS equivalence moves. 8

1.7 Cusps and crossings in the Ng resolution procedure. 10

2.1 The standard contact structure on $\mathbb{R}^3$ and a Legendrian curve. 19

2.2 Front projections of Legendrian unknots. 21

2.3 A front projection of a Legendrian trefoil. 21

2.4 The Reidemeister moves for front projections. 23

2.5 Lagrangian projections of Legendrian unknots. 24

2.6 A Lagrangian projection of a Legendrian trefoil. 24

2.7 The Reidemeister moves for Lagrangian projections. 25

2.8 Cusps and crossings in the Ng resolution procedure. 27

2.9 Strands of fixed slope. 27

2.10 Stretching a left cusp. 28
2.11 Stretching a crossing. 28
2.12 Stretching a right cusp. 28
2.13 A Ng resolved trefoil. 29
2.14 The writhe of an oriented crossing. 32
2.15 Oriented cusps. 32
2.16 Geometric stabilization. 33
2.17 The Chekanov examples. 34
2.18 A capping path and a convex immersed polygon for a Lagrangian trefoil. 36
2.19 A Maslov potential near left and right cusps. 37
2.20 A Reeb sign of a crossing. 38
2.21 An augmentation as a chain map. 44
2.22 Generating family example. 46
2.23 Graded normal rulings of a Legendrian trefoil. 51
2.24 Configurations of a normal switch. 51
2.25 Departures and returns. 52

3.1 An ordered chain complex. 56
3.2 A marked front projection. 59
3.3 A MCS on a Legendrian trefoil. 65
3.4 The matrix moves in a transition past a right cusp. 66
3.5 MCS equivalence move 0. 68

3.6 MCS equivalence moves 1 - 13 70
3.7 MCS equivalence moves 14 - 21 71
3.8 MCS equivalence moves 22, the Explosion Move. 71

4.1 A chain homotopy between DGA morphisms. 89
4.2 A chain homotopy between augmentations. 91

5.1 The process of adding a dip to L_Σ. 101
5.2 A dip in a Lagrangian projection. 102
5.3 Inserts in a sufficiently dipped diagram. 102
5.4 Disks in a dipped diagram. 104
5.5 Disks contributing to ∂q_s and ∂z_r. 108
5.6 A disk contributing to ∂A_j. 109
5.7 Disks contributing to $R(\partial B_j)$. 110
5.8 Types of disks contributing to $L(\partial B_j)$ when I_j is of type (1) or (4). 111
5.9 Types of disks contributing to $L(\partial B_j)$ when I_j is of type (2). . 112
5.10 Types of disks contributing to $L(\partial B_j)$ when I_j is of type (3). . 113
5.11 A partial dip. 121
5.12 Disks in which $a^{i+1,i}$ is a negative convex corner. 128

6.1 Labeling points in L_Σ. 140
6.2 Assigning an augmentation to an MCS. 146
6.3 Type II and II^{-1} moves. 148
6.4 Two "far away" type II^{-1} moves. 149

6.5 Dip creation in Algorithm 1. 154
6.6 Assigning an MCS to an augmentation. 156
6.7 MCS equivalence moves 1 - 13 with dips indicated. 167
6.8 MCS equivalence moves 14 - 21 with dips indicated. 168
6.9 The Explosion move with dips indicated. 168
6.10 Simple switches. 171
6.11 Simple returns. 172
6.12 A handleslide mark stuck at a crossing. 173
6.13 The ordering of V. 175
6.14 Sweeping a handleslide into/out of V. 177
6.15 Sweeping into V from the left. 178
6.16 Sweeping V past cusps. 178
6.17 Sweeping V past a crossing. 178
6.18 Sweeping V past a crossing with a handleslide. 180
6.19 Sweeping V past a right cusp with accumulation. 183
6.20 Removing a handleslide at a cusp. 184
6.21 Explosion at a right cusp. 185
6.22 Sweeping V past a right cusp with accumulation. 189
6.23 Removing a handleslide at a cusp. 190
6.24 Explosion at a right cusp. 191

7.1 Unmarking graded returns that are paired with ungraded departures. 197

7.2 Exploding handleslide marks. 197
7.3 Graded departure-return pairs. 198
7.4 A marked graded departure-return pair. 204
7.5 A marked graded departure-return pair. 204

List of Symbols

K	A Legendrian knot. We also use K to refer to a Legendrian isotopy class.
Σ	The front projection of a Legendrian knot K.
L	The Lagrangian projection of a Legendrian knot K.
L_Σ	The Ng resolution of the front projection Σ.
L_Σ^d	A dipped diagram of the Ng resolution of Σ.
ϵ	An augmentation on a Lagrangian projection.
$\simeq$	The chain homotopy equivalence relation on augmentations.
H	A chain homotopy between augmentations.
$[\epsilon]$	An augmentation chain homotopy class.
$Aug(L)$	The set of augmentations of L.
$Aug(L_\Sigma)$	The set of augmentations of L_Σ.
$Aug^{ch}(L_\Sigma)$	The set of augmentation chain homotopy classes of L_Σ.
$Aug_{occ}(L_\Sigma^d)$	The set of occ-simple augmentations of L_Σ^d.
$Aug_{occ}^m(L_\Sigma)$	The set of minimal occ-simple augmentations of L_Σ^d.
$MCS(\Sigma)$	The set of MCSs of Σ.

$\sim$	The equivalence relation on MCSs.
F	A linear-quadratic generating family for Σ.
μ	A Maslov potential on Σ.
D	A dip region of L^d_Σ.
A	The a-lattice of a dip region of L^d_Σ.
B	The b-lattice of a dip region of L^d_Σ.
I	An insert region between dips of L^d_Σ.
N	A graded normal ruling on Σ.
$N(\Sigma)$	The set of graded normal rulings of Σ.

Chapter 1

Introduction

1.1 Legendrian knot theory

A Legendrian knot K is a smooth knot in $\mathbb{R}^3$ whose tangent space sits in the 2-plane distribution ξ, where ξ is the kernel of the one form $\alpha = dz - ydx$; see Figure 1.1. The 2-plane distribution ξ is the *standard contact structure* on $\mathbb{R}^3$ and Legendrian knot theory is the study of Legendrian knots up to isotopy through Legendrian knots. In fact, this theory is the local version of a much larger theory which studies contact structures and Legendrian submanifolds of 3-manifolds.

Although smooth knot theory has many invariants, Legendrian knot theory is a younger field with few invariants. The Thurston-Bennequin and rotation numbers are known as the "classical" Legendrian invariants. By the work of Bennequin [3], these invariants provide the first connection between

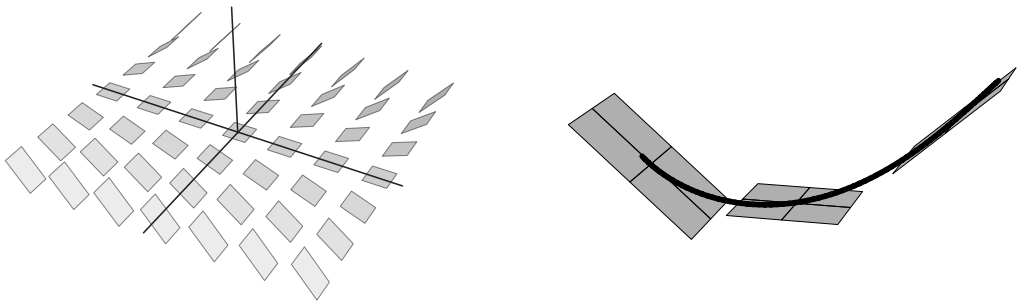

Figure 1.1: (a) The standard contact structure on $\mathbb{R}^3$. (b) A Legendrian curve. Thank you to Josh Sabloff for this figure.

the geometry of a Legendrian knot and its topology. Bennequin proved an inequality relating the Thurston-Bennequin and rotation numbers of a Legendrian knot with its genus. As a consequence, Bennequin was able to prove that $\mathbb{R}^3$ admits an exotic contact structure. More recent work has provided other connections between the classical invariants and invariants of smooth knots; see [9, 16, 28, 34, 38]. As we will see in Chapter 2, the Thurston-Bennequin and rotation numbers distinguish infinitely many Legendrian knot classes within each smooth knot class.

In [6], Chekanov proves that the classical invariants do not distinguish every pair of distinct Legendrian isotopy classes. In fact, modern Legendrian invariants exist that distinguish Legendrian isotopy classes that are indistinguishable using the Thurston-Bennequin and rotation numbers. We will study connections between modern Legendrian invariants derived from Symplectic Field Theory and from the theory of generating families. Specifically, we relate augmentations, derived from Symplectic Field Theory, and Morse complex sequences, derived from generating families.

We begin with a description of the Chekanov-Eliashberg Differential Graded Algebra (abbreviated CE-DGA), from which augmentations are computed. The CE-DGA is a special case of the Symplectic Field Theory of [11, 12] and developed in [12] and [6]. The CE-DGA assigns to a Legendrian knot K a differential graded algebra. The algebra is generated by the crossings of the projection of K onto the xy-plane, called the *Lagrangian projection* of K and denoted L. We let $(\mathcal{A}(L), \partial)$ denote the CE-DGA of K.

Geometrically, the CE-DGA is Floer theoretic in nature. In fact, the generators of $\mathcal{A}(L)$ are the critical points of an action functional on the infinite-dimensional space of curves beginning and ending on K. Instead of analyzing gradient flow lines of the action functional, the boundary map is computed from certain pseudo-holomophic curves in the symplectization of $(\mathbb{R}^3, \xi)$. In contrast to Morse theory, the pseudo-holomorphic curves may begin at a single critical point and end at a collection of critical points. In this manner, $\mathcal{A}(L)$ becomes an noncommutative algebra and not merely a vector space. We refer the interested reader to [7] and [14] for a more detailed introduction to the CE-DGA.

In [6], Chekanov proves that the homology of $(\mathcal{A}(L), \partial)$ is a Legendrian invariant, called the *Legendrian contact homology* of K. In addition, if we consider $(\mathcal{A}(L), \partial)$ up to a certain algebraic equivalence, then the resulting DGA class is also a Legendrian invariant. The pseudo-holomorphic curves determining the differential of $(\mathcal{A}(L), \partial)$ project to combinatorial disks in $\mathbb{R}^2$, which may be counted algorithmically. Thus, $(\mathcal{A}(L), \partial)$ may be calculated

algorithmically, although it may be computationally intensive. On the other hand, determining if two CE-DGAs are equivalent is difficult.

However, we may derive from $(\mathcal{A}(L), \partial)$ other Legendrian invariants that have proved to be useful in distinguishing Legendrian isotopy classes. *Augmentations* are certain algebra homomorphisms from $(\mathcal{A}(L), \partial)$ to $\mathbb{Z}_2$. These maps have been used to construct Legendrian isotopy invariants that have provided connections between the CE-DGA and Legendrian invariants coming from the theory of generating families; see [17, 19, 29]. We denote the set of augmentations of $(\mathcal{A}(L), \partial)$ by $Aug(L)$. The existence of an augmentation is a Legendrian isotopy invariant and, in fact, we can normalize the cardinality of $|Aug(L)|$ by an appropriate power of two to form a numerical invariant; see [25, 29]. There is a natural algebraic equivalence relation on $Aug(L)$. We denote the set of equivalence classes of augmentations of L by $Aug^{ch}(L)$. We prove in Chapter 4 that the cardinality of $Aug^{ch}(L)$ is a Legendrian isotopy invariant for K.

A second source of modern invariants is the theory of generating families. These invariants are studied extensively in [8, 30, 21, 40, 41]. A *generating family* for a Legendrian knot K is a one-parameter family of maps $F_x : \mathbb{R}^n \to \mathbb{R}$ that encodes the xz-projection of K. We let Σ denote the xz-projection of K and call it the *front projection* of K. F_x encodes Σ in the following manner. The parameter x in F_x corresponds to the x-axis in the xz-projection. If we fix a point x_0 along the x-axis, then the critical values of $F_{x_0} : \mathbb{R}^n \to \mathbb{R}$ correspond to the points of $\Sigma \cap (\{x_0\} \times \mathbb{R})$; see Figure 1.2. In other language,

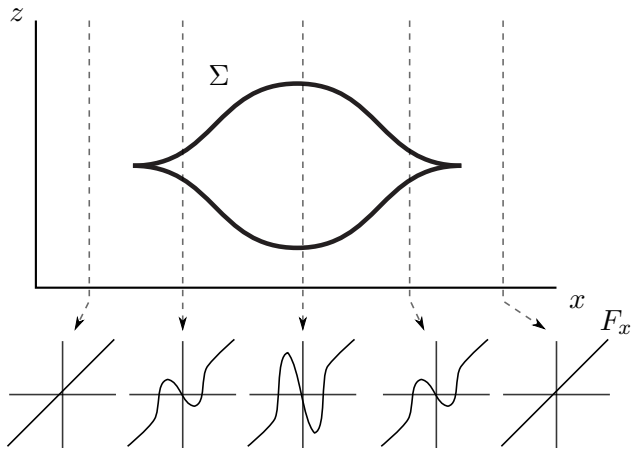

Figure 1.2: A generating family for a Legendrian unknot.

this says that Σ is the Cerf diagram of the one-parameter family F_x; see [4]. The existence of a generating family is a Legendrian isotopy invariant. If K and K' are Legendrian isotopic and K admits a generating family then so does K'. However, not all Legendrian knot classes admit generating families.

From a generating family, we may derive a combinatorial object called a *graded normal ruling* as follows. Suppose a Legendrian knot K admits a generating family $F_x : \mathbb{R}^n \to \mathbb{R}$ and g_x is a metric on the domain $\mathbb{R}^k$ for each x. If F_x and g_x are suitably generic, then for all but finitely many values of x, the function/metric pair (F_x, g_x) gives a Morse-Smale chain complex (C_x, ∂_x, g_x) and we can explicitly describe the changes in (C_x, ∂_x, g_x) as x varies. Each Morse-Smale chain complex (C_x, ∂_x, g_x) has trivial homology and, as we will see, a canonical pairing of its generators. A graded normal ruling is a combinatorial object that encodes the pairing of the generators of (C_x, ∂_x, g_x) as x varies. In [8], Chekanov and Pushkar prove that if two

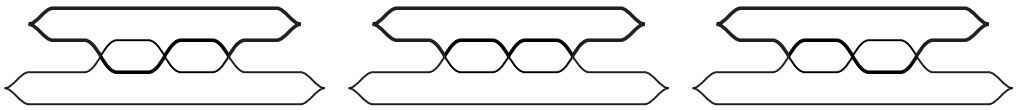

Figure 1.3: The three graded normal rulings of the standard Legendrian trefoil. The two ruling paths are indicated in each trefoil.

knots are Legendrian isotopic then there exists a bijection between their sets of graded normal rulings. In addition, this bijection respects a certain Euler characteristic on the rulings and, thus, a polynomial Legendrian invariant may be formed from the set of graded normal rulings.

The homological pairing encoded by a graded normal ruling is only part of the information contained in the sequence of complexes (C_x, ∂_x, g_x) coming from a suitably generic generating family (F_x, g_x). In particular, the pairing does not detect certain geometric handleslides occurring in (F_x, g_x). In this thesis we form an algebraic/combinatorial object called a *Morse complex sequence* that encodes the entire sequence (C_x, ∂_x, g_x)[1]. Our formulation will be purely algebraic in nature. We will not work explicitly with generating families, although we gain important geometric intuition from the theory of generating families.

A *Morse complex sequence*, abbreviated *MCS*, is a finite sequence of $\mathbb{Z}_2$ chain complexes $(C_1, \partial_1), \ldots, (C_m, \partial_m)$, written $\mathcal{C} = (C_1, \partial_1) \ldots (C_m, \partial_m)$, where consecutively ordered chain complexes (C_i, ∂_i) and (C_{i+1}, ∂_i) are related by one of four elementary moves determined by the singularities of

[1]In [31], Pushkar defines an essentially identical object. See Section 1.4 for a more detailed discussion on the origin of this object.

Σ and possible handleslide marks. A precise definition is given in Definition 3.2.3. An example is given in Figure 1.4. An MCS may be encoded graphically as a collection of vertical arcs on Σ; see Figure 1.5. We let $MCS(\Sigma)$ denote the set of MCSs of Σ.

For a suitably generic generating family F_x, it is possible to define an MCS from the Morse-Smale chain complexes (C_x, ∂_x, g_x) of (F_x, g_x). There is a natural equivalence relation on $MCS(\Sigma)$ coming from our understanding of the evolution of one-parameter families of functions and metrics[2]. In [20], Hatcher and Wagoner describe these equivalence moves in the context of 2-parameter families of functions and metrics, however, they were not concerned with the associated Legendrian knot theory. The equivalence relation manifests itself as a series of local moves involving the vertical arcs in the graphical representation of an MCS. Examples of MCS equivalence moves are given in Figure 1.6. We let $\widehat{MCS}(\Sigma)$ denote the set of MCSs of Σ up to equivalence.

Before stating the results of this thesis, we note several existing connections between augmentations, generating families, and graded normal rulings. In particular, see any of [8, 17, 18, 19, 23, 29, 36]. For a fixed Legendrian knot K with Lagrangian projection L and front projection Σ, the following results are known.

Theorem 1.1.1 ([17, 18, 29, 36])**.** $(\mathcal{A}(L), \partial)$ has a graded augmentation

[2]In the language of Legendrian knot theory, this equivalence relation first appears in [31]. See Section 1.4 for a more detailed discussion on the origin of this equivalence relation.

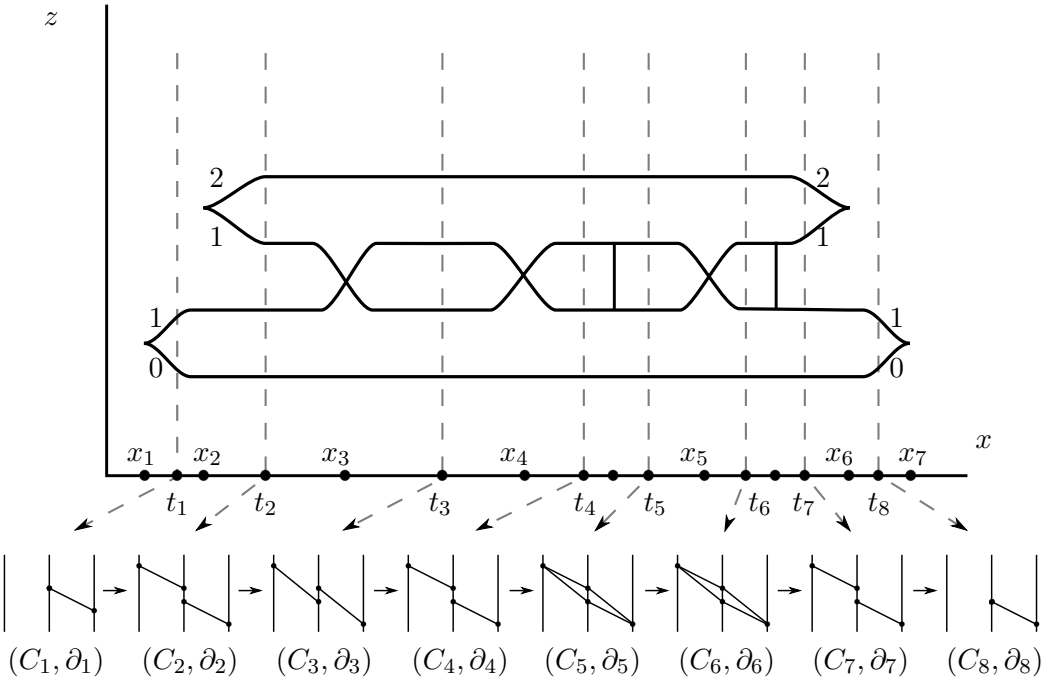

Figure 1.4: An example of an MCS on a generic front projection of a Legendrian trefoil. This MCS includes handleslide moves between t_4 and t_5 and between t_6 and t_7. In both cases, the handleslide occurs between the two generators of index 1. The graphics in the bottom row encode the ordered chain complexes of $\mathcal{C}$. This graphical notation is described in Chapter 2.

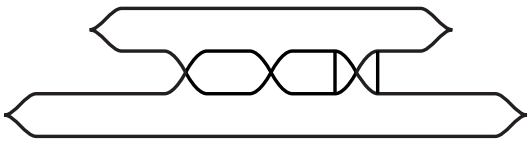

Figure 1.5: The graphical presentation of the MCS in Figure 1.4. The two vertical lines indicate the two handleslide moves.

Figure 1.6: Two MCS equivalence moves.

if and only if Σ has a graded normal ruling. In particular, there exists a many-to-one map from the set of augmentations of $(\mathcal{A}(L), \partial)$ to the set of graded normal rulings of Σ.

The backward direction of the first statement was proved by Fuchs in [17] and Fuchs and Ishkhanov proved the forward direction in [18]. Sabloff independently proved the forward direction in [36]. Ng and Sabloff proved the second statement in [29].

Theorem 1.1.2 ([8, 19])**.** *K admits a generating family if and only if Σ has a graded normal ruling.*

Chekanov and Pushkar proved the forward direction in [8]. The backward direction is stated without proof in [8] as well. Fuchs and Rutherford prove the backwards direction in [19].

1.2 Results

The results of this thesis show that chain homotopy classes of augmentations are intimately related to equivalence classes of MCSs. Before stating the results, we define the Ng resolution of a front projection. Given a Legendrian knot K with front projection Σ, we form the *Ng resolution* of Σ, denoted L_Σ, by resolving the cusps and crossings as indicated in Figure 1.7. The resulting planar curve is a Lagrangian projection for K. The Ng resolution procedure is discussed in detail in Chapter 2. Given Σ and L_Σ, we have the following results.

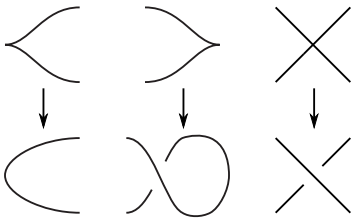

Figure 1.7: Cusps and crossings in the Ng resolution procedure.

Theorem 1.2.1 (MBH)**.** For a fixed Legendrian knot K with front projection Σ and Ng resolution L_Σ, there exists a surjective map $\widehat{\Psi} : \widehat{MCS}(\Sigma) \to Aug^{ch}(L_\Sigma)$.

Theorem 1.2.1 is an immediate consequence of the following three lemmata.

Lemma 1.2.2 (MBH, [19])**.** For a fixed Legendrian knot K with front projection Σ and Ng resolution L_Σ, there exists a map $\Psi : MCS(\Sigma) \to Aug^{ch}(L_\Sigma)$.

Lemma 1.2.3 (MBH)**.** There is an explicit algorithm that assigns to an augmentation $\epsilon \in Aug(L_\Sigma)$ an MCS $\mathcal{C}_\epsilon$ so that $\Psi(\mathcal{C}_\epsilon) = [\epsilon]$. Hence, the map $\widehat{\Psi}$ is surjective.

Lemma 1.2.4 (MBH)**.** If $\mathcal{C}_1 \sim \mathcal{C}_2$ then $\Psi(\mathcal{C}_1) = \Psi(\mathcal{C}_2)$. Hence, the map $\widehat{\Psi} : \widehat{MCS}(\Sigma) \to Aug^{ch}(L_\Sigma)$ defined by $\widehat{\Psi}([\mathcal{C}]) = \Psi(\mathcal{C})$ is well-defined.

In Section 6.5, we describe two standard forms for MCSs on Σ. We use explicit algorithms to prove that every MCS is equivalent to an MCS in $S\bar{R}$-form and an MCS in C-form. Given a graded normal ruling N, the $S\bar{R}$-form allows us to calculate bounds on the number of MCS classes with graded

normal ruling N. From the C-form of an MCS $\mathcal{C}$, it is easy to write down the augmentation class $\widehat{\Psi}([\mathcal{C}])$. In addition, the algorithm in the proof of Lemma 1.2.3 gives an MCS in C-form.

Theorem 1.2.5 (MBH)**.** Every MCS is equivalent to an MCS in $S\bar{R}$-form and an MCS in C-form.

In certain situations, we can prove that $\widehat{\Psi}$ is injective. In particular, we have the following.

Theorem 1.2.6 (MBH)**.** If Σ has exactly two left cusps, then $\widehat{\Psi} : \widehat{MCS}(\Sigma) \to Aug^{ch}(L_\Sigma)$ is a bijection.

In the case of a front projection with exactly two left cusps, we can also explicitly calculate $|Aug^{ch}(L_\Sigma)| = |\widehat{MCS}(\Sigma)|$. The language in this corollary is defined in Chapter 7.

Corollary 1.2.7 (MBH)**.** Suppose Σ has exactly two left cusps and let $N(\Sigma)$ denote the set of graded normal rulings on Σ. For each $N \in N(\Sigma)$, define $\nu(N)$ to be the number of graded departure-return pairs in N. Then $|Aug^{ch}(L_\Sigma)| = |\widehat{MCS}(\Sigma)| = \sum_{N \in N(\Sigma)} 2^{\nu(N)}$

1.3 Outline of the rest of the thesis

In Chapter 2, we provide the necessary background material in Legendrian knot theory. We review the "classical invariants" of Legendrian knots, namely

the Thurston-Bennequin and rotation numbers, and note a few of their strengths and weaknesses. The front and Lagrangian projections of a Legendrian knot are used to develop combinatorial descriptions of the Chekanov-Eliashberg DGA, augmentations, and graded normal rulings. The Ng resolution procedure from [27] is detailed. The Ng resolution procedure is a standard first step when looking for connections between the CE-DGA and the theory of generating families.

Chapter 3 begins with a brief discussion of one-parameter families of function/metric pairs. This discussion provides motivation for the definition of a Morse complex sequence (MCS) on a front projection Σ of a Legendrian knot. Ordered chain complexes are defined followed by the definition of an MCS as a sequence of ordered chain complexes satisfying certain algebraic conditions. These algebraic conditions are encoded as matrix equations. A natural equivalence relation on MCSs exists coming from the evolution of the metric in a one-parameter family of function/metric pairs. Each MCS induces a graded normal ruling on Σ and equivalent MCSs induce identical graded normal rulings.

Chapter 4 reviews properties of differential graded algebras, DGA morphisms and DGA chain homotopies. In particular, an augmentation is a DGA morphism from the CE-DGA to the trivial $\mathbb{Z}_2$ DGA. Chain homotopy gives an equivalence relation on the set of augmentations of the CE-DGA. Chapter 4 includes a proof that the cardinality of the set of chain homotopy classes of augmentations is a Legendrian knot invariant.

In Chapter 5 we develop techniques that allow us to gain local control over the boundary map of the CE-DGA. In particular, the splash/dip construction first introduced in [17] allows us to write down the boundary map of the CE-DGA of a "dipped" version of L_Σ as a system of local matrix equations. Adding dips changes the topology of L_Σ considerably. However, we are able to keep track of the extension of the augmentations of L_Σ to augmentations on the dipped version of L_Σ. In fact, the resulting matrix equations from these extended augmentations look very similar to the matrix equations in the definition of an MCS.

In Chapter 6 we develop the connections between MCSs and augmentations. In particular, Lemma 1.2.2 follows from Lemmata 6.1.7 and 6.2.6, Lemma 1.2.3 follows from Theorem 6.3.1, and Lemma 1.2.4 follows from Lemma 6.4.4. In Section 6.5, we describe the $S\bar{R}$-form and the C-form of MCSs on Σ and prove Theorem 1.2.5 using explicit algorithms involving MCS moves.

In Chapter 7 we prove Theorem 1.2.6 and Corollary 1.2.7.

1.4 Origins of the MCS

In this section I describe how I came to know the idea behind Morse complex sequences. In the spring and summer of 2008, I was working on extending graded normal rulings from Legendrian knots to Legendrian surfaces in $\mathbb{R}^5$ in the hopes of constructing an invariant of Legendrian surfaces. I had some

success defining an appropriate extension, however, there were problems that I could not overcome. In September 2008, I attended the American Institute of Mathematics (AIM) workshop on Legendrian and Transverse Knots. Through many fruitful conversations with Sergei Chmutov, Dmitry Fuchs, Victor Goryunov, Paul Melvin, Dan Rutherford, Joshua Sabloff, and Lisa Traynor, it became clear that constructing such an object on Legendrian surfaces requires understanding the handleslide data in one-parameter families of function/metric pairs. The problem of incorporating handleslides into the graded normal ruling theory was taken up by these attendees and myself. We were motivated by the recent work of Fuchs and Rutherford in [19] and ideas suggested by Petya Pushkar in a personal correspondence with Dmitry Fuchs in 2000 [31].

On the concluding day of the AIM workshop, Fuchs received an email from Pushkar describing progress he has made incorporating handleslide data into graded normal rulings. In [33], Pushkar outlines his theory of *spring sequences* and claims a number of results. This theory was also outlined in [31]. Spring sequences are essentially equivalent to the decorated graded normal rulings devised by our group at AIM and the Morse complex sequences defined in this thesis. In [33], Pushkar claims considerably more than our group could claim or even conjecture. He claims, under an equivalence relation defined in [31], there is a natural bijection between the sets of equivalence classes of spring sequences of two Legendrian isotopic knots. In addition, he claims that there exists a connection between certain algebraic classes of

augmentations and equivalence classes of spring sequences. Pushkar also outlines an extension of spring sequences to an invariant of Legendrian surfaces. The techniques he outlines in his extension are analogous to techniques I had developed, though the theory he claims is more developed than my own.

As far as I am aware, [31] is the first appearance of the idea of generalizing the theory of graded normal ruling by using a finite sequence of chain complexes to form a new algebraic/combinatorial object on Legendrian knots. The equivalence relation on spring sequences defined by Pushkar in [31] appears in the earlier work of Hatcher and Wagoner [20], although they were working in the context of 2-parameter families of functions and metrics and were not concerned with the associated Legendrian knots. The claim that there exists a connection between certain algebraic classes of augmentations and equivalence classes of MCSs first appears in [33], as does the claim that MCSs can be extended to a Legendrian surface invariant. It is my understanding that proofs of the claims in [31] and [33] have not been published.

I was given a copy of [33] by Dmitry Fuchs on the last day of the September 2008 AIM workshop and was emailed a copy of [31] by Dmitry Fuchs soon thereafter. Along with the work done by our group at AIM, these notes directly influenced the definition of a Morse complex sequence and the equivalence relation on the set of MCSs given in this thesis. The results claimed by Pushkar in [33] also directed my efforts. In addition, Sergei Chmutov emailed to the AIM group notes and blackboard photos of a talk given by Pushkar in November 2008 at CIRM; see [32]. The proofs of the results stated in

Section 1.2, with the exception of half of Lemma 1.2.2, which is attributed to [19], are my original work. In addition, the results in Chapters 6 and 7 not attributed to previous papers are also my original work.

1.5 Future directions

As noted in Section 1.4, Pushkar claims in [33] a number of results concerning MCSs. Of those claimed, this thesis addresses the connection between MCS equivalence classes and chain homotopy classes of augmentations. Given that we prove $\widehat{\Psi} : \widehat{MCS}(\Sigma) \to Aug^{ch}(L_\Sigma)$ is surjective, it is natural to ask:

Question 1. Is $\widehat{\Psi} : \widehat{MCS}(\Sigma) \to Aug^{ch}(L_\Sigma)$ injective?

The results in this thesis concern a fixed Legendrian knot K with front projection Σ. In order to define a Legendrian isotopy invariant from MCSs, we must answer the following question.

Question 2. Suppose K and K' are Legendrian isotopic with front projections Σ and Σ'. What is the relationship between $\widehat{MCS}(\Sigma)$ and $\widehat{MCS}(\Sigma')$?

In [33], Pushkar claims that there is a natural bijection between $\widehat{MCS}(\Sigma)$ and $\widehat{MCS}(\Sigma')$. Understanding the answer to this question is also a necessary first step in understanding the following question.

Question 3. Can we use MCSs to define a combinatorial object on Legendrian surfaces in $\mathbb{R}^5$ giving a Legendrian isotopy invariant?

In June 2009, Dmitry Fuchs, Paul Melvin, Dan Rutherford, Joshua Sabloff, Lisa Traynor and I met again at the American Institute of Mathematics to continue our work from the September 2008 workshop. At the June meeting, our work concerned the precise geometric relationship between MCSs and generating families. In particular, MCSs are geometrically motivated by the theory of generating families, but the precise relationship between MCSs and generating families is unclear. This leads us to ask:

Question 4. Does every MCS on Σ determine a generating family of Σ?

Question 5. Is it possible to define an equivalence relation on generating families motivated by the MCS equivalence relation?

The group at AIM had partial success answering these two questions and I anticipate that our further collaboration will provide more insights into MCSs and their role in Legendrian knot theory.

Chapter 2

Background

We begin by laying the basic framework of Legendrian knot theory. The statements of definitions and results in this chapter come from [35], except in Section 2.5, where they come from [21]. An in-depth survey of Legendrian knot theory can be found in [13].

2.1 Legendrian knots in $\mathbb{R}^3$

Legendrian knots are smooth knots in $\mathbb{R}^3$ that satisfy a certain geometric condition, namely their tangent spaces lie within a specified plane field. The plane field is called the *standard contact structure* on $\mathbb{R}^3$ and is defined as follows:

Definition 2.1.1. The *standard contact structure* ξ on $\mathbb{R}^3$ is the 2-plane distribution defined as the kernel of the 1-form $\alpha = dz - ydx$; see Figure 2.1

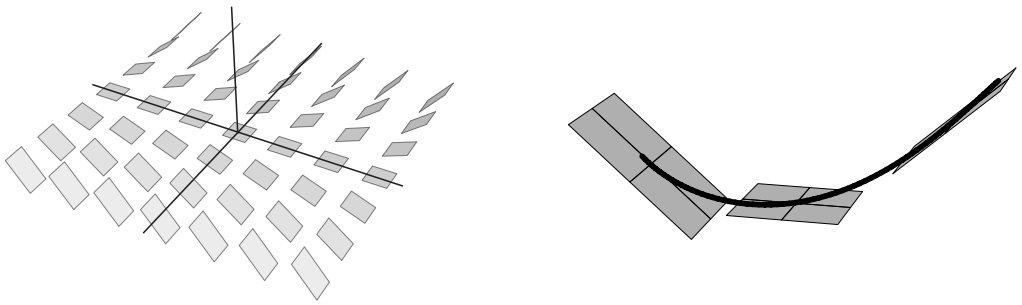

Figure 2.1: (a) The standard contact structure on $\mathbb{R}^3$. (b) A Legendrian curve. Thank you to Josh Sabloff for this Figure.

(a).

The standard contact structure ξ assigns to each point in $\mathbb{R}^3$ a two dimensional subspace of the tangent space. At the point $\{x, y, z\}$, the subspace is spanned by the vectors ∂_y and $\partial_x + y\partial_z$. It is easy to check that $\alpha \wedge d\alpha$ is a volume form on $\mathbb{R}^3$ and hence is non-zero. Thus the Frobenius Theorem implies that ξ is completely non-integrable. Intuitively, this means that the twisting of the planes of ξ makes it impossible, even locally, for the tangent space of a surface to coincide with the plane field. However, it is certainly possible for the tangent space of a curve to sit inside the plane field. Such curves are called *Legendrian*; see Figure 2.1 (b).

Definition 2.1.2. A *Legendrian knot* is a smooth embedding $K : S^1 \to \mathbb{R}^3$ such that for all t, $K'(t) \in \xi(K(t))$, or equivalently, $\alpha(K'(t)) = 0$.

In a slight abuse of notation, we will use K to denote both the embedding map and the image of the map. Two Legendrian knots that can be smoothly deformed into each other through Legendrian knots are called *Legendrian*

isotopic. More precisely,

Definition 2.1.3. K_0 and K_1 are *Legendrian isotopic* if there exists a smooth map $L : S^1 \times I \to \mathbb{R}^3$ such that for each fixed $t \in [0,1]$, $L_t : S^1 \to \mathbb{R}^3$ is a Legendrian knot, $L_0 = K_0$, and $L_1 = K_1$.

Legendrian knots are plentiful. Every topological knot has a Legendrian knot C^0 close to it[1]. In particular, every smooth knot class has a Legendrian representative. Two Legendrian knots that are Legendrian isotopic are isotopic as smooth knots. This leads us to ask:

Question 6. Do there exist Legendrian knots that are smoothly isotopic but not Legendrian isotopic?

We will see shortly that the answer to this question is an emphatic yes. There are infinitely many Legendrian knot classes for a particular smooth knot class. The task of finding invariants that can distinguish Legendrian knots classes has been a fruitful area of research for the last 25 years. Before delving into Legendrian knot invariants, we will lay out the tools and techniques needed to visualize and work with these knots.

As in smooth knot theory, we will study Legendrian knots using projections onto planes in $\mathbb{R}^3$. There are two projections from $\mathbb{R}^3$ to $\mathbb{R}^2$ that preserve the geometric information of ξ and hence allow us to keep track of the Legendrian properties of K. The *front projection* of $\mathbb{R}^3 = \{(x, y, z)\}$ projects away the y coordinate while the *Lagrangian projection* projects away the z

[1]Though not the original source, Theorem 2.5 in [13] gives a nice proof of this result.

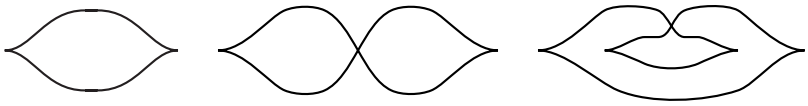

Figure 2.2: Front projections of Legendrian unknots.

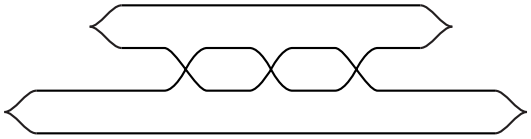

Figure 2.3: A front projection of a Legendrian trefoil.

coordinate. We will use both projections extensively. In addition, there are Reidemeister-type theorems that tell us how the projections of Legendrian isotopic knots are related.

2.1.1 The front projection

Definition 2.1.4. The *front projection* of a Legendrian knot K is the image of K under the projection map $\pi_f : \mathbb{R}^3 \to \mathbb{R}^2$ by $(x, y, z) \mapsto (x, z)$. We let Σ denote the image $\pi_f(K)$; see Figures 2.2 and 2.3.

We will always assume that the immersed points of Σ are transverse double points. This is a generic condition in the sense that any Legendrian knot can be Legendrian isotoped within an small neighborhood of itself to ensure this condition is satisfied.

The Legendrian properties of K can be easily seen in the front projection Σ. In particular, the Legendrian condition $\alpha(K'(t)) = dz - ydx(K'(t)) = 0$ implies that at every point of K, $y = \frac{dz}{dx}$. In Σ, the Legendrian condition

$y = \frac{dz}{dx}$ manifests itself in the following three ways.

1. The slope $\frac{dz}{dx}$ at each point of Σ is finite so Σ has no vertical tangencies . Instead we see cusps that are parameterized, up to a change of coordinates, by $x(t)^3 = z(t)^2$. A *strand* in Σ is a smooth arc in Σ connecting a left cusp to a right cusp.

2. We can uniquely reconstruct K from Σ since the y-coordinate of each point in Σ is equal to the slope at that point. In the same manner, any closed curve in the xz-plane that has no vertical tangencies but has cusps and transverse self-intersection points will uniquely determine the front projection of a Legendrian knot.

3. If we set the convention that the y-axis points *into* the page, then at a transverse double point we do not need to specify which strand appears in front. The Legendrian condition $y = \frac{dz}{dx}$ implies that the strand with the smaller slope appears in front of the strand with the larger slope.

In smooth knot theory, the Reidemeister moves take the three dimensional problem of classifying smooth knots up to isotopy and reduces it to a two dimensional problem of relating smooth knot projections by a system of projection moves. In a similar manner, the problem of classifying Legendrian knots up to Legendrian isotopy can be reduced to classifying front projections up to a system of projection moves. In particular,

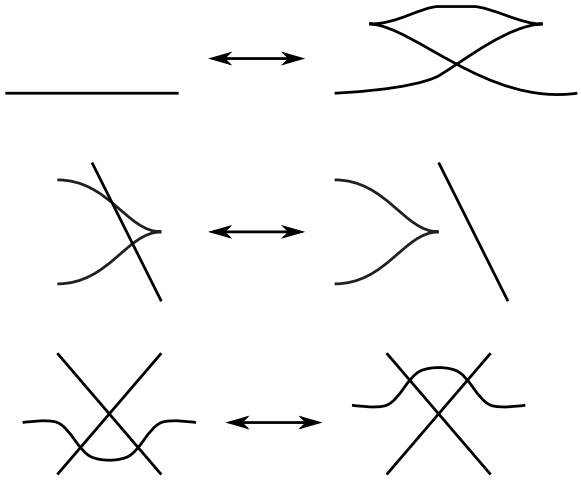

Figure 2.4: The Reidemeister moves for front projections. Reflections in the x and z directions give additional moves.

Theorem 2.1.5 ([37])**.** Two Legendrian knots are Legendrian isotopic if and only if their front projections are related by a finite sequence of the moves pictured in Figure 2.4.

This theorem gives a program for developing and using Legendrian invariants. Given K, we need only think of an intelligent way of assigning to Σ an object (integer, polynomial, group, etc.) so that the object does not change when we perform each of the moves in Figure 2.4. The resulting object will then be a Legendrian isotopy invariant. Of course, this program is not at all easy.

2.1.2 The Lagrangian projection

Definition 2.1.6. The *Lagrangian projection* of a Legendrian knot K is the image of K under the projection map $\pi_L : \mathbb{R}^3 \to \mathbb{R}^2$ by $(x, y, z) \mapsto (x, y)$. We

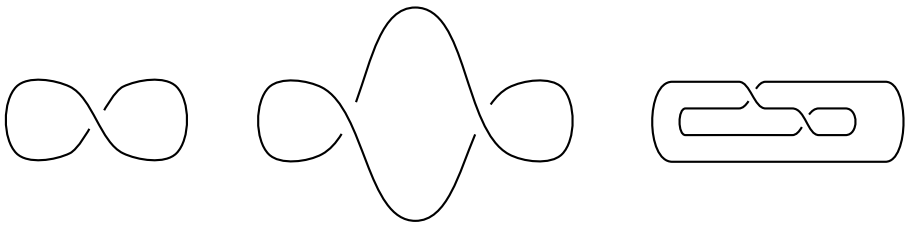

Figure 2.5: Lagrangian projections of Legendrian unknots.

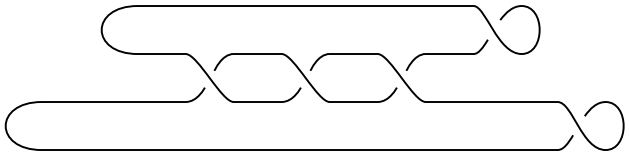

Figure 2.6: A Lagrangian projection of a Legendrian trefoil.

let L denote the image $\pi_L(K)$; see Figures 2.5 and 2.6.

Theorem 2.1.7 ([37])**.** If two Legendrian knots are Legendrian isotopic then their Lagrangian diagrams are related by a finite sequence of the moves pictured in Figure 2.7.

The converse to Theorem 2.1.7 is not true. In fact, a Lagrangian Reidemeister move does not always result in another Lagrangian projection. Conditions on the area bounded by L must be satisfied in order for a Lagrangian Reidemeister move to result in another Lagrangian projection; see Section 4 in [22]. A simple application of Stokes theorem shows that L bounds zero signed area in the $\{x, y\}$-plane. It is often more convenient to work with front projections since no such limitations exist for Reidemeister moves on front projections.

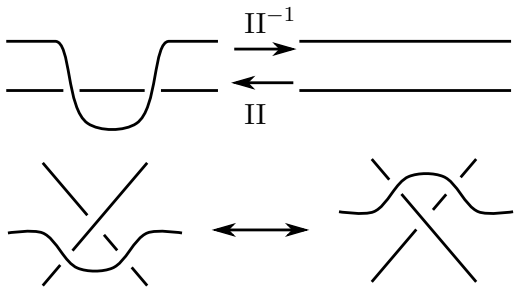

Figure 2.7: Reidemeister moves on Lagrangian projections. We obtain other moves through rotation by 180 degrees about each of the three coordinate axes. We have indicated the type II and type II^{-1} moves.

2.1.3 The Ng resolution

In [27], Ng describes an algorithm connecting a front projection with a topologically similar Lagrangian projection. As in smooth knot theory, Legendrian knot invariants are often easier to compute from a projection of the knot than from the knot itself. Thus, the Ng resolution algorithm is a useful tool in finding connections between different Legendrian invariants. In fact, generating families and normal rulings are naturally defined using the front projection, while the CE-DGA is easily formulated using the Lagrangian projection. Each of these invariants has a combinatorial formulation based on the topology of their projections. The Ng resolution algorithm is the first step in finding connections between these invariants.

Definition 2.1.8. Given a Legendrian knot K with front projection Σ, we form the *Ng resolution*, denoted L_Σ, by:

1. Smoothing the left cusps of Σ as in Figure 2.8 (a),

2. Smoothing and twisting the right cusps of Σ as in Figure 2.8 (b), and

3. Resolving the double points of Σ as in Figure 2.8 (c).

We caution the reader that L_Σ is not the Lagrangian projection of the Legendrian knot with front Σ. Indeed, Ng's algorithm isotopes Σ to another front projection Σ' and L_Σ is the Lagrangian projection of the Legendrian knot with front Σ'.

The resolution procedure isotopes Σ to Σ' as follows. The procedure begins to the left of Σ and proceeds to the right. At each crossing or cusp, the procedure isotopes Σ as indicated in Figures 2.10, 2.11 and 2.12. Figures 2.10, 2.11 and 2.12 describe the isotopy on Σ and the result of this isotopy in the Lagrangian projection. In particular, Σ' is formed by stretching Σ in the x direction and modifying the slopes of the strands comprising Σ. After isotoping Σ, the strands of the resulting front projection have constant, decreasing slopes from top to bottom except at finitely many places where the slopes of two consecutive strands are exchanged. By the Legendrian condition $y = \frac{dz}{dx}$, strands with constant slope result in strands with slope 0 in the resulting Lagrangian projection; see Figure 2.9. The exchanging of two slopes results in a crossing in the resulting Lagrangian projection; see Figure 2.11 and 2.12. The full procedure for the front projection of a trefoil is detailed in Figure 2.13. Ng proves in [27] that Σ and Σ' are front projections of Legendrian isotopic knots.

Remark 2.1.9. In this remark we define a height function on the crossings

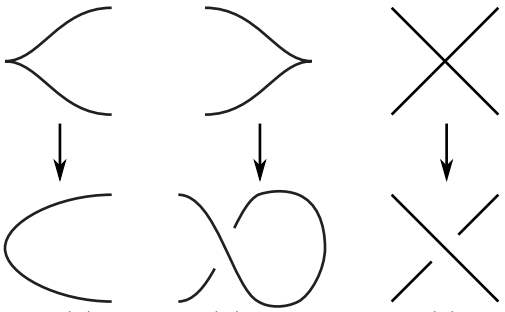

Figure 2.8: Cusps and crossings in the Ng resolution procedure.

Figure 2.9: Strands with fixed slope in the front projection (left) and the resulting strands in the Lagrangian projection (right).

of L_Σ. Let T denote the crossings of L_Σ and let $p \in T$. In Σ', the crossing p is created when two strands t_p and b_p have the same slope. We define a height function $h : T \to \mathbb{R}^+$ in the following manner. We define $h(p)$ to be the absolute value of the difference in the z-coordinates of t_p and b_p at the instant when they have the same slope. This height function corresponds to the height function we define in Section 2.3.3. It is an important part of the construction of the differential of the CE-DGA associated to L_Σ.

For now we make one note about $h : T \to \mathbb{R}^+$. We can construct Σ' so that as we move from left to right along the x-axis, the distance between the strands of Σ' is strictly increasing. Hence, the height function $h : T \to \mathbb{R}^+$ is strictly increasing as we move from left to right along the x-axis in L_Σ.

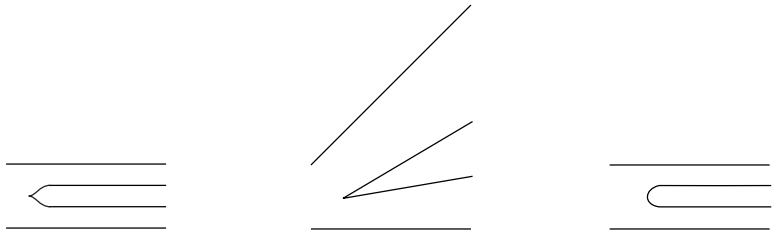

Figure 2.10: The resolution procedure near a left cusp of the original front projection. From left to right, the three projections are Σ, Σ', and L_Σ.

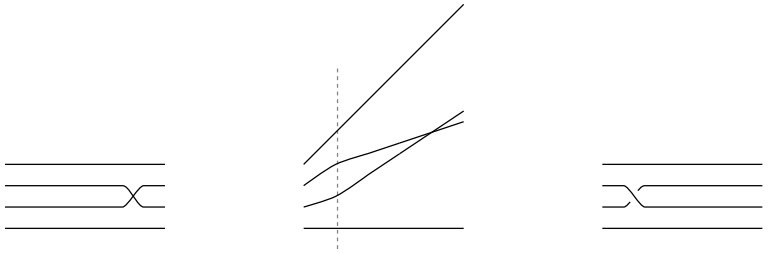

Figure 2.11: The resolution procedure near a crossing of the original front projection. The dotted line indicates where the slopes of two strands are interchanged. From left to right, the three projections are Σ, Σ', and L_Σ.

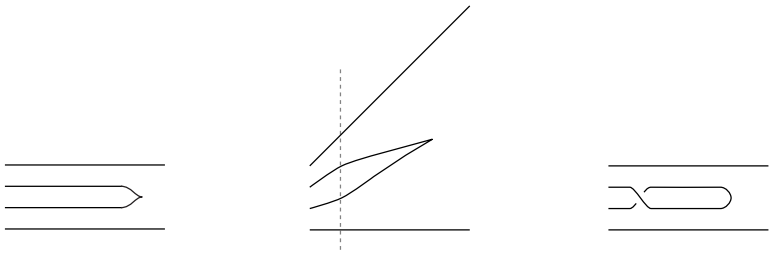

Figure 2.12: The resolution procedure near a right cusp of the original front projection. The dotted line indicates where the slopes of two strands are interchanged. From left to right, the three projections are Σ, Σ', and L_Σ.

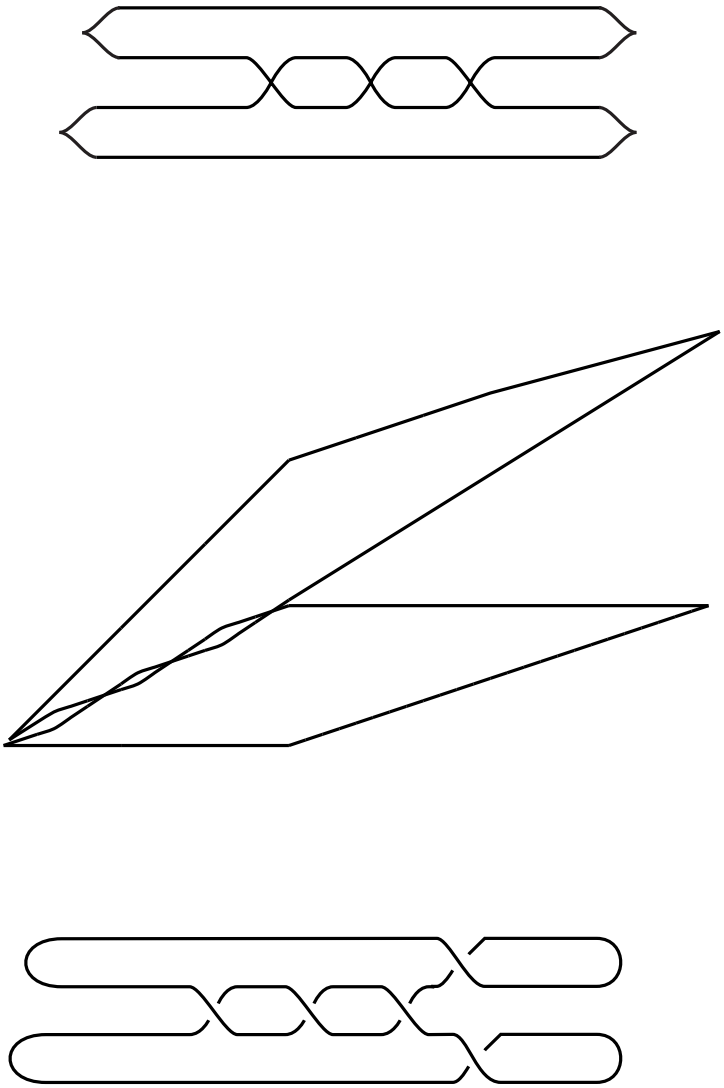

Figure 2.13: The complete resolution procedure for the front projection of a trefoil. From top to bottom, the three projections are Σ, Σ', and L_Σ.

At this point we have enough tools and techniques at our disposal to begin working with Legendrian invariants. In the case of smooth knot theory, many invariants exists of varying degrees of power and complexity. In Legendrian knot theory, only a handful of invariants exist, although their origins run the gamut of geometry, topology, algebra and combinatorics.

2.2 Classical Legendrian knot invariants

In 1983, Bennequin's published [3]. This paper had a profound effect on both Legendrian knot theory and contact topology. Bennequin's work showed that Legendrian knots could be studied using topological techniques from smooth knot theory. Since the publication of [3], Legendrian knot theory has grown considerably, as has the range of topological and geometric tools used to study Legendrian knots. Bennequin also exhibited the existence of an exotic contact structure on $\mathbb{R}^3$. This helped originate the dichotomy between tight and overtwisted contact structures in modern contact topology. The following two Legendrian invariants were central to Bennequin's work.

Two Legendrian knot invariants exist that measure different "twisting" relationships between Legendrian knots and the contact structure ξ. These two invariants are often referred to as the "classical invariants," since they were the first to provide an answer to Question 6.

The *Thurston-Bennequin number* measures the twisting of the contact planes around K as we move along K. More precisely,

Definition 2.2.1. Let K' be the knot resulting from a small transverse push-off of K in the direction of a vector field transverse to ξ. Then the *Thurston-Bennequin number*, denoted $tb(K)$, is the linking number of K and K'.

The *rotation number*, denoted $r(K)$, measures the winding number of the tangent space of K inside a trivialization of ξ. The rotation number requires that we fix an orientation on K and changing the orientation on K changes the sign of $r(K)$. More precisely,

Definition 2.2.2. The *rotation number* of an oriented Legendrian knot K is the winding number of the oriented tangent direction of K with respect to the trivialization $\{\partial_y, \partial_x + y\partial_z\}$ of ξ.

We can easily compute $tb(K)$ and $r(K)$ from the front and Lagrangian projections of K. Before giving formulae for $tb(K)$ and $r(K)$, we define two useful numbers. The *cusp number* of a front projection is the total number of cusps appearing in the projection and is denoted $c(\Sigma)$. The *writhe* of an oriented knot projection P is the signed count of its crossings and is denoted $w(P)$. The sign convention on the crossings is given in Figure 2.14. On an oriented front projection, we will also keep track of *downward-pointing* and *upward-pointing cusps*; see Figure 2.15 for a description.

Proposition 2.2.3. The Thurston-Bennequin number and rotation number of K are computed from the front projection Σ in the following way:

1. $tb(K) = w(\Sigma) - \frac{1}{2}c(\Sigma)$ and

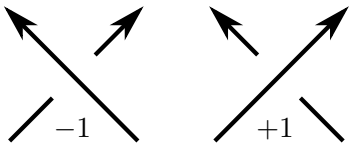

Figure 2.14: The writhe contribution of an oriented crossing.

Figure 2.15: Downward-pointing and upward-pointing cusps on an oriented projection.

2. Given an orientation on K, $r(K) = \frac{1}{2}(\#$ downward-pointing cusps $-\#$ upward-pointing cusps).

The Thurston-Bennequin number and rotation number of K are computed from the Lagrangian projection L in the following way:

1. The Thurston-Bennequin number of K is the writhe of its Lagrangian projection L, and

2. Given an orientation on K, the rotation number $r(K)$ is the rotation number of the tangent space of L with respect to the trivialization $\{\partial_x, \partial_y\}$ of the tangent space of $\mathbb{R}^2 = \{(x, y)\}$.

Example. We calculate the tb and r of the front projections of the Legendrian unknots in Figure 2.2 and note that from left to right the pair (tb, r) is $(-1, 0)$, $(-2, \pm 1)$, and $(-1, 0)$. The first and third knot are Legendrian isotopic by a Reidemeister I move. As we can see, the middle unknot is not Legendrian isotopic to the other two.

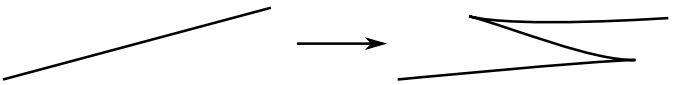

Figure 2.16: Geometric stabilization of a Legendrian front projection. The resulting front projection is not Legendrian isotopic to the original.

Given a front projection, there is a simple algorithm for constructing another front projection with the same smooth knot type but different Legendrian knot type. We do so by changing a strand of Σ as described in Figure 2.16. Note that this operation changes the Thurston-Bennequin number by -1 and the rotation number by ± 1, depending on the orientation on the original Legendrian knot. By repeated applications of this process, we can construct infinitely many Legendrian isotopy classes within a given smooth knot type.

It is natural to ask if tb and r distinguish every pair of Legendrian isotopy classes within a smooth knot type.

Question 7. Do there exist Legendrian knots with the same smooth knot type and the same classical invariants that are not Legendrian isotopic?

The answer is yes. Chekanov demonstrated in [6] two Legendrian 5_2 knots that have the same tb and r but are not Legendrian isotopic; see Figure 2.17. Chekanov used a new Legendrian invariant derived from a differential graded algebra to distinguish these two Legendrian isotopy classes. Although unpublished, at the same time Eliashberg had similar examples providing an affirmative answer to Question 7.

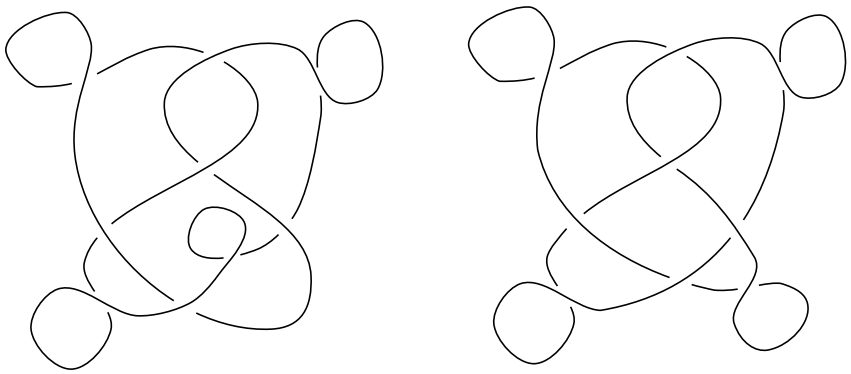

Figure 2.17: Chekanov's examples of two Legendrian 5_2 knots with identical tb and r, but are not Legendrian isotopic.

2.2.1 A Word of Caution

In the following sections we will discuss modern Legendrian invariants that came after tb and r. We are primarily concerned with finding new connections between generating families, graded normal rulings, and augmentations. It is known that if $r(K) \neq 0$ then K does not admit any of these objects. Hence, we will restrict ourselves to Legendrian knots with rotation number 0. The definitions that follow are all stated with the assumption $r(K) = 0$ in mind. In many cases, there are reformulations of these definitions for the case $r(K) \neq 0$. In addition, we will define the CE-DGA over $\mathbb{Z}_2$, even though the CE-DGA may be formulated over $\mathbb{Z}[t, -t]$.

2.3 The Chekanov-Eliashberg DGA

In [6] and [12], Chekanov and Eliashberg develop a differential graded algebra, from here on referred to as the CE-DGA, that has led to the discovery of

several new Legendrian isotopy invariants. The CE-DGA is defined using the Lagrangian projection of a Legendrian knot. We first define the algebra, followed by the grading and the differential.

Let K be a Legendrian knot with Lagrangian projection L. Label the crossings of L by $q_1, \ldots, q_n$ and let $Q = \{q_1, \ldots, q_n\}$. Then the algebra of the CE-DGA is defined as:

2.3.1 The Algebra

Definition 2.3.1. Let $A(L)$ denote the $\mathbb{Z}_2$ vector space freely generated by the elements of Q. Then the algebra $\mathcal{A}(L)$ is the unital tensor algebra $TA(L)$. We consider $\mathcal{A}(L)$ to be a *based* algebra since the algebra basis Q is part of the data of $\mathcal{A}(L)$.

An element of $\mathcal{A}(L)$ looks like the sum of noncommutative words in the letters q_i. For example: $1 + q_1 + q_3 + q_5q_3q_1 + q_3q_5q_1$

2.3.2 The Grading

In the CE-DGA, the generators in Q are graded by elements of $\mathbb{Z}$. We define a grading $|q_i|$ on the generators q_i and extend it to a grading on all of the elements of $\mathcal{A}(L)$ by requiring $|ab| = |a| + |b|$ for all $a, b \in \mathcal{A}(L)$.

First we isotope K slightly so that the two strands meeting at each crossing of L are orthogonal. The grading $|q_i|$ measures the winding number of a path in L that begins and ends at q_i.

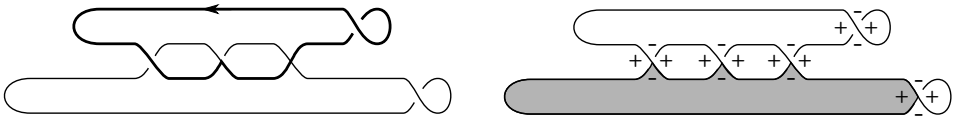

Figure 2.18: We label the crossings of this projection $q_1, \ldots, q_5$ from left to right. (a) A capping path for q_2. (b) A convex immersed polygon contributing the monomial $q_3q_2q_1$ to ∂q_5.

Definition 2.3.2. Let γ_i be a path in K that begins at q_i and follows L until it first returns to q_i. Such a path is called a *capping path* for crossing q_i; see Figure 2.18 (a).

We let $r(\gamma_i)$ denote the fractional winding number of the tangent space of γ_i with respect to the trivialization $\{\partial_x, \partial_y\}$ of the tangent space of $\mathbb{R}^2 = \{(x, y)\}$.

Definition 2.3.3. The *grading of a crossing* q_i is defined to be:

$$|q_i| = 2r(\gamma_i) - \frac{1}{2} \tag{2.1}$$

The orthogonality of the crossing strands at q_i ensures that $2r(\gamma_i) - \frac{1}{2}$ is an integer. Each crossing q_i has two possible capping paths. It is easy to check that $|q_i|$ is independent of the choice of capping path.

If L_Σ is the Ng resolution of some front projection Σ then we can calculate the grading of the crossings of L_Σ from Σ. Let $q_1, \ldots, q_n$ denote both the crossings in Σ and the resolved crossings in L_Σ. Let $z_1, \ldots, z_m$ denote the crossings in L_Σ created during the resolution of a the right cusps of Σ. By using capping paths, it is easy to calculate that $|z_j| = 1$ for all j. We calculate

Figure 2.19: A Maslov potential near left and right cusps.

the gradings $|q_i|$ by affixing an integer to each strand of Σ and looking at the difference between these integers at each crossing q_i.

Definition 2.3.4. A *Maslov potential* on Σ is an assignment μ to each strand of Σ an element of $\mathbb{Z}$ such that the assignment satisfies the relation shown in Figure 2.19.

Any two Maslov potentials μ_1 and μ_2 differ by a constant, i.e. there exists $a(\mu_1, \mu_2) \in \mathbb{Z}$ such that $\mu_1 - \mu_2 = a(\mu_1, \mu_2)$. Given a front projection Σ and Maslov potential μ, we define a grading on the crossings on Σ in the following manner.

Definition 2.3.5. For each crossing q_i we let q_i^T (resp. q_i^B) denote the strand with the smaller (resp. larger) slope and define the grading of q_i to be $|q_i| = \mu(q_i^T) - \mu(q_i^B)$.

A capping path γ_i in the Ng resolution L_Σ projects to a path γ in Σ. It is easy see that $|q_i| = D - U$, where D (respectively, U) is the number of downward (respectively, upward) pointing cusps coming from the path γ. Thus, by the definition of a Maslov potential at cusps, the grading defined in Definition 2.3.5 equals the grading defined in Definition 2.3.3.

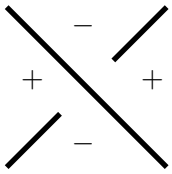

Figure 2.20: The Reeb sign of a crossing.

2.3.3 The Differential

Definition 2.3.6. A *Reeb chord* of a Legendrian knot K is a path γ in $\mathbb{R}^3$ that begins and ends on L and has constant x and y coordinates.

Since, the Lagrangian projection projects away the z-coordinate, the Reeb chords of K are in 1-1 correspondence with the crossings of L. We let γ_i denote the Reeb chord associated with a crossing q_i.

Definition 2.3.7. The *height* h of a Reeb chord γ_i is defined to be the absolute value of the difference in the z-coordinates of the two end points of γ_i.

We define a height function h on the crossings of L by letting $h(q_i) = h(\gamma_i)$. When the heights of the Reeb chords are all distinct, h provides an ordering on the crossings of L. A Legendrian knot may be perturbed slightly so that this is the case. As we will see, the height of q_i is related to ∂q_i in the CE-DGA. Along with the height $h(q_i)$, we also decorate each corner of crossing q_i with a *Reeb sign* as described in Figure 2.20.

Definition 2.3.8. Let D be the unit disk in $\mathbb{R}^2$ and let $\mathcal{X} = \{x_0, \ldots, x_n\}$ be a set of distinct points along ∂D in counter-clockwise order. A *convex*

immersed polygon is a continuous map $f : D \to \mathbb{R}^2$ so that:

1. The map f is an orientation-preserving immersion on the interior of D;
2. The restriction of the map f to $\partial D \setminus \mathcal{X}$ is an immersion whose image lies inside L; and
3. The image of each $x_i \in \mathcal{X}$ under f is a crossing of L, and the image of a neighborhood of x_i covers a convex corner at the crossing. Call a corner of an immersed polygon *positive* if it covers a positive Reeb sign and *negative* otherwise.

As a simple application of Stokes theorem to a convex immersed disk f, we have:

Lemma 2.3.9. Let f be a convex immersed polygon and let γ_i be the Reeb chord that lies over the corner $f(x_i)$. The following relationship holds:

$$\sum_{x_i \text{ positive}} h(\gamma_i) - \sum_{x_j \text{ negative}} h(\gamma_j) = Area(f(D)) \tag{2.2}$$

The convex immersed polygon bounds positive area in $\mathbb{R}^2$ since we require that f is orientation-preserving. Hence we have the following:

Corollary 2.3.10. Every convex immersed polygon has at least one positive corner.

In the case of an immersed polygon with a single positive corner, the height of the positive corner is greater than the height of each of the negative corners. The differential ∂q_i of the generator q_i is a mod 2 count of

convex immersed polygons with a single positive corner at q_i. We extend this differential to all elements of $\mathcal{A}(L)$ using linearity and the Leibniz rule.

Definition 2.3.11. Let $\tilde{\Delta}(q_i; q_{j_1}, \ldots, q_{j_k})$ be the set of convex immersed polygons with a positive corner at q_i and negative corners at $q_{j_1}, \ldots, q_{j_k}$. The negative corners are ordered by the counter-clockwise order of the marked points along ∂D in the definition of a convex immersed polygon. Let $\Delta(q_i; q_{j_1}, \ldots, q_{j_k})$ be $\tilde{\Delta}(q_i; q_{j_1}, \ldots, q_{j_k})$ modulo smooth reparameterization.

Definition 2.3.12. The differential ∂ on the algebra $\mathcal{A}(L)$ is defined on a generator $q_i \in Q$ by the formula:

$$\partial q_i = \sum_{\Delta(q_i; q_{j_1}, \ldots, q_{j_k})} \#(\Delta(q_i; q_{j_1}, \ldots, q_{j_k})) q_{j_1} \ldots q_{j_k} \tag{2.3}$$

where $\#(\Delta(\ldots))$ is the mod 2 count of the elements in $\#(\Delta(\ldots))$. We extend ∂ to all of $\mathcal{A}(L)$ by linearity and the Leibniz rule.

The convex immersed polygon contributing the monomial $q_3 q_2 q_1$ to ∂q_5 is given in Figure 2.18 (b).

Lemma 2.3.13. The set $\Delta(q_i; q_{j_1}, \ldots, q_{j_k})$ is finite and the sum in Equation 2.3 has finitely many terms.

Theorem 2.3.14 ([6])**.** The differential ∂ satisfies:

1. $|\partial q| = |q| - 1$ modulo $2r(K)$, and
2. $\partial \circ \partial = 0$.

If $h(q) > h(p)$ for crossings q, p in L, then by Corollary 2.3.10 p does not appear in ∂q. In the case of a Ng resolution L_Σ, we noted in Section 2.1.3 that the heights of the crossings increase as we move from left to right along the x-axis. Thus the negative corners of a convex immersed polygon contributing to ∂ in $(\mathcal{A}(L_\Sigma), \partial)$ always appear to the left of the positive corner. In Chapter 5, this fact will help us find convex immersed polygon contributing to ∂.

2.3.4 Legendrian Invariance of the CE-DGA

Each Lagrangian projection of a Legendrian knot has an associated CE-DGA. In [6], Chekanov defines an algebraic equivalence on DGAs, called *stable tame isomorphism*, and proves that the CE-DGAs of two Lagrangian projections related by Reidemeister moves are equivalent. Thus, up to stable tame isomorphism, the CE-DGA is a Legendrian isotopy invariant. In general, it is difficult to decide if two CE-DGAs are stable tame isomorphic. This equivalence relation also preserves the homology of the DGA and so the homology of $(\mathcal{A}(L), \partial)$ is a Legendrian isotopy invariant, called the *Legendrian contact homology* of K.

Definition 2.3.15. Given two algebras $\mathcal{A}$ and $\mathcal{A}'$, a grading-preserving identification of their generating sets $Q \leftrightarrow Q'$, and a generator q_j for $\mathcal{A}$, an *elementary isomorphism* ϕ is an graded algebra map that is defined by:

$$\phi(q_i) = \begin{cases} q_i' & i \neq j \\ q_j' + u & i = j,\ u \text{ a term in } \mathcal{A}' \text{ not containing } q_j' \end{cases}$$

A composition of elementary isomorphisms is called a *tame isomorphism*.

Definition 2.3.16. A *tame isomorphism of DGAs* between $(\mathcal{A}, \partial)$ and $(\mathcal{A}', \partial')$ is a tame isomorphisms Φ that is also a chain map, i.e. $\Phi \circ \partial = \partial' \circ \Phi$.

Definition 2.3.17. Given a DGA $(\mathcal{A}, \partial)$ with generating set Q, its *degree i stabilization* $S_i(\mathcal{A}, \partial)$ is the algebra generated by the set $Q \cup \{e_1, e_2\}$, where

$$|e_1| = i \text{ and } |e_2| = i - 1 \tag{2.4}$$

and the differential is extended to the new generators by

$$\partial e_1 = e_2 \text{ and } \partial e_2 = 0 \tag{2.5}$$

Definition 2.3.18. Two DGAs $(\mathcal{A}, \partial)$ and $(\mathcal{A}', \partial')$ are *stable tame isomorphic* if there exists stabilizations $S_{i_1}, \dots, S_{i_m}$ and $S'_{j_1}, \dots, S'_{j_n}$ and a tame isomorphism of DGAs

$$\psi : S_{i_1}(\dots S_{i_m}(\mathcal{A}) \dots) \to S'_{j_1}(\dots S'_{j_n}(\mathcal{A}') \dots) \tag{2.6}$$

so that the composition of maps is a chain map, i.e. $\partial \circ \psi = \psi \circ \partial'$

where ∂ (resp. ∂') indicates the boundary map of $S_{i_1}(\dots S_{i_m}(\mathcal{A})\dots)$ (resp. $S'_{j_1}(\dots S'_{j_n}(\mathcal{A}')\dots)$.

Theorem 2.3.19 ([6])**.** If Legendrian knots K and K' are Legendrian isotopic with Lagrangian projections L and L' respectively, then the CE-DGAs $(\mathcal{A}(L), \partial)$ and $(\mathcal{A}(L'), \partial')$ are stable tame isomorphic.

Corollary 2.3.20. The homology of the CE-DGA of a Legendrian knot K is a Legendrian isotopy invariant. We call this invariant the *Legendrian contact homology*.

2.4 Augmentations

The CE-DGA of a Lagrangian projection L and its resulting Legendrian contact homology is, in general, difficult to compute. Luckily we can derive from $(\mathcal{A}(L), \partial)$ other Legendrian invariants that have proved to be useful in distinguishing Legendrian isotopy classes. In [6], Chekanov implicitly defines a class of DGA chain maps called *augmentations*, which he uses to distinguish the Legendrian knots in Figure 2.17.

Definition 2.4.1. An *augmentation* is an algebra map $\epsilon : (\mathcal{A}(L), \partial) \to \mathbb{Z}_2$ satisfying:

1. $\epsilon(1) = 1$,
2. $\epsilon \circ \partial = 0$, and

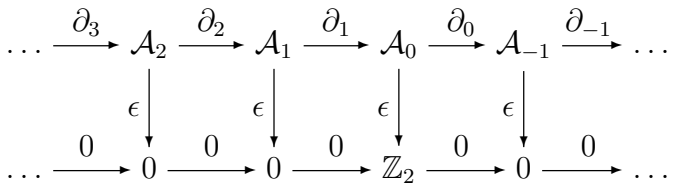

Figure 2.21: An augmentation as a chain map.

3. $\epsilon(q_i) = 1$ implies $|q_i| = 0$.

We let $Aug(L)$ denote the set of augmentations of $(\mathcal{A}(L), \partial)$.

We think of an augmentation $\epsilon \in Aug(L)$ as a chain map between the CE-DGA $(\mathcal{A}(L), \partial)$ and the DGA whose only nonzero chain group is a copy of $\mathbb{Z}_2$ in grading 0 with differential identically zero.

It is easy to check that a tame isomorphism between DGAs induces a bijection on the corresponding sets of augmentations. Stabilizing a DGA may double the number of augmentations depending on the grading of the new generators. Hence, the number of augmentations is not a Legendrian invariant. However, the existence of an augmentation certainly is a Legendrian isotopy invariant.

2.5 Generating families

A generating family encodes a Legendrian front projection as the Cerf diagram of a one-parameter family of smooth functions $F_x : \mathbb{R}^n \to \mathbb{R}$; see [1, 4, 21, 39, 42] for a more complete introduction to the theory of generating

families. From this one-parameter family of functions we are able to derive several Legendrian isotopy invariants. Considerable success has been had using generating families to distinguish Legendrian knots; see [8, 19, 41, 40, 30]

Definition 2.5.1. Suppose $F : \mathbb{R} \times \mathbb{R}^k \to \mathbb{R}$, $(x, \mathbf{v}) \mapsto F(x, \mathbf{v})$ is a smooth function such that the map $(\frac{\partial F}{\partial v_1}, \frac{\partial F}{\partial v_2}, ..., \frac{\partial F}{\partial v_k}) : \mathbb{R} \times \mathbb{R}^k \to \mathbb{R}^k$ has 0 as a regular value. Then

$$C_F := \{(x, \mathbf{v}) \in \mathbb{R} \times \mathbb{R}^k \mid \partial_{v_i} F = 0 \text{ for } i = 1, 2, ..., k\} \tag{2.7}$$

is a 1-dimensional submanifold of $\mathbb{R} \times \mathbb{R}^k$ called the *critical locus of* F and we can immerse C_F into $(\mathbb{R}^3, \xi_{std})$ as a Legendrian submanifold by $i_F : C_F \to \mathbb{R}^3$ by

$$i_F((x_0, \mathbf{v}_0)) = (x_0, \partial_x F(x_0, \mathbf{v}_0), F(x_0, \mathbf{v}_0)) \tag{2.8}$$

In this manner, F generates a (possibly immersed) Legendrian submanifold $K_F := i_F(C_F)$ of $(\mathbb{R}^3, \xi_{std})$. We say F *generates* K_F or F is a *generating family* for K_F.

We think of a generating family $F : \mathbb{R} \times \mathbb{R}^k \to \mathbb{R}$ as the 1-parameter family of functions $F_x : \mathbb{R}^k \to \mathbb{R}$. By adding further conditions to F we can ensure that K_F is an embedding Legendrian knot. In partic For a fixed $x_0 \in \mathbb{R}$, the points of K_F with x-coordinate equal to x_0 correspond to the critical points of the function $F_{x_0} : \mathbb{R}^k \to \mathbb{R}$; see Figure 2.22.

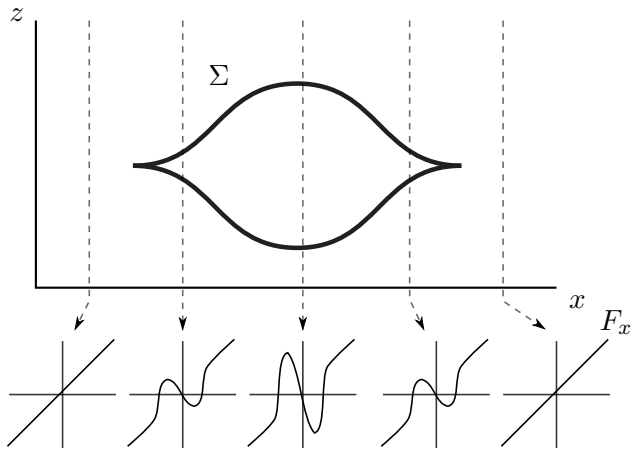

Figure 2.22: A generating family for a Legendrian unknot.

As we saw in the Chapter 1, we will primarily concern ourselves with the Morse-Smale complexes coming from the 1-parameter family $F : \mathbb{R}\times\mathbb{R}^k \to \mathbb{R}$. In order for F_{x_0} to have a well-defined Morse-Smale complex, we require that F is sufficiently nice outside of a compact set of the domain. In the next definition, we make this condition precise. In particular, this condition ensures that, for a generic metric on the domain of F_{x_0}, the gradient flow lines go off to infinity nicely.

Definition 2.5.2. Suppose F is as defined in Definition 2.5.1. Consider the fiber direction of the domain of F as a Cartesian product $\mathbb{R} \times \mathbb{R}^{k'}$ with coordinates $(l, \mathbf{v})$. If outside a compact set of the domain $\mathbb{R} \times \mathbb{R} \times \mathbb{R}^{k'}$, $F(x, l, \mathbf{v}) = J_x(l) + Q_{x,l}(\mathbf{v})$ where J_x is a nonzero linear function of l and $Q_{x,l}$ is a nondegenerage quadratic function of v, then we say F is *linear-quadratic at infinity*. We'll use the abbreviation LQ for linear-quadratic at infinity.

Definition 2.5.3. Two generating families $F_i : \mathbb{R} \times \mathbb{R}^{k_i} \to \mathbb{R}$, $i \in \{0, 1\}$ are

equivalent if and only if they can be made equal after a succession of the following two operations:

(1) Given a generating family $F : \mathbb{R} \times \mathbb{R}^k \to \mathbb{R}$, suppose $\Phi : \mathbb{R} \times \mathbb{R}^k \to \mathbb{R} \times \mathbb{R}^k$ is a fiber-preserving diffeomorphism, i.e. $\Phi(x, \mathbf{v}) = (x, \phi_x(\mathbf{v}))$ where ϕ_x is a diffeomorphism. Then we say $F' = F \circ \Phi$ is obtained from F by a *fiber-preserving diffeomorphism*.

(2) Given a generating family $F : \mathbb{R} \times \mathbb{R}^k \to \mathbb{R}$, suppose $Q : \mathbb{R}^j \to \mathbb{R}$ is a nondegenerate quadratic function. Define $F' : \mathbb{R} \times \mathbb{R}^k \times \mathbb{R}^j \to \mathbb{R}$ by $F'(x, \mathbf{v_1}, \mathbf{v_2}) = F(x, \mathbf{v_1}) + Q(\mathbf{v_2})$. Then we say F' is obtained from F by a *stabilization*.

Theorem 2.5.4 ([21, 40])**.** Let K_F be a Legendrian submanifold of $(\mathbb{R}^3, \xi_{std})$ generated by an LQ generating family $F : \mathbb{R} \times \mathbb{R} \times \mathbb{R}^k \to \mathbb{R}$. Let $(\phi_t)_{t\in[0,1]}$ be a compactly supported contact isotopy of $(\mathbb{R}, \xi_{std})$ with $\phi_0 = id$. Then there exists $j > 0$ and a path of LQ generating families $(F_t)_{t\in[0,1]}$ defined on $\mathbb{R} \times \mathbb{R} \times \mathbb{R}^k \times \mathbb{R}^j$ such that

(1) F_0 and F are equivalent by $F_0(x, l, \mathbf{v}, \mathbf{w}) = F(x, l, \mathbf{v}) + Q(\mathbf{w})$, where Q is a nondegenerate quadratic functions on $\mathbb{R}^j$;

(2) $F_t = F_0$ outside a compact set of the domain;

(3) F_t generates $\phi_t(K_F)$ for $t \in [0, 1]$.

In the case of Lagrangian submanifolds in symplectic manifolds, a formulation of Theorem 2.5.4 appears in [39] and [42]. Chekanov also gives a

formulation of Theorem 2.5.4 in [5].

Theorem 2.5.4 implies that the existence of a LQ generating family for a Legendrian submanifold of $(\mathbb{R}^3, \xi_{std})$ is a Legendrian isotopy invariant. This gives us a useful Legendrian isotopy invariant for studying Legendrian knots and links.

2.6 Normal rulings

Determining whether or not a Legendrian knot in $\mathbb{R}^3$ comes from a generating family may seem difficult, but it can be reduced to a combinatorial problem of finding "graded normal rulings" on the front projection. A graded normal ruling is a combinatorial object encoded in the generating family for a given Legendrian knot. It has a simple description in terms of the front projection of a Legendrian knot and, in fact, the existence of a graded normal ruling is equivalent to the existence of a generating family. Although rooted in the work of Eliashberg [10], graded normal rulings were brought to prominence by Chekanov and Pushkar in [8, 7] to solve Arnold's four cusp conjecture and by Fuchs in [17], where he related them to augmentations. In addition, Chekanov and Pushkar defined a polynomial Legendrian invariant from graded normal rulings.

We begin by motivating the definition of graded normal ruling. The geometric motivation for a graded normal ruling on Σ comes from examining the one-parameter family of Morse chain complexes that result from a suitably

generic LQ generating family F for Σ. For a generic x and metric g_x, the function $F_x : \mathbb{R}^n \to \mathbb{R}$ induces a Morse-Smale chain complex (C_x, ∂_x, g_x). As x varies, there are finitely many points where the Morse-Smale chain complex changes. The possible changes include: the birth of two critical points, the death of two critical points, the interchanging of critical values of two critical points, and a handleslide of one critical point over another of the same index. The LQ condition ensures that for a sufficiently large positive number c, the chain complex (C_x, ∂_x, g_x) computes the relative homology $H_*(M_c, M_{-c}; \mathbb{Z}_2)$ where $M_a = \{y \in \mathbb{R}^n | F_x(y) \leq a\}$. This homology is trivial and so by [2] a canonical pairing of the critical points of (C_x, ∂_x, g_x) exists. The graded normal ruling invariant encodes the pairing of the critical points of (C_x, ∂_x, g_x) as x varies. Section 12 of [8] provides a more detailed explanation of the connection between generating families and graded normal rulings. We now turn to precisely defining graded normal rulings.

Definition 2.6.1. A *ruling* on the front diagram Σ is a one-to-one correspondence between the set of left cusps and the set of right cusp and, for each corresponding pair of cusps, two paths in Σ that join them such that the ruling paths satisfy:

1. Any two paths in the ruling meet only at crossings or at cusps; and
2. The two paths joining corresponding cusps meet only at the cusps, hence their interiors are disjoint.

The two paths joining a pair of corresponding cusps are called *companions*

of one another. Together the two paths bound a disk in the plane. We call this disk a *ruling disk*. At a crossing, two paths interact. Either these two paths simply pass through each other or one path lies entirely above the other. In the latter case, we call the crossing a *switch*.

Definition 2.6.2. We say a ruling is *graded* if each switched crossing has grading 0, where the grading comes from a Maslov potential as defined in Section 2.3. A ruling is called *normal* if at each switch the two paths interacting at the crossing and their companion strands are arranged as in one of the three cases pictured in Figure 2.24.

Let $N(\Sigma)$ denote the set of graded normal ruling of a Legendrian knot with front projection Σ. Given two front projections Σ and Σ' related by a sequence of Reidemeister moves, there is a bijection between their sets of graded normal rulings.

Theorem 2.6.3 ([8])**.** If K and K' are Legendrian isotopic, then there is an explicit bijection between $N(\Sigma)$ and $N(\Sigma')$.

Figure 2.23 shows the three graded normal rulings of the standard Legendrian trefoil. In addition, this bijection respects a certain Euler characteristic on the rulings and, thus, a polynomial Legendrian isotopy invariant may be formed from the set of graded normal rulings; see [8].

In a normal ruling, there are two types of unswitched crossings. A *departure* is an unswitched crossing in which just before the crossing the two ruling disks are either disjoint or one is nested inside the other and just after

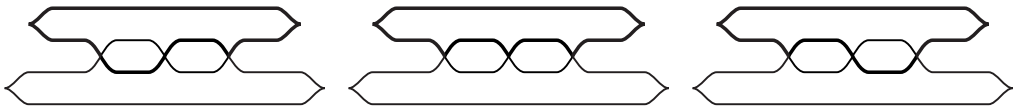

Figure 2.23: The three graded normal rulings of the standard Legendrian trefoil.

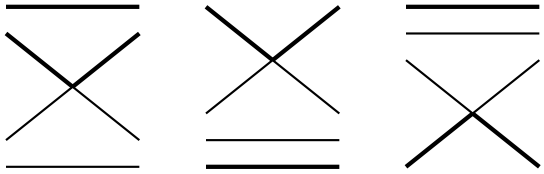

Figure 2.24: The three possible configurations of a normal switch.

the crossing the two disks partially overlap. A *return* is the reverse. Just before the crossing the two ruling disks partially overlap and just after the crossing the two ruling disks are either disjoint or one is nested inside the other; see Figure 2.25.

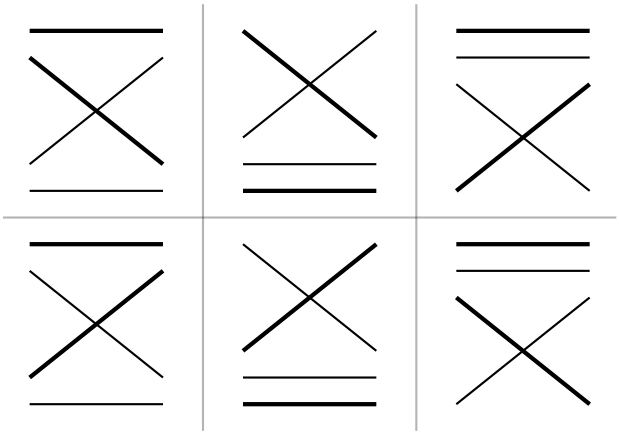

Figure 2.25: The top (bottom) row shows the possible departures (returns).

Chapter 3

Defining Morse Complex Sequences

Suppose a Legendrian knot K admits a LQ generating family $F : \mathbb{R}\times\mathbb{R}^k \to \mathbb{R}$ and g is a metric on the domain $\mathbb{R}\times\mathbb{R}^k$. If F and g are suitably generic[1], then for all but finitely many values of x the function/metric pair (F_x, g_x) gives a Morse-Smale chain complex (C_x, ∂_x, g_x). If (F_x, g_x) fails to be Morse-Smale at x_0, then the chain complex immediately preceding x_0 and the chain complex immediately following x_0 are related by one of four elementary moves: two new critical points with adjacent index are born, two existing critical points with adjacent index die, the critical values of two critical points are interchanged, or a handleslide move occurs between two critical points of the

[1]Our discussion of generating families provides geometric motivation for the definition of a Morse chain sequence. We do not precisely define the term "suitably generic," but refer the reader to [1], [20], and [24].

same index. The last move occurs at an instant x_0 when (F_{x_0}, g_{x_0}) has a gradient flow line flowing between two critical points of the same index. In this manner, a LQ generating family determines a sequence of Morse-Smale chain complexes.

Each Morse-Smale chain complex (C_x, ∂_x, g_x) in the sequence coming from F has trivial homology and, as we will see, a canonical pairing of its critical points. The graded normal ruling invariant encodes the pairing of the generators of (C_x, ∂_x, g_x) as x varies. However, this pairing is only part of the information contained in the sequence of complexes. In this Section, we will define a new object[2] called a *Morse complex sequence* which aims to encode the entire sequence. Our formulation will be purely algebraic in nature.

Generating families provide the geometric motivation for our definition of an MCS and for the definition of the equivalence relation on MCSs. However, we will not work explicitly with generating families. Instead, we derive algebraic and combinatorial objects from generating families and work with those instead. Indeed, there are no proofs in this thesis involving generating families.

Throughout this chapter we will work with a fixed front projection Σ with Maslov potential μ. We begin by defining the chain complexes that make up a Morse complex sequence.

[2]See Section 1.4 for a discussion of the origins of this object.

3.1 Ordered chain complexes

Definition 3.1.1. An *ordered chain complex* is a $\mathbb{Z}_2$ vector space C with ordered basis $y_1 < y_2 < \ldots < y_m$, a $\mathbb{Z}$ grading on $y_1, \ldots, y_m$, denoted $|y_j|$ and a linear map $\partial : C \to C$, that satisfies:

1. $\partial \circ \partial = 0$,
2. $|\partial y_j| = |y_j| - 1$, and
3. $\partial y_j = \sum_{i<j} a_{j,i} y_i$, where $a_{j,i} \in \mathbb{Z}_2$.

We will often think of $y_1, \ldots, y_m$ as the standard basis of row vectors $e_1, \ldots, e_m$ and ∂ as the lower triangular matrix defined by:

$$(\partial)_{j,i} = \begin{cases} a_{j,i} & i < j \\ 0 & i \geq j \end{cases}$$

In this manner, ∂y_j is the vector-matrix multiplication $y_j \partial$ and, by 1. in Definition 3.1.1, $\partial^2 = 0$. Although it is unorthodox to use vector-matrix multiplication, we will see later that the noncommutative structure of the CE-DGA makes this preferable to matrix-vector multiplication. We will also let $\langle \partial y_j | y_i \rangle$ denote the contribution of the generator y_i to the ∂y_j, i.e. $\langle \partial y_j | y_i \rangle = a_{j,i}$. We denote an ordered chain complex by (C, ∂) when the ordered basis and grading are understood.

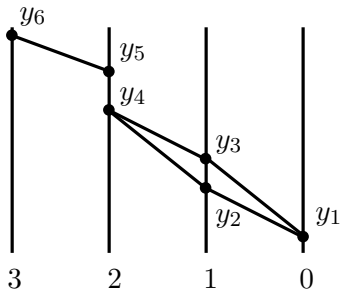

Figure 3.1: The graphical presentation of an ordered chain complex.

In [2], Barannikov encodes an ordered chain complex graphically. For example, let (C, ∂) be an ordered chain complex with ordered generators $y_1 < y_2 < \ldots < y_6$, graded $|y_6| = 3$, $|y_5| = |y_4| = 2$, $|y_3| = |y_2| = 1$, $|y_1| = 0$, and with boundary map ∂ defined by:

- $\partial y_6 = y_5$
- $\partial y_4 = y_3 + y_2$
- $\partial y_3 = \partial y_2 = y_1$
- $\partial y_5 = \partial y_1 = 0$

The graphical representation of (C, ∂) can be seen in Figure 3.1. In this figure, the vertical lines represent the gradings of the generators, the height of the vertices on the vertical lines indicates the ordering of the generators, and the sloped lines connecting vertices represent the boundary map ∂.

As we have seen, ordered chain complexes arise naturally in topology and geometry. If $f : M \to \mathbb{R}$ is a Morse-Smale function with respect to a metric on a compact manifold M, then f induces an ordered chain complex

generated by the critical points $\{y_1, \ldots, y_m\}$ of f, graded by the index of y_j, ordered by the critical values $f(y_1) < \ldots < f(y_m)$, and where $\langle \partial y_j | y_i \rangle$ is the mod 2 count of the gradient flow lines between y_j and y_i.

3.1.1 Useful Matrix Notation

Before going further, we set the matrix notation that will be used throughout this thesis. All of these matrices have entries in $\mathbb{Z}_2$ and all of our matrix operations are done mod $\mathbb{Z}_2$.

1. Suppose $k > l$. We let $\delta_{k,l}$ denote a square matrix with 1 in the (k, l) position and zeros everywhere else.

2. We let $E_{k,l} = I + \delta_{k,l}$ where I denotes the identity matrix. Note that $E_{k,l}^{-1} = E_{k,l}$.

3. We let $P_{i+1,i}$ denote the permutation matrix obtained by interchanging rows i and $i+1$ of the identity matrix. Note that $P_{i+1,i}^{-1} = P_{i+1,i}$.

4. We let J_{i-1} denote the matrix obtained by inserting two columns of zeros after column $i-1$ in the identity matrix. J_{i-1}^T is the transpose of J_{i-1}.

We note a few facts about J_{i-1},J_{i-1}^T, and $E_{k,l}$ matrix. Suppose J_{i-1} is an $m \times (m+2)$ matrix and N is a square matrix of dimension $m+2$. Then:

1. $J_{i-1}N$ removes rows i and $i+1$ from N;

2. NJ_{i-1}^T removes columns i and $i+1$ from N;

3. $E_{k,l}N$ adds row l to row k; and

4. $NE_{k,l}$ add column k to column l.

3.2 Morse complex sequences on Σ

A Morse complex sequence is a set of vertical marks on a front projection Σ along with a sequence of ordered chain complexes. Before giving a precise definition, we would like to ensure that the singularities of Σ are nicely arranged.

Definition 3.2.1. A front projection Σ of a Legendrian knot K is said to be *σ-generic* if:

1. the singularities of Σ are of 3 types:

   (a) left cusps;

   (b) right cusps; and

   (c) transverse intersections of two strands.

2. the x-coordinates of the singularities are all distinct

Every Legendrian knot K can be Legendrian isotoped in an arbitrarily small neighborhood of itself so that Σ is σ-generic.

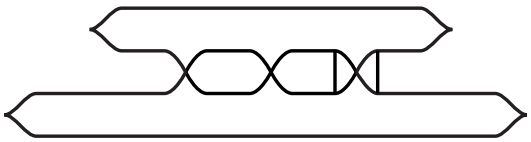

Figure 3.2: A marked front projection.

Definition 3.2.2. A *handleslide mark* on a σ-generic front projection Σ with Maslov potential μ is an arc in the xz-plane with fixed x-coordinate and endpoints on Σ. We require that the arc not intersect the crossings or cusps of Σ. We also require that the end points of a handleslide mark sit on strands of Σ with the same Maslov potential. A *marked front projection* is a σ-generic front projection with a collection of handleslide marks; see Figure 3.2.

The next definition is long, but can be summed up as follows. A *Morse complex sequence* is a marked front projection and a finite sequence of ordered chain complexes $(C_1, \partial_1) \dots (C_m, \partial_m)$ that satisfy:

1. Each vector space in $(C_1, \partial_1) \dots (C_m, \partial_m)$ is generated by the intersection points of a vertical line with the front projection Σ. For C_j, the vertical line γ_j sits to the left of the j^{th} singularity or handleslide mark. The generators are ordered by their z-coordinates and graded by the Maslov potential on the strands.

2. (C_1, ∂_1) has trivial homology. C_1 has only two generators and their gradings differ by one, so requiring that (C_1, ∂_1) has trivial homology uniquely defines ∂_1.

3. ∂_{j+1} is determined by ∂_j and the singularity or handleslide mark between γ_j and γ_{j+1}.

See Figure 3.3 for an example of an MCS. Now for the precise definition.

Definition 3.2.3. Let Σ be a σ-generic front projection with Maslov potential μ. A *Morse complex sequence* $\mathcal{C}$ *on* Σ is a marked front projection and a finite sequence of ordered chain complexes $(C_1, \partial_1) \dots (C_m, \partial_m)$ satisfying the following.

1. Let $x_0, \dots, x_m$ denote the x-coordinates of the crossings, cusps and handleslide marks of the marked front projection and choose $\{t_1, \dots, t_m\} \in \mathbb{R}$ so that $t_j \in (x_{j-1}, x_j)$ for all j. Then C_j is generated by the m_j points of intersection in $\Sigma \cap (\{t_j\} \times \mathbb{R})$. We label the generators $y_1^j, \dots, y_{m_j}^j$ so that $y_1^j < \dots < y_{m_j}^j$ with respect to the z-axis. Each generator is graded by $|y_i^j| = \mu(y_i^j)$.

2. In (C_1, ∂_1), $\partial_1 y_2^1 = y_1^1$ and $\partial_1 y_1^1 = 0$.

3. ∂_{j+1} and ∂_j are related as follows:

   (a) If x_j is a handleslide mark between strands k and l with $k > l$, then the map $\phi_{k,l} : (C_j, \partial_j) \to (C_{j+1}, \partial_{j+1})$ defined by

$$\phi_{k,l}(y_i^j) = \begin{cases} y_i^{j+1} & \text{if } i \neq k \\ y_k^{j+1} + y_l^{j+1} & \text{if } i = k \end{cases} \tag{3.1}$$

is a chain isomorphism. As matrices:

$$\partial_{j+1} = E_{k,l}\partial_j E_{k,l}^{-1} \tag{3.2}$$

(b) If x_j is a crossing between strands $i+1$ and i, then the map $\psi_{i+1} : (C_j, \partial_j) \to (C_{j+1}, \partial_{j+1})$ defined by

$$\psi_{i+1}(y_k^j) = \begin{cases} y_k^{j+1} & \text{if } k \notin \{i, i+1\} \\ y_{i+1}^{j+1} & \text{if } k = i \\ y_i^{j+1} & \text{if } k = i+1 \end{cases} \tag{3.3}$$

is a chain isomorphism. As matrices:

$$\partial_{j+1} = P_{i+1}\partial_j P_{i+1}^{-1} \tag{3.4}$$

(c) Suppose x_j is a left cusp between strands $i+1$ and i and let V be the ordered chain complex generated by y_{i+1}^{j+1} and y_i^{j+1} with differential ∂ defined by $\partial y_{i+1}^{j+1} = y_i^{j+1}$ and $\partial y_i^{j+1} = 0$. Then $C_{j+1} \cong C_j \oplus V$ by the identification of generators given by:

i. $y_k^j \mapsto y_k^{j+1}$ if $k < i$, and

ii. $y_k^j \mapsto y_{k+2}^{j+1}$ if $k \geq i$.

The differential ∂_{j+1} is the direct sum of ∂ and the extension of ∂_j by the identification of generators given above. As matrices, ∂_{j+1} is obtained from ∂_j by inserting two rows (columns) of zeros after row (column) $i-1$ in ∂_j and then changing the $(i+1, i)$ entry to 1.

(d) If x_j is a right cusp between strands $i+1$ and i, then $(C_{j+1}, \partial_{j+1})$ is chain isomorphic to the quotient of $(C_{j+1}, \partial_{j+1})$ by the subcomplex generated by $\{y_{i+1}^j, \partial_j y_{i+1}^j\}$. The matrix ∂_{j+1} is computed explicitly as follows. (We have dropped the j superscripts in the following computation so that it is easier to read.)

i. Let $y_{i+1} < y_{u_1} < y_{u_2} < \ldots < y_{u_s}$ denote the generators of C_j satisfying $\langle \partial_j y | y_i \rangle = 1$;

ii. Let $y_{v_r} < \ldots < y_{v_1} < y_i$ denote the generators of C_j satisfying $\langle \partial y_{i+1} | y \rangle = 1$; and

iii. Let $E = E_{i,v_r} \ldots E_{i,v_1} E_{u_1,i+1} \ldots E_{u_s,i+1}$.

Then, as matrices:

$$\partial_{j+1} = J_{i-1} E \partial_j E^{-1} J_{i-1}^T \tag{3.5}$$

We write $\mathcal{C} = (C_1, \partial_1) \ldots (C_m, \partial_m)$ and let $\mathcal{C}$ denote both the marked

front projection and the finite sequence of ordered chain complexes. We will say (C_j, ∂_j) is the ordered chain complex *associated to* the crossing, cusp or handleslide mark x_{j-1}.

The situation at a right cusp is the most complex. Let us dissect what is going on in the matrix equation $\partial_{j+1} = J_{i-1} E \partial_j E^{-1} J_{i-1}^T$. The equation $E\partial_j E^{-1}$ represents a series of handleslide moves on the chain complex (C_j, ∂_j). After the handleslide move $E_{u_s,i+1}$, y_i no longer appears in $\partial_j y_{u_s}$. In fact, each handleslide $E_{u_j,i+1}$ removes y_i from $\partial_j y_{u_i}$. These moves may change the differential in other ways, but we concentrate only on how they effect y_{i+1} and y_i. After the series of handleslides $E_{u_1,i+1} \dots E_{u_s,i+1}$, y_i only appears in $\partial_j y_{i+1}$. Each of the handleslides in $E_{i,v_r} \dots E_{i,v_1}$ simplifies $\partial_j y_{i+1}$ by removing the terms y_{v_j}. Thus, in $E\partial_j E^{-1}$, $\partial_j y_{i+1} = y_i$ and y_i appears in no other $\partial_j y_k$. Thus the generators y_{i+1} and y_i form an acyclic subcomplex. Conjugating $E\partial E^{-1}$ by J_{i-1} has the effect of quotienting out this subcomplex. As matrices, conjugating by J_{i-1} removes rows and columns $i+1$ and i from $E\partial_j E^{-1}$. This process is detailed in Figure 3.4.

Remark 3.2.4. We note the following:

1. In an MCS, the vector spaces and differentials in $(C_1, \partial_1) \dots (C_m, \partial_m)$ do not depend on the set $\{t_1, \dots, t_m\}$ chosen in Condition 1. of Definition 3.2.3.

2. It follows from Definition 3.2.3 that at a right cusp x_j between strands $i+1$ and i, $\langle \partial_j y_{i+1}^j | y_i^j \rangle = 1$ and at a crossing x_j, between strands $i+1$

and i, $\langle \partial_j y^j_{i+1} | y^j_i \rangle = 0$.

3. Not every marked front projection is associated with an MCS. As we will see, an MCS determines a graded normal ruling of the front diagram and every graded normal ruling determines at least one MCS. If Σ does not admit a graded normal ruling, which is certainly possible, then Σ does not admit an MCS.

4. If a marked front projection is part of an MCS, then the sequence $(C_1, \partial_1) \dots (C_m, \partial_m)$ may be reconstructed from the marked front projection using Conditions 1. - 3. of Definition 3.2.3. Thus, a marked front projection may be associated with at most one MCS.

Proposition 3.2.5. In an MCS $\mathcal{C}$, the homologies of (C_j, ∂_j) and $(C_{j+1}, \partial_{j+1})$ are isomorphic. Thus by Condition 2. of Definition 3.2.3, all of the homologies in $\mathcal{C}$ are trivial.

Proof. In the case of a handleslide or crossing, the matrices $E_{k,l}$ and $P_{i+1,i}$ are invertible so they give chain isomorphisms between (C_j, ∂_j) and $(C_{j+1}, \partial_{j+1})$, hence the homologies of (C_j, ∂_j) and $(C_{j+1}, \partial_{j+1})$ are isomorphic.

In the case of a left cusp, $(C_{j+1}, \partial_{j+1})$ is obtained by direct summing an acyclic chain complex with (C_j, ∂_j). Thus the homologies of (C, ∂) and (C', ∂') are isomorphic.

In the case of move 3, we noted above that the equation $J_{i-1} E \partial E^{-1} J^T_{i-1}$ quotients out an acyclic subcomplex. Thus the homologies of (C_j, ∂_j) and $(C_{j+1}, \partial_{j+1})$ are isomorphic. □

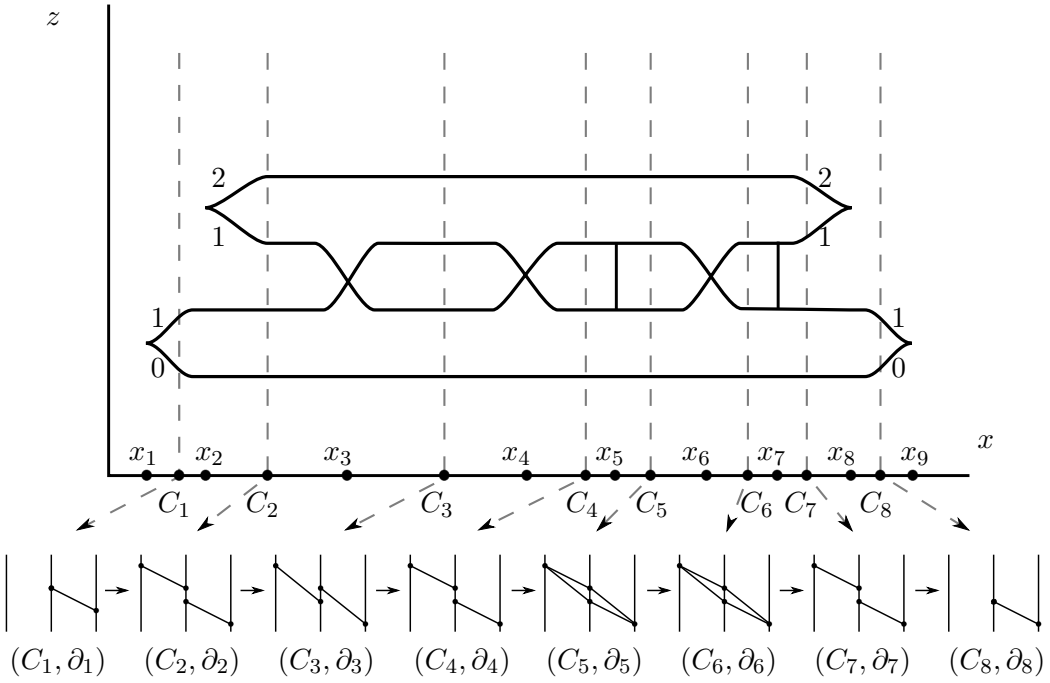

Figure 3.3: An example of an MCS on a σ-generic front projection of a Legendrian trefoil. This MCS includes handleslide marks between C_4 and C_5 and between C_6 and C_7. In both cases, the handleslide occurs between the two generators of index 1.

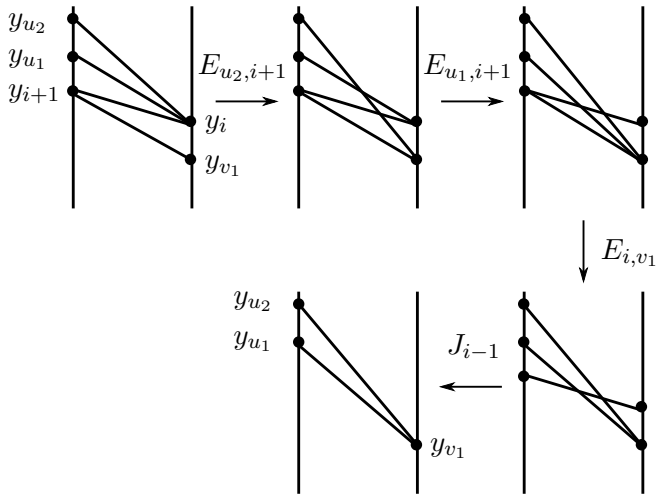

Figure 3.4: The sequence of matrix moves occurring at a right cusp. We concentrate on how the generators y_{i+1} and y_i are effected and do not display the entire ordered chain complex.

3.3 An Equivalence Relation on $MCS(\Sigma)$

Let $MCS(\Sigma)$ denote the set of all MCS's on Σ. In this section, we describe a set of local moves, called *MCS moves*[3], that we use to form an equivalence relation on $MCS(\Sigma)$. We will call two MCSs $\mathcal{C}$ and $\mathcal{C}'$ *equivalent* and write $\mathcal{C} \sim \mathcal{C}'$ if they are related by a finite sequence of MCS moves. As we noted in part 4 of Remark 3.2.4, the chain complexes in an MCS are completely determined by its associated marked front projection. Thus, MCS moves are defined as graphical changes in the handleslide marks of $\mathcal{C}$. We will verify that each equivalence move leaves the ordered chain complexes of $\mathcal{C}$ unchanged outside of the region in which the move takes place.

All of these moves are geometrically motivated from the theory of generating families. Suppose a Legendrian knot K admits a LQ generating family $F : \mathbb{R} \times \mathbb{R}^k \to \mathbb{R}$ and g is a metric on the domain $\mathbb{R} \times \mathbb{R}^k$. If F and g are suitably generic, then we have a one-parameter family of function/metric pairs (F_x, g_x) giving a sequence of Morse-Smale chain complexes (C_x, ∂_x, g_x). Now consider fixing the function F and evolving the metric g through a one-parameter family so that we have a two-parameter family of function/metric pairs (F_x, g_x^t). If the one-parameter families (F_x, g_x^0) and (F_x, g_x^1) are both suitably generic, then we would like to understand how the sequences (C_x, ∂_x, g_x^0) and (C_x, ∂_x, g_x^1) are related. In [20], Hatcher and Wagoner describe possible relationships between (C_x, ∂_x, g_x^0) and (C_x, ∂_x, g_x^1).

[3]See Section 1.4 for a discussion of the origins of these moves.

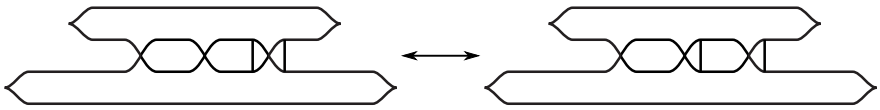

Figure 3.5: MCS equivalence move 0.

The resulting relationships directly motivate the MCS moves we define.

The first MCS move, denoted *MCS move 0*, is to allow handleslide marks to slide left and right along the strands of Σ without moving past other handleslide marks or singularities. An example of this move is seen in Figure 3.5.

The other moves are given in Figures 3.6, 3.7, and 3.8. In each figure, we have only drawn the strands of Σ that are involved in the equivalence move. Other strands may exist between those drawn, but we assume that no other crossings, cusps or handleslides appear.

The move in Figure 3.8, which we call the *Explosion move*, requires explanation. Suppose (C, ∂) is an ordered chain complex with generating set $y_1 < \ldots < y_m$ and a pair of generators $y_l < y_k$ such that $|y_l| = |y_k| + 1$. Let $y_{u_1} < y_{u_2} < \ldots < y_{u_s}$ denote the generators of C_j satisfying $\langle \partial y | y_k \rangle = 1$; see the left three arrows in Figure 3.8. Let $y_{v_r} < \ldots < y_{v_1} < y_i$ denote the generators of C_j appearing in $\partial_j y_l$; see the right two arrows in Figure 3.8. Let $E = E_{k,v_r} \ldots E_{k,v_1} E_{u_1,l} \ldots E_{u_s,l}$. Then over $\mathbb{Z}_2$, the following formula holds:

$$\partial = E \partial E^{-1}. \tag{3.6}$$

The MCS equivalence move in Figure 3.8 says that we can either introduce

or remove the handleslides represented by E. The handleslide marks may be added in any order since they commute past each other using the moves defined in Figure 3.6. We note that this may add many more chain complexes to an MCS, however, Equation 3.6 implies that this change in $\mathcal{C}$ is local in the sense that it does not change any of the other chain complexes in $\mathcal{C}$. The next proposition shows that all of the MCS moves are local in this sense.

Geometrically, the Explosion move is the result of a flow line flowing from a critical point of index i to a critical point of index $i+1$ in the two-parameter evolution of function/metric pairs (F_x, g_x^t) described above.

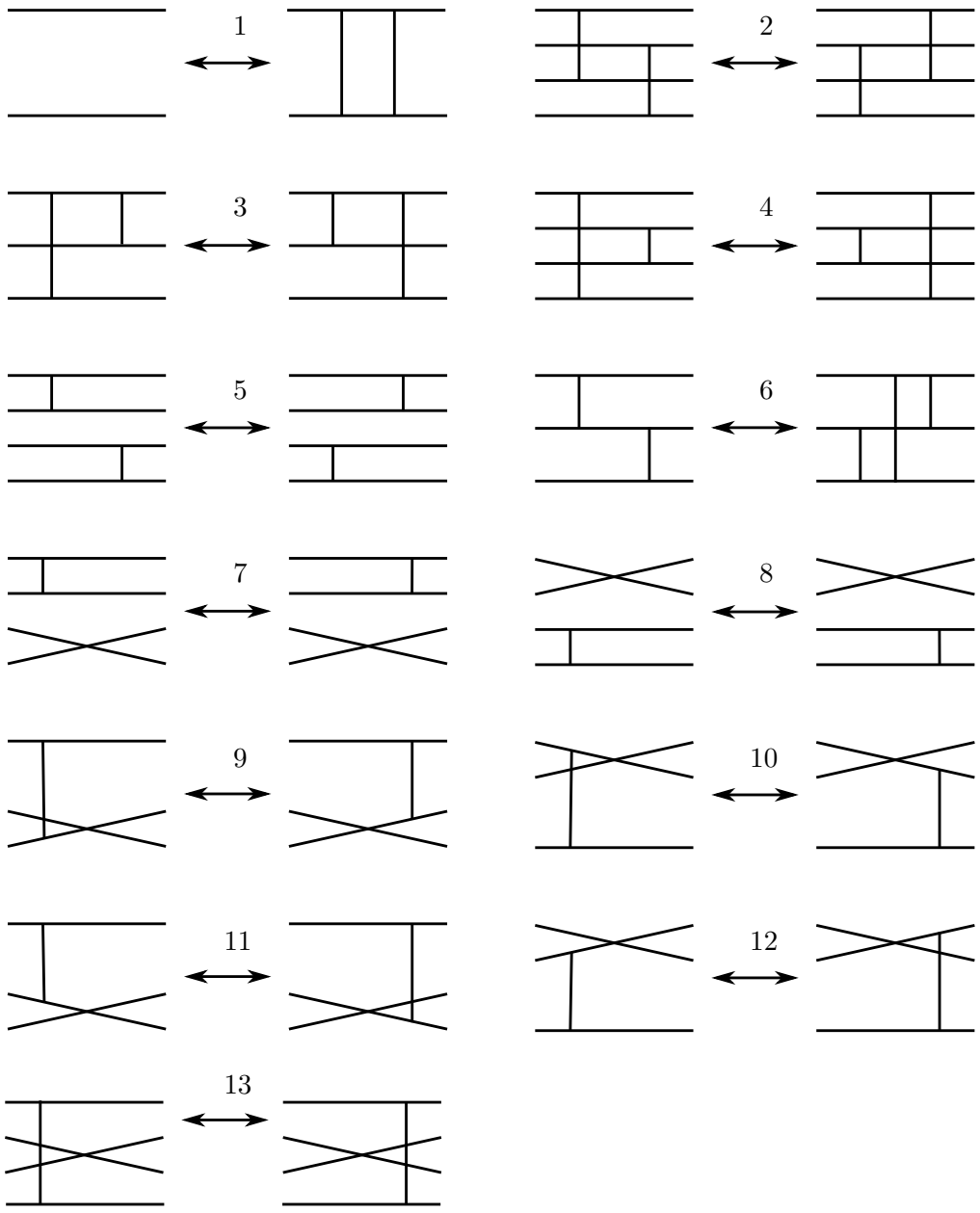

Figure 3.6: MCS equivalence moves 1 - 13. We also allow the horizontal reflection of moves 3 and 6.

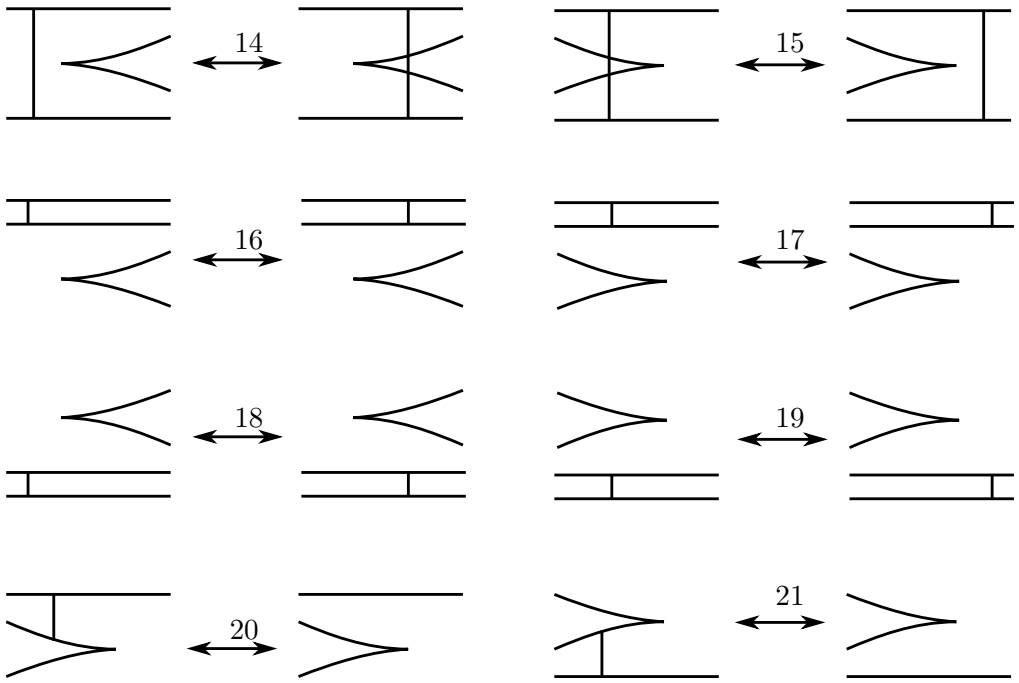

Figure 3.7: MCS equivalence moves 14 - 21.

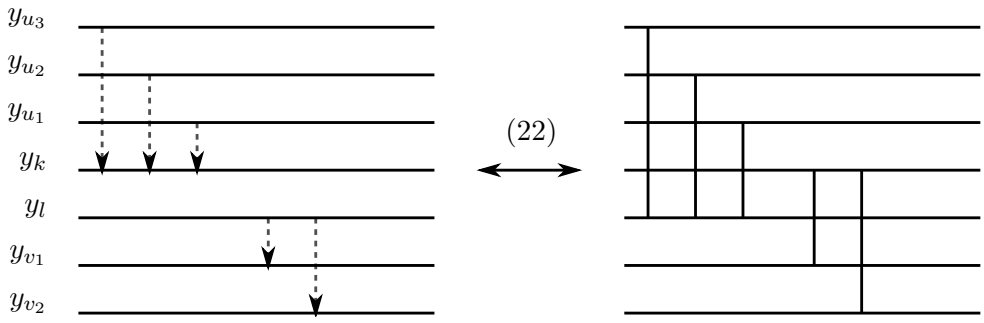

Figure 3.8: MCS equivalence move 22. Also known as the Explosion Move.

Proposition 3.3.1. Suppose $\mathcal{C} = (C_1, \partial_1) \dots (C_m, \partial_m)$ is an MCS on Σ and that in the interval $[a, b]$ of the x-axis we modify the marked front projection of $\mathcal{C}$ by one of the local moves in Figures 3.6, 3.7, or 3.8. Then the resulting marked front projection $\mathcal{C}'$ is an MCS. In addition, the ordered chain complexes of $\mathcal{C}$ and $\mathcal{C}'$ agree outside of the interval $[a, b]$.

Proof. For each MCS move in Figures 3.6 and 3.7 there are two directions to check. They correspond to the two directions of the double arrow in each figure. In the argument below, we begin by checking the left-to-right case. The right-to-left cases follows by a similar argument.

Let $x_0 < \dots < x_m$ denote the x-coordinates of the crossings, cusps and handleslide marks of $\mathcal{C}$ and let $y_0 < \dots < y_n$ denote the x-coordinates of the crossings, cusps and handleslide marks of $\mathcal{C}'$. Since $\mathcal{C}$ and $\mathcal{C}'$ have the same handleslide marks outside of $[a, b]$, we know that $\{x_0, \dots, x_m\}$ and $\{y_0, \dots, y_n\}$ agree outside of $[a, b]$.

In order to show that $\mathcal{C}'$ is an MCS, we need to define a sequence of ordered chain complexes $(C'_1, \partial'_1) \dots (C'_n, \partial'_n)$ that satisfies Conditions 1. - 3. of Definition 3.2.3.

Let x_{j-1} denote the largest element of $\{x_0, \dots, x_m\}$ that is smaller than a. We note that for all $0 < i < j$, $x_i = y_i$ and x_i and y_i represent the same crossing, cusp or handleslide mark in both $\mathcal{C}$ and $\mathcal{C}'$. We define $(C'_i, \partial'_i) = (C_i, \partial_i)$ for all $1 < i \leq j$. Since $\mathcal{C}$ is an MCS, we know that $(C_1, \partial_1) \dots (C_j, \partial_j)$ satisfies Conditions 1. - 3. and hence so do $(C'_1, \partial'_1) \dots (C'_j, \partial'_j)$.

Now let x_τ denote the smallest element of $\{x_{j+1}, \dots, x_m\}$ that is larger

than b and let y_ρ denote the smallest element of $\{y_{j+1}, \ldots, y_n\}$ that is larger than b. Note that $x_\tau < \ldots < x_m$ and $y_\rho < \ldots < y_n$ represent the same crossings, cusps and handleslide marks in $\mathcal{C}$ and $\mathcal{C}'$. Let $\gamma : \{\rho, \ldots, n\} \to \{\tau, \ldots, m\}$ be the bijection defined by: $x_k = y_l$ if and only if $\gamma(l) = k$. We define $(C'_i, \partial'_i) = (C_{\gamma(i)}, \partial_{\gamma(i)})$ for all $i > \rho$. Since $\mathcal{C}$ is an MCS, we know that $(C_\tau, \partial_\tau) \ldots (C_m, \partial_m)$ satisfies Conditions 1. - 3. and hence so do $(C'_{\rho+1}, \partial'_{\rho+1}) \ldots (C'_n, \partial'_n)$.

We are left to define (C'_i, ∂'_i) for all $j < i < \rho$. We use (C'_j, ∂'_j) and Condition 3. to build (C'_i, ∂'_i) inductively from $i = j + 1$ to $i = \rho$. In order for the entire sequence $(C'_1, \partial'_1) \ldots (C'_n, \partial'_n)$ to satisfy Conditions 1. - 3., we must show that the ordered chain complex $(C'_\rho, \partial'_\rho)$ defined by this inductive argument agrees with (C_τ, ∂_τ) so that the three sequences we have defined, namely $(C'_1, \partial'_1) \ldots (C'_j, \partial'_j)$, $(C'_{j+1}, \partial'_{j+1}) \ldots (C'_\rho, \partial'_\rho)$ and $(C'_{\rho+1}, \partial'_{\rho+1}) \ldots (C'_n, \partial'_n)$, fit together correctly.

In each of the cases below, we show that the ordered chain complex $(C'_\rho, \partial'_\rho)$ built inductively from (C'_j, ∂'_j) and Condition 3. is equal to (C_τ, ∂_τ). We know that the vector spaces C'_ρ and C_τ have the same generating set as described by Condition 1., hence, we only need to show that $\partial'_\rho = \partial_\tau$. As we will see, this task is really an exercise in working with simple matrices.

Move 1:

Suppose the handleslide marks that are introduced occur between strands k and l with $k > l$. Then $\mathcal{C}$ and $\mathcal{C}'$ look like:

$$\mathcal{C}: \ \ldots \longrightarrow (C_j, \partial_j) \longrightarrow \ldots$$

$$\mathcal{C}': \ \ldots \longrightarrow (C'_j, \partial'_j) \xrightarrow{E_{k,l}} (C'_{j+1}, \partial'_{j+1}) \xrightarrow{E_{k,l}} (C'_{j+2}, \partial'_{j+2}) \longrightarrow \ldots$$

We must show that $\partial'_{j+2} = \partial_j$. This follows immediately from the fact that $E_{k,l}E_{k,l} = I$ and $\partial_j = \partial'_j$. The right-to-left case follows similarly.

Moves 2 - 5:

Suppose one handleslide mark occurs between strands k_1 and l_1 with $k_1 > l_1$ and the other occurs between strands k_2 and l_2 with $k_2 > l_2$. Suppose also that $k_1 \neq l_2$ and $k_2 \neq l_1$. Then $\mathcal{C}$ and $\mathcal{C}'$ look like:

$$\mathcal{C}: \ \ldots \longrightarrow (C_j, \partial_j) \xrightarrow{E_{k_1,l_1}} (C_{j+1}, \partial_{j+1}) \xrightarrow{E_{k_2,l_2}} (C_{j+2}, \partial_{j+2}) \longrightarrow \ldots$$

$$\mathcal{C}': \ \ldots \longrightarrow (C'_j, \partial'_j) \xrightarrow{E_{k_2,l_2}} (C'_{j+1}, \partial'_{j+1}) \xrightarrow{E_{k_1,l_1}} (C'_{j+2}, \partial'_{j+2}) \longrightarrow \ldots$$

We must show that $\partial'_{j+2} = \partial_{j+2}$. This follows immediately from the fact that $E_{k_1,l_1}E_{k_2,l_2} = E_{k_2,l_2}E_{k_1,l_1}$ and $\partial_j = \partial'_j$. The right-to-left case follows similarly. This argument also verifies that the horizontal reflection of MCS move 3 is a valid move.

Move 6:

Suppose the strands involved in the handleslide marks of this move are numbered $a > b > c$. Then $\mathcal{C}$ and $\mathcal{C}'$ look like:

$$\mathcal{C}: \ \ldots \longrightarrow (C_j, \partial_j) \xrightarrow{E_{a,b}} (C_{j+1}, \partial_{j+1}) \xrightarrow{E_{b,c}} (C_{j+2}, \partial_{j+2}) \longrightarrow \ldots$$

$$\mathcal{C}': \ \ldots \longrightarrow (C'_j, \partial'_j) \xrightarrow{E_{b,c}} (C'_{j+1}, \partial'_{j+1}) \xrightarrow{E_{a,c}} (C'_{j+2}, \partial'_{j+2}) \xrightarrow{E_{a,b}} (C'_{j+3}, \partial'_{j+3}) \longrightarrow \ldots$$

We must show that $\partial'_{j+3} = \partial_{j+2}$. This follows immediately from the fact that $E_{a,b}E_{b,c} = E_{b,c}E_{a,c}E_{a,b}$ and $\partial_j = \partial'_j$. The right-to-left case follows similarly. This argument also verifies that the horizontal reflection of MCS Move 6 is a valid move.

Moves 7, 8, and 13:

Suppose the handleslide mark occurs between strands k and l with $k > l$ and the crossing occurs between strands $i+1$ and i. Suppose also that $k, l \notin \{i+1, i\}$. Then $\mathcal{C}$ and $\mathcal{C}'$ look like:

$$\mathcal{C}: \ \ldots \longrightarrow (C_j, \partial_j) \xrightarrow{E_{k,l}} (C_{j+1}, \partial_{j+1}) \xrightarrow{P_{i+1,i}} (C_{j+2}, \partial_{j+2}) \longrightarrow \ldots$$

$$\mathcal{C}': \ \ldots \longrightarrow (C'_j, \partial'_j) \xrightarrow{P_{i+1,i}} (C'_{j+1}, \partial'_{j+1}) \xrightarrow{E_{k,1}} (C'_{j+2}, \partial'_{j+2}) \longrightarrow \ldots$$

We must show that $\partial'_{j+2} = \partial_{j+2}$. This follows immediately from the fact that $E_{k,l}P_{i+1,i} = P_{i+1,i}E_{k,l}$ and $\partial_j = \partial'_j$. The right-to-left case follows similarly.

Move 9:

Suppose the handleslide mark occurs between strands k and i with $k > i$

and the crossing occurs between strands $i+1$ and i. Suppose also that $k \neq i+1$. Then $\mathcal{C}$ and $\mathcal{C}'$ look like:

$$\mathcal{C}: \ \ldots \longrightarrow (C_j, \partial_j) \xrightarrow{E_{k,i}} (C_{j+1}, \partial_{j+1}) \xrightarrow{P_{i+1,i}} (C_{j+2}, \partial_{j+2}) \longrightarrow \ldots$$

$$\mathcal{C}': \ \ldots \longrightarrow (C'_j, \partial'_j) \xrightarrow{P_{i+1,i}} (C'_{j+1}, \partial'_{j+1}) \xrightarrow{E_{k,i+1}} (C'_{j+2}, \partial'_{j+2}) \longrightarrow \ldots$$

We must show that $\partial'_{j+2} = \partial_{j+2}$. This follows immediately from the fact that $E_{k,i}P_{i+1,i} = P_{i+1,i}E_{k,i+1}$ and $\partial_j = \partial'_j$. The right-to-left case follows similarly.

Move 10:

Suppose the handleslide mark occurs between strands $i+1$ and l with $i+1 > l$ and the crossing occurs between strands $i+1$ and i. Suppose also that $l \neq i$. Then $\mathcal{C}$ and $\mathcal{C}'$ look like:

$$\mathcal{C}: \ \ldots \longrightarrow (C_j, \partial_j) \xrightarrow{E_{i+1,l}} (C_{j+1}, \partial_{j+1}) \xrightarrow{P_{i+1,i}} (C_{j+2}, \partial_{j+2}) \longrightarrow \ldots$$

$$\mathcal{C}': \ \ldots \longrightarrow (C'_j, \partial'_j) \xrightarrow{P_{i+1,i}} (C'_{j+1}, \partial'_{j+1}) \xrightarrow{E_{i,l}} (C'_{j+2}, \partial'_{j+2}) \longrightarrow \ldots$$

We must show that $\partial'_{j+2} = \partial_{j+2}$. This follows immediately from the fact that $E_{i,l}P_{i+1,i} = P_{i+1,i}E_{i+1,l}$ and $\partial_j = \partial'_j$. The right-to-left case follows similarly.

Move 11:

Suppose the handleslide mark occurs between strands k and $i+1$ with $k > i+1$ and the crossing occurs between strands $i+1$ and i. Then $\mathcal{C}$ and $\mathcal{C}'$ look like:

$$\mathcal{C}: \ \ldots \longrightarrow (C_j, \partial_j) \xrightarrow{E_{k,i+1}} (C_{j+1}, \partial_{j+1}) \xrightarrow{P_{i+1,i}} (C_{j+2}, \partial_{j+2}) \longrightarrow \ldots$$

$$\mathcal{C}': \ \ldots \longrightarrow (C'_j, \partial'_j) \xrightarrow{P_{i+1,i}} (C'_{j+1}, \partial'_{j+1}) \xrightarrow{E_{k,i}} (C'_{j+2}, \partial'_{j+2}) \longrightarrow \ldots$$

We must show that $\partial'_{j+2} = \partial_{j+2}$. This follows immediately from the fact that $E_{k,i}P_{i+1,i} = P_{i+1,i}E_{k,i+1}$ and $\partial_j = \partial'_j$. The right-to-left case follows similarly.

Move 12:

Suppose the handleslide mark occurs between strands i and l with $i > l$ and the crossing occurs between strands $i+1$ and i. Then $\mathcal{C}$ and $\mathcal{C}'$ look like:

$$\mathcal{C}: \ \ldots \longrightarrow (C_j, \partial_j) \xrightarrow{E_{i,l}} (C_{j+1}, \partial_{j+1}) \xrightarrow{P_{i+1,i}} (C_{j+2}, \partial_{j+2}) \longrightarrow \ldots$$

$$\mathcal{C}': \ \ldots \longrightarrow (C'_j, \partial'_j) \xrightarrow{P_{i+1,i}} (C'_{j+1}, \partial'_{j+1}) \xrightarrow{E_{i+1,l}} (C'_{j+2}, \partial'_{j+2}) \longrightarrow \ldots$$

We must show that $\partial'_{j+2} = \partial_{j+2}$. This follows immediately from the fact that $E_{i+1,l}P_{i+1,i} = P_{i+1,i}E_{i,l}$ and $\partial_j = \partial'_j$. The right-to-left case follows similarly.

Move 14, 16, and 18:

Suppose the handleslide mark occurs between strands k and l in the left-hand picture and between strands k' and l' in the right-hand picture. Recall that the numbering of the strands before the cusp is different than the numbering of the strands after the cusp. Suppose the left cusp occurs just above strand i. Then $\mathcal{C}$ and $\mathcal{C}'$ look like:

$$\mathcal{C}: \quad \ldots \longrightarrow (C_j, \partial_j) \xrightarrow{E_{k,l}} (C_{j+1}, \partial_{j+1}) \xrightarrow{B_i} (C_{j+2}, \partial_{j+2}) \longrightarrow \ldots$$

$$\mathcal{C}': \quad \ldots \longrightarrow (C'_j, \partial'_j) \xrightarrow{B_i} (C'_{j+1}, \partial'_{j+1}) \xrightarrow{E_{k',l'}} (C'_{j+2}, \partial'_{j+2}) \longrightarrow \ldots$$

In the diagram above, B_i indicates the transition across a left cusp above strand i. We must show that $\partial'_{j+2} = \partial_{j+2}$. Since the handleslide does not involve the acyclic subcomplex introduced at a left cusp, we can either handleslide before the acyclic subcomplex is introduced or after, thus $\partial'_{j+2} = \partial_{j+2}$. The right-to-left case follows similarly.

Move 15, 17, and 19:

Suppose the handleslide mark occurs between strands k and l in the left-hand picture and between strands k' and l' in the right-hand picture. Recall that the numbering of the strands before the cusp is different than the numbering of the strands after the cusp. Suppose the right cusp occurs between strands $i+1$ and i. Then $\mathcal{C}$ and $\mathcal{C}'$ look like:

$$\mathcal{C}: \quad \ldots \longrightarrow (C_j, \partial_j) \xrightarrow{E_{k,l}} (C_{j+1}, \partial_{j+1}) \xrightarrow{D_i} (C_{j+2}, \partial_{j+2}) \longrightarrow \ldots$$

$$\mathcal{C}': \quad \ldots \longrightarrow (C'_j, \partial'_j) \xrightarrow{D_i} (C'_{j+1}, \partial'_{j+1}) \xrightarrow{E_{k',l'}} (C'_{j+2}, \partial'_{j+2}) \longrightarrow \ldots$$

In the diagram above, D_i indicates a transition past a right cusp between strands $i+1$ and i. We must show that $\partial'_{j+2} = \partial_{j+2}$. Since the handleslide does not involve the acyclic subcomplex quotiented out during a transition past a right cusp, we can either handleslide before it is quotiented out or after, thus $\partial'_{j+2} = \partial_{j+2}$. The right-to-left case follows similarly.

In terms of matrix computations, this follows from the following argument. Note that if the handleslide matrix $E_{k,l}$ has dimension p then $E_{k',l'}$ has dimension $p-2$. The equality $\partial'_{j+2} = \partial_{j+2}$ follows immediately from the following:

1. $E_{k',l'} J_{i-1} = J_{i-1} E_{k,l}$,
2. $J_{i-1}^T E'^{-1}_{k',l} = E_{k,l}^{-1} J_{i-1}^T$, and
3. $E_{k,l}$ commutes with each of the handleslides appearing in $E = E_{i,v_r} \ldots E_{i,v_1} E_{u_1,i+1} \ldots E_{u_s,i+1}$.

Thus:

$$\begin{aligned}
\partial'_{j+2} &= E_{k',l'}\partial'_{j+1}E^{-1}_{k',l'} \\
&= E_{k',l'}J_{i-1}E\partial'_jE^{-1}J^T_{i-1}E^{-1}_{k',l'} \\
&= E_{k',l'}J_{i-1}E\partial_jE^{-1}J^T_{i-1}E^{-1}_{k',l'} \\
&= J_{i-1}EE_{k,l}\partial_jE^{-1}_{k,l}E^{-1}J^T_{i-1} \\
&= J_{i-1}E\partial_{j+1}E^{-1}J^T_{i-1} \\
&= \partial_{j+2}
\end{aligned}$$

Move 20:

Suppose the handleslide mark occurs between strands k and $i+1$ with $k > i+1$ and the right cusp occurs between strands $i+1$ and i. Then $\mathcal{C}$ and $\mathcal{C}'$ look like:

$$\mathcal{C}: \quad \ldots \longrightarrow (C_j, \partial_j) \xrightarrow{E_{k,i+1}} (C_{j+1}, \partial_{j+1}) \xrightarrow{D_i} (C_{j+2}, \partial_{j+2}) \longrightarrow \ldots$$

$$\mathcal{C}': \quad \ldots \longrightarrow (C'_j, \partial'_j) \xrightarrow{D'_i} (C'_{j+1}, \partial'_{j+1}) \longrightarrow \ldots$$

In the diagram above, D_i and D'_i indicate transitions past a right cusp between strands $i+1$ and i. Let E represent the sequence of handleslide moves appearing in the formula for ∂_{j+2} as described in Condition 3c of Definition 3.2.3. Let F denote the corresponding sequence of handleslide moves in the formula for ∂'_{j+1}. We must show that $\partial'_{j+1} = \partial_{j+2}$.

The handleslide move $E_{k,i+1}$ occurring between (C_j, ∂_j) and $(C_{j+1}, \partial_{j+1})$ flips the parity of entry (k, i) between matrices ∂_j and ∂_{j+1}. Hence, the matrices ∂'_j and ∂_{j+1} differ at entry (k, i). Thus, if $E_{k,i+1}$ appears in F then it does not appear in E and, vice versa, if $E_{k,i+1}$ does not appear in F then it does appear in E. Either way, $F = EE_{k,i+1}$ and so

$$\begin{aligned}
\partial'_{j+1} &= J_{i-1}F\partial'_j F^{-1}J_{i-1}^T \\
&= J_{i-1}EE_{k,i+1}\partial_j E_{k,i+1}^{-1}E^{-1}J_{i-1}^T \\
&= J_{i-1}E\partial_{j+1}E^{-1}J_{i-1}^T \\
&= \partial_{j+2}
\end{aligned}$$

The right-to-left case follows similarly as does the case of Move 21.

Move 22 (Explosion Move):

The localness of the Explosion Move was detailed in the discussion surrounding Equation 3.6.

□

We let $\widehat{MCS}(\Sigma)$ denote the equivalence classes of $MCS(\Sigma)/\sim$ and let $[\mathcal{C}]$ denote an equivalence class in $\widehat{MCS}(\Sigma)$.

3.4 Associating a Normal Ruling to an MCS

The geometric motivation for a graded normal ruling on Σ comes from examining the one-parameter family of Morse chain complexes that result from a generating family F for Σ. The graded normal ruling invariant encodes a pairing of critical points in each of the Morse chain complexes. In this section we show how to associate a graded normal ruling to an MCS.

Definition 3.4.1 ([2])**.** An ordered chain complex (C, ∂) with generators $y_1, \ldots, y_m$ is in *simple form* if for all i either $\partial y_i = 0$ or there exists some j such that $\partial y_i = y_j$.

Lemma 3.4.2 ([2])**.** Let (C, ∂) be an ordered chain complex. Then after a series of handleslide moves we can reduce (C, ∂) to simple form. In addition, this simple form is unique.

It should be noted that Lemma 3.4.2 arises in the work of J.H.C. Whitehead in the 1930's.

Remark 3.4.3. The following two observations follow directly from Lemma 3.4.2.

1. If two ordered chain complexes (C, ∂) and (C', ∂') are chain isomorphic by a handleslide move, i.e. $\partial = E_{k,l}\partial' E_{k,l}^{-1}$, then the uniqueness result in Lemma 3.4.2 implies that they have the same simple form.

2. If in an ordered chain complex (C, ∂), two consecutive generators y_{j+1} and y_j satisfy $\langle \partial y_{j+1} | y_j \rangle = 1$, then a handleslide move applied to the

matrix ∂ will not change the parity of entry $(j+1, j)$. So in the simple form of (C, ∂), y_{j+1} and y_j must be paired.

Definition 3.4.4. Suppose (C, ∂) is an ordered chain complex with generators $y_1, \ldots, y_m$ and trivial homology. By Lemma 3.4.2, there exists a fixed-point free involution $\tau : \{1, \ldots, m\} \to \{1, \ldots, m\}$ that satisfies: In the simple form of (C, ∂), for all i either $\partial y_i = y_{\tau(i)}$ or $\partial y_{\tau(i)} = y_i$. We call τ the *pairing* of (C, ∂) since it pairs the generators $y_1, \ldots, y_m$.

The following lemma assigns a normal ruling to an MCS. In Section 12.4 of [8], Chekanov and Pushkar prove this lemma for a generating family. The notation we set in Lemma 3.4.5 will be used in the proof of Lemma 3.4.6.

Lemma 3.4.5. The pairing determined by the simple forms of the ordered chain complexes in an MCS $\mathcal{C} = (C_1, \partial_1) \ldots (C_m, \partial_m)$ determines a graded normal ruling on Σ.

Proof. By Proposition 3.2.5, the ordered chain complexes appearing in an MCS all have trivial homology, so by Lemma 3.4.2 each (C_i, ∂_i) has a pairing τ_i. We will use these pairings to define a graded normal ruling on Σ.

Let $x_0, \ldots, x_n$ denote the cusps and crossings of $\mathcal{C}$ such that $x_0 < \ldots < x_n$. In each open interval (x_{i-1}, x_i), choose ρ_i so that $(C_{\rho_i}, \partial_{\rho_i})$ is associated to the crossing or cusp x_{i-1}. Equivalently, $(C_{\rho_i}, \partial_{\rho_i})$ is chosen to be the first ordered chain complex of $\mathcal{C}$ immediately following the singularity x_{i-1}. We define a pairing on the strands of $\Sigma \cap ((x_{i-1}, x_i) \times \mathbb{R})$ using the pairing τ_{ρ_i} of

$(C_{\rho_i}, \partial_{\rho_i})$. In particular, for each $x \in (x_{i-1}, x_i)$ we define the pairing on the points of $\Sigma \cap (\{x\} \times \mathbb{R})$ to be the pairing τ_{ρ_i}.

Suppose (C_k, ∂_k) is another ordered chain complex associated to a crossing, cusp or handleslide mark in $[x_{i-1}, x_i)$, then by the definition of an MCS, $(C_{\rho_i}, \partial_{\rho_i})$ and (C_k, ∂_k) are related by a sequence of handleslide moves. Thus, by part 1 of Remark 3.4.3, $\tau_{\rho_i} = \tau_k$ and so the pairing we defined on the strands of $\Sigma \cap ((x_{i-1}, x_i) \times \mathbb{R})$ is well-defined.

It remains to check that:

1. The two strands entering a left cusp or a right cusp are paired; and

2. The switched crossings are graded and normal.

Suppose that x_{i-1} is a left cusp between strands $j+1$ and j. Then in $(C_{\rho_i}, \partial_{\rho_i})$, $\partial_{\rho_i} y_{j+1} = y_j$. Thus, by part 2 of Remark 3.4.3, y_{j+1} and y_j must be paired in the simple form of $(C_{\rho_i}, \partial_{\rho_i})$. Hence the strands entering the left cusp x_{i-1} must be paired.

If x_i is a right cusp between strands $j+1$ and j, then by part 2 of Remark 3.2.4, the ordered chain complex (C_k, ∂_k) immediately preceding x_i must satisfy $\langle \partial_k y_{j+1} | y_j \rangle = 1$. Thus the matrix ∂_k has a 1 in position $(j+1, j)$. From here the argument follows from part 2 of Remark 3.4.3 as in the case of a left cusp.

Suppose x_i represents a switch. Let α and β denote the two strands meeting at x_i and let γ denote the companion strand of α to the left of the crossing. Then the Maslov potential of α and γ differ by 1 since the

corresponding generators are paired in an ordered chain complex. After the crossing, strand γ is paired with β so the Maslov potential of β and γ differ by 1. Since γ must sit either above or below both α and β, this implies that the Maslov potential of α and β must be the same. Hence the crossing at x_i has grading 0 and the switch at x_i is graded. The fact that all switches are normal follows directly from Lemma 4 in [2].

□

Given an MCS $\mathcal{C}$, we let $N_{\mathcal{C}} \in N(\Sigma)$ denote the graded normal ruling associated to $\mathcal{C}$ by Lemma 3.4.5.

Proposition 3.4.6. If $\mathcal{C}_1 \sim \mathcal{C}_2$ then $N_{\mathcal{C}_1} = N_{\mathcal{C}_2}$.

Proof. We need only check that $N_{\mathcal{C}_1} = N_{\mathcal{C}_2}$ when $\mathcal{C}_1$ and $\mathcal{C}_2$ differ by a single MCS move.

Let $\mathcal{C}_1 = (C_1, \partial_1) \dots (C_m, \partial_m)$ and $\mathcal{C}_2 = (C'_1, \partial'_1) \dots (C'_n, \partial'_n)$. Let $x_0, \dots, x_n$ denote the cusps and crossings of Σ such that $x_0 < \dots < x_n$. Here we allow x_i to refer both to the singularity and its x-coordinate. In each open interval (x_{i-1}, x_i), choose ρ_i so that $(C_{\rho_i}, \partial_{\rho_i})$ is associated to the crossing or cusp x_{i-1}. Similarly, choose σ_i so that $(C'_{\sigma_i}, \partial'_{\sigma_i})$ is associated to x_{i-1}.

As described in the proof of Lemma 3.4.5, $N_{\mathcal{C}_1}$ is defined using the pairings τ_{ρ_i} of $(C_{\rho_i}, \partial_{\rho_i})$ and $N_{\mathcal{C}_2}$ is defined using the pairings τ_{σ_i} of $(C'_{\sigma_i}, \partial'_{\sigma_i})$. In order to show that $N_{\mathcal{C}_1} = N_{\mathcal{C}_2}$, we must show that $\tau_{\rho_i} = \tau_{\sigma_i}$ for all i.

MCS moves 1 - 6 and the Explosion Move: These moves occur away from crossings and cusps. We know from Proposition 3.3.1 that the ordered chain

complexes in $\mathcal{C}_1$ and $\mathcal{C}_2$ are equal outside of the region in which the MCS move is happening. Hence, $(C_{\rho_i}, \partial_{\rho_i}) = (C'_{\sigma_i}, \partial'_{\sigma_i})$ for all i and so $\tau_{\rho_i} = \tau_{\sigma_i}$ for all i.

MCS moves 7 - 19: Let x_{j-1} denote the singularity (either cusp or crossing) involved in the MCS move. By Proposition 3.3.1, $(C_{\rho_i}, \partial_{\rho_i}) = (C'_{\sigma_i}, \partial'_{\sigma_i})$ for all $i \neq j$. Thus we need to show that $\tau_{\rho_j} = \tau_{\sigma_j}$. Note that $(C_{\rho_j}, \partial_{\rho_j})$ and $(C'_{\sigma_j}, \partial'_{\sigma_j})$ are related by a single handleslide move. In particular, if the handleslide appearing in the MCS move is between strands k and l, then $\partial_{\rho_j} = E_{k,l}\partial'_{\sigma_j}E_{k,l}$. Thus $\tau_{\rho_j} = \tau_{\sigma_j}$.

MCS moves 20 and 21: Let x_{j-1} denote the right cusp involved in the MCS move. By Proposition 3.3.1, $(C_{\rho_i}, \partial_{\rho_i}) = (C'_{\sigma_i}, \partial'_{\sigma_i})$ for all i and so $\tau_{\rho_i} = \tau_{\sigma_i}$ for all i.

□

We let $N_{[\mathcal{C}]} \in N(\Sigma)$ denote the graded normal ruling associated to the MCS class $[\mathcal{C}]$.

As noted in the Chapter 1, there are a number of results connecting graded normal rulings and augmentations. In the following chapters, we will explore connections between MCSs and augmentations[4]. In particular, we will find a surjection from the set of MCS classes for a front projection Σ to the set of chain homotopy classes of augmentations on the Ng resolution L_Σ. The next chapter reviews definitions and results concerning morphisms between differential graded algebras. From these, we derive the definition of a chain

[4]See Section 1.4 for a discussion of the origins of these results.

homotopy between augmentations. We also show that the cardinality of the set of chain homotopy classes of augmentations on a Lagrangian projection is a Legendrian knot invariant.

Chapter 4

Chain Homotopy Classes of Augmentations

4.1 Chain homotopy equivalence

Let K be a Legendrian knot in $\mathbb{R}^3$ with Lagrangian projection L. An augmentation $\epsilon \in Aug(L)$ is a chain map between the CE-DGA $(\mathcal{A}(L), \partial)$ and the DGA whose only nonzero chain group is a copy of $\mathbb{Z}_2$ in grading 0 with differential identically zero; see Figure 2.21. We place an equivalence relation on the augmentations in $Aug(L)$ by considering chain homotopic augmentations to be equivalent. We have to be careful when we define a chain homotopy, since our chain groups are algebras and not simply vector spaces. We begin by defining the necessary objects on arbitrary DGAs and then restrict to the case of augmentations and CE-DGAs. Although the CE-DGAs we work with

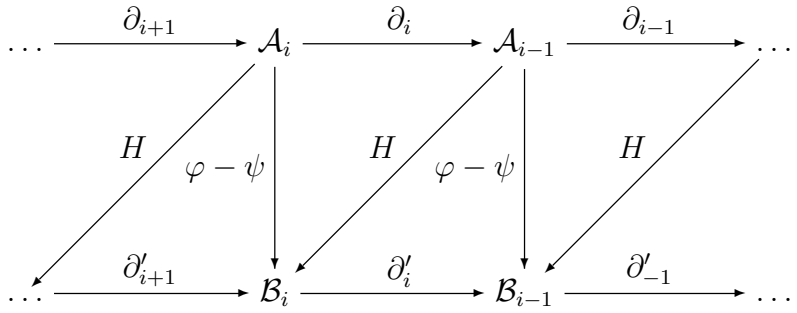

Figure 4.1: A chain homotopy H between DGA morphisms φ and ψ.

are over $\mathbb{Z}_2$ and graded by $\mathbb{Z}$, the following definitions only require that the DGAs be over a commutative ring R and graded by a cyclic group Γ. The definitions and lemmata in this section follow directly from Section 2.3 of [22].

Definition 4.1.1. Let $(\mathcal{A}, \partial)$ and $(\mathcal{B}, \partial')$ be differential graded algebras over a commutative ring R and graded by a cyclic group Γ. A *DGA morphism* $\varphi : (\mathcal{A}, \partial) \to (\mathcal{B}, \partial')$ is an algebra homomorphism satisfying:

1. $|\varphi(a)| = |a|$ for all $a \in \mathcal{A}$, and
2. $\varphi \circ \partial = \partial' \circ \varphi$.

In particular, augmentations are DGA morphisms.

Definition 4.1.2. Let $(\mathcal{A}, \partial)$ and $(\mathcal{B}, \partial')$ be differential graded algebras over a commutative ring R and graded by a cyclic group Γ. Let $\varphi, \psi : (\mathcal{A}, \partial) \to (\mathcal{B}, \partial')$ be DGA morphisms. Then a *chain homotopy between φ and ψ* is a linear map $H : (\mathcal{A}, \partial) \to (\mathcal{B}, \partial')$ satisfying:

1. For all $a \in \mathcal{A}$, $|H(a)| = |a| + 1$,

2. For all $a, b \in \mathcal{A}$, $H(ab) = H(a)\psi(b) + (-1)^{-|a|}\varphi(a)H(b)$, and

3. $\varphi - \psi = H \circ \partial + \partial' \circ H$.

We refer to Condition 2 as the *derivation product property*; see Figure 4.1.

If $(\mathcal{A}, \partial)$ and $(\mathcal{B}, \partial')$ have fixed generating sets, then when constructing chain homotopies between DGA morphisms, we may restrict our attention to the generators of $(\mathcal{A}, \partial)$. The next lemma follows directly from Lemma 2.18 in [22].

Lemma 4.1.3 ([22])**.** Let $(\mathcal{A}, \partial)$ and $(\mathcal{B}, \partial')$ be differential graded algebras over a commutative ring R and graded by a cyclic group Γ with generating sets Q and Q' respectively. Let $\varphi, \psi : (\mathcal{A}, \partial) \to (\mathcal{B}, \partial')$ be DGA morphisms.

If a map $H : Q \to \mathcal{B}$ satisfies $|H(q)| = |q| + 1$ for all $q \in Q$ then H can be uniquely extended by linearity and the derivation product property to a map $H : (\mathcal{A}, \partial) \to (\mathcal{B}, \partial')$ satisfying $|H(a)| = |a| + 1$ for all $a \in \mathcal{A}$.

Moreover, if the extension satisfies $\varphi(q) - \psi(q) = H \circ \partial(q) + \partial' \circ H(q)$ for all $q \in Q$, then $\varphi - \psi = H \circ \partial + \partial' \circ H$ on all of $\mathcal{A}$ and, thus, H is a chain homotopy between φ and ψ.

In the case of augmentations of a CE-DGA $(\mathcal{A}(L), \partial)$, $(\mathcal{B}, \partial')$ is the DGA whose only nonzero chain group is a copy of $\mathbb{Z}_2$ in grading 0 with differential identically zero. So a chain homotopy H is nonzero only on elements of $\mathcal{A}_{-1}$. Since $\partial' = 0$, Condition 3 of Definition 4.1.2 is equivalent to $\epsilon_1 - \epsilon_2 =$

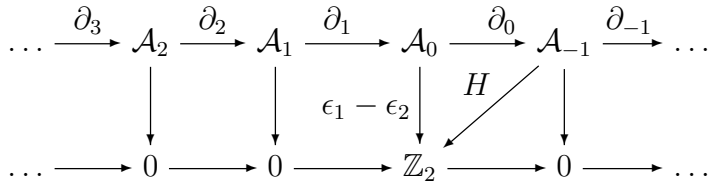

Figure 4.2: A chain homotopy H between augmentations ϵ_1 and ϵ_2.

$H \circ \partial$. $(\mathcal{A}(L), \partial)$ has a fixed generating set $Q = \{q_1, \ldots, q_n\}$ corresponding to the crossings of L. We have the following corollary by combining these observations with Lemma 4.1.3.

Corollary 4.1.4. Let $(\mathcal{A}(L), \partial)$ be the CE-DGA of the Lagrangian projection L with generating set Q and let $\epsilon_1, \epsilon_2 \in Aug(L)$.

If a map $H : Q \to \mathbb{Z}_2$ is nonzero only on generators of grading -1, then H can be uniquely extended by linearity and the derivation product property to a map, also denoted H, on all of $(\mathcal{A}(L), \partial)$ that is nonzero only on elements of grading -1.

Moreover, if the extension satisfies $\varphi(q) - \psi(q) = H \circ \partial(q) + \partial' \circ H(q)$ for all $q \in Q$, then $\varphi - \psi = H \circ \partial + \partial' \circ H$ on all of $\mathcal{A}(L)$ and, thus, H is a chain homotopy between ϵ_1 and ϵ_2.

We say ϵ_1 and ϵ_2 are *chain homotopic* and write $\epsilon_1 \simeq \epsilon_2$ if a chain homotopy H exists between ϵ_1 and ϵ_2.

Lemma 4.1.5 ([15])**.** $\simeq$ is an equivalence relation.

We let $[\epsilon]$ denote the chain homotopy class of ϵ in $Aug^{ch}(L) := Aug(L) / \simeq$.

4.2 Stable tame isomorphism classes of CE-DGAs

In the case of the CE-DGA, the number of chain homotopy classes is a Legendrian invariant.

Proposition 4.2.1. If L and L' are Lagrangian projections of Legendrian isotopic knots K and K', then there is a bijection between $Aug^{ch}(L)$ and $Aug^{ch}(L')$.

Proof. By Theorem 2.3.19, $(\mathcal{A}(L), \partial)$ and $(\mathcal{A}(L'), \partial')$ are tame isomorphic after a finite sequence of stabilizations on each CE-DGA. A tame isomophism is a composition of the elementary isomorphisms defined in Definition 2.3.15, thus we need only consider the case of a single elementary isomorphism and a single stabilization. Let $(\mathcal{A}, \partial)$ and $(\mathcal{B}, \partial')$ be DGAs over $\mathbb{Z}_2$, graded by $\mathbb{Z}$, with generating sets $Q = \{q_1, \ldots, q_n\}$ and $P = \{p_1, \ldots, p_n\}$ respectively such that $|q_i| = |p_i|$ for all i.

Case 1: Elementary isomorphism between DGAs

Suppose $\phi : (\mathcal{A}, \partial) \to (\mathcal{B}, \partial')$ is an elementary isomorphism and $\phi \circ \partial = \partial' \circ \phi$. Let $\Phi : Aug(\mathcal{B}) \to Aug(\mathcal{A})$ be the map defined by $\epsilon' \mapsto \epsilon' \circ \phi$. We will show that Φ is a bijection and that Φ sends chain homotopic augmentations to chain homotopic augmentations.

Recall that ϕ is a graded algebra map defined by:

$$\phi(q_i) = \begin{cases} p_i & i \neq j \\ p_j + u & i = j \text{ and } u \text{ is a term in } \mathcal{B} \text{ not containing } p_j \end{cases}$$

Let $\epsilon = \epsilon' \circ \phi$. Since ϕ is grading-preserving, $\epsilon(q) = \epsilon' \circ \phi(q) = 1$ implies $|q| = 0$. Thus ϵ satisfies the grading condition of an augmentation. Also, $\epsilon \circ \partial = 0$ follows from the fact that ϕ is a chain map and $\epsilon' \circ \partial' = 0$:

$$\begin{aligned} \epsilon \circ \partial(q) &= \epsilon' \circ \phi \circ \partial(q) \\ &= \epsilon' \circ \partial' \circ \phi(q) \\ &= 0 \end{aligned}$$

Hence, $\epsilon = \epsilon' \circ \phi$ is an augmentation in $Aug(\mathcal{A})$. Let $\psi : (\mathcal{B}, \partial') \to (\mathcal{A}, \partial)$ be the graded algebra map defined by:

$$\psi(p_i) = \begin{cases} q_i & i \neq j \\ q_j + \psi(u) & i = j \text{ and } u \text{ is a term in } \mathcal{B} \text{ not containing } p_j \end{cases}$$

The map ψ is an elementary isomorphism between $(\mathcal{B}, \partial')$ and $(\mathcal{A}, \partial')$. The maps $\psi \circ \phi$ and $\phi \circ \psi$ are the identity map. The map $\Psi : Aug(\mathcal{A}) \to Aug(\mathcal{B})$ defined by $\epsilon \mapsto \epsilon \circ \psi$ is the inverse of Φ, hence, Φ is a bijection.

Finally, we show that Φ maps chain homotopic augmentations to chain homotopic augmentations. Let H' by a chain homotopy between $\epsilon'_1, \epsilon'_2 \in Aug(\mathcal{B})$. Then $H = H' \circ \phi$ is a chain homotopy between $\epsilon_1 = \epsilon'_1 \circ \phi$ and $\epsilon_2 = \epsilon'_2 \circ \phi$. This follows from the fact that ϕ is grading-preserving and a chain map. Thus, $\Phi : Aug(\mathcal{B}) \to Aug(\mathcal{A})$ by $\epsilon' \mapsto \epsilon' \circ \phi$ is a bijection that induces a bijection between $Aug^{ch}(\mathcal{B})$ and $Aug^{ch}(\mathcal{A})$.

Case 2: Stabilization

Suppose $(S_i(\mathcal{A}), \partial)$ is an index i stabilization of $(\mathcal{A}, \partial)$ and $i \neq 0$. Recall $S_i(\mathcal{A}, \partial)$ is the algebra generated by the set $Q \cup \{e_1, e_2\}$, where

$$|e_1| = i \text{ and } |e_2| = i - 1$$

and the differential is extended to the new generators by

$$\partial e_1 = e_2 \text{ and } \partial e_2 = 0$$

An augmentation ϵ' on $S_i(\mathcal{A}, \partial)$ must send both e_1 and e_2 to 0, since $|e_1| \neq 0$ and $\epsilon' \circ \partial(e_1) = \epsilon'(e_2) = 0$. Thus each augmentation $\epsilon \in Aug(\mathcal{A})$ extends uniquely to an augmentation in $S_i(\mathcal{A}, \partial)$ by sending both e_1 and e_2 to 0 and every augmentation in $S_i(\mathcal{A}, \partial)$ restricts to an augmentation in $(\mathcal{A}, \partial)$. This gives a bijection between $Aug(\mathcal{A})$ and $Aug(S_i(\mathcal{A}))$. Chain homotopies extend and restrict in a similar manner, thus we have a bijection between $Aug^{ch}(\mathcal{A})$ and $Aug^{ch}(S_i(\mathcal{A}))$.

Now suppose $i = 0$. Recall $S_0(\mathcal{A}, \partial)$ is the algebra generated by the set $Q \cup \{e_1, e_2\}$, where

$$|e_1| = 0 \text{ and } |e_2| = -1$$

and the differential is extended to the new generators by

$$\partial e_1 = e_2 \text{ and } \partial e_2 = 0$$

Every augmentation $\epsilon \in Aug(\mathcal{A})$ extends to two different augmentations in $S_0(\mathcal{A}, \partial)$; one sends both e_1 and e_2 to 0 and the other sends e_1 to 1 and e_2 to 0. Likewise, when we restrict an augmentation in $S_i(\mathcal{A}, \partial)$ to an augmentation in $Aug(\mathcal{A})$, we get a two-to-one map. However, it is easy to see that the two images of ϵ in $Aug(S_0(\mathcal{A}))$ are chain homotopic by the chain homotopy H that sends e_2 to 1 and all of the other generators to 0. Thus we have a bijection between $Aug^{ch}(\mathcal{A})$ and $Aug^{ch}(S_0(\mathcal{A}))$.

□

As an immediate corollary to Proposition 4.2.1 we have the following

Corollary 4.2.2. Given a Legendrian isotopy class K with Lagrangian projection L, the number $A^{ch}(K) = |Aug^{ch}(L)|$ is independent of L and, hence, is a Legendrian isotopy invariant.

Suppose L and L' are two Lagrangian projections of the Legendrian isotopy class K related by two different sequences of Reidemeister moves giving

stable tame isomorphisms ψ, ψ'. By Proposition 4.2.1, the induced maps $\Psi, \Psi' : Aug^{ch}(L) \to Aug^{ch}(L')$ are bijections. We might hope that these maps are actually equal, in which case we could unambiguously refer to the augmentation classes of K. Unfortunately, this is not the case. In [22], Kalman shows that this bijection may depend on the sequence of Reidemeister moves.

The following lemma will be a necessary part of our later work connecting augmentation classes and MCS classes. We note that a more general statement holds for arbitrary DGAs.

Lemma 4.2.3. Suppose L and L' are Lagrangian projections with CE-DGAs $(\mathcal{A}(L), \partial)$ and $(\mathcal{A}(L'), \partial')$ respectively. Let $f : (\mathcal{A}(L), \partial) \to (\mathcal{A}(L'), \partial')$ be a DGA morphism. Then f induces a map $F : Aug^{ch}(L') \to Aug^{ch}(L)$ by $[\epsilon] \mapsto [\epsilon \circ f]$. If $g : (\mathcal{A}(L), \partial) \to (\mathcal{A}(L'), \partial')$ is also a DGA morphism and H is a chain homotopy between f and g, then $F = G$.

Proof. We must check that F is a well-defined map, i.e. $\epsilon \circ f$ is an augmentation and $\epsilon \simeq \epsilon'$ implies $\epsilon \circ f \simeq \epsilon' \circ f$. The first statement follows from the fact that f is degree preserving and a chain map and $\epsilon \circ \partial' = 0$, hence $\epsilon \circ f(q) = 1$ implies $|q| = 1$ and $\epsilon \circ f \circ \partial = \epsilon \circ \partial' \circ f = 0$. If H is a chain homotopy between ϵ and ϵ', then $H \circ f$ is a chain homotopy between $\epsilon \circ f$ and $\epsilon' \circ f$.

Suppose $g : (\mathcal{A}(L), \partial) \to (\mathcal{A}(L'), \partial')$ is also a DGA morphism and H is a chain homotopy between f and g. We show $F = G$ by showing that $\epsilon \circ f$ and $\epsilon \circ g$ are chain homotopic, thus:

$$\begin{aligned} F([\epsilon]) &= [\epsilon \circ f] \\ &= [\epsilon \circ g] \\ &= G([\epsilon]) \end{aligned}$$

The chain homotopy property $f - g = H \circ \partial - \partial' \circ H$ and the augmentation property $\epsilon \circ \partial' = 0$ imply:

$$\begin{aligned} \epsilon \circ f - \epsilon \circ g &= \epsilon \circ (f - g) \\ &= \epsilon \circ (H \circ \partial - \partial' \circ H) \\ &= \epsilon \circ H \circ \partial \end{aligned}$$

Let $H' = \epsilon \circ H : (\mathcal{A}(L), \partial) \to \mathbb{Z}_2$. Since, ϵ is an algebra homomorphism and H is a chain homotopy between f and g, we see that H' is a chain homotopy between $\epsilon \circ f$ and $\epsilon \circ g$.

□

We will concentrate on understanding the chain homotopy classes of a fixed Lagrangian projection. We use the Ng resolution and a procedure called "adding dips" to modify a Lagrangian projection so that the disks counted by the boundary map of the CE-DGA are easy to find. The dips allow us to localize the disks. In particular, this gives a system of local matrix equations for the augmentation condition $\epsilon \circ \partial$ and for the chain homotopy

condition $\epsilon_1 - \epsilon_2 = H \circ \partial$. Understanding the chain homotopy classes of augmentations then reduces to the problem of understanding solutions to these sets of matrix equations.

Chapter 5

Dipped Resolution Diagrams

In this chapter we develop techniques that allow us to gain control over the differential in the Chekanov-Eliashberg DGA. In [17], Fuchs modifies the Lagrangian projection of a Legendrian knot so that the differential in the CE-DGA is easy to compute. The modifications to the Lagrangian projection increase the number of generators significantly. This philosophy of simplifying the differential at the cost of increasing the number of generators has proved to be useful; see [19, 18, 29, 36]. We will use the version of this philosophy implemented by Sabloff in [36].

5.1 Adding dips to a Ng resolution diagram

Given a Legendrian knot K with σ-generic front projection Σ and Ng resolution L_Σ, it is possible to perform a series of Lagrangian Reidemeister type

II moves on L_Σ so that the boundary map of the CE-DGA of the resulting Lagrangian projection is easy to write down.

In Section 2.1.3, we defined the Ng resolution procedure which assigns to Σ a topologically similar Lagrangian projection L_Σ. This is done by isotoping Σ to another front projection Σ'. L_Σ is the Lagrangian projection of the Legendrian knot with front projection Σ'. The full procedure is detailed in Section 2.1.3.

We perform a series of type II moves on L_Σ by making small indentations in the strands of Σ'. The indentations becomes more pronounced as we move from the bottom strand to the top strand. Although these indentations appear uninteresting in the front projection Σ', they result in a sequence of type II moves occurring in L_Σ. The collection of crossings created in L_Σ is called a *dip*, denoted D, and the process of performing type II moves to create D is called *adding a dip*; see Figure 5.1. We create the small indentations on Σ' one at a time from the bottom strand to the top. This allows us to precisely keep track of the type II moves occurring in L_Σ. At the location of the dip, label the strands of L_Σ from bottom to top with the integers $1, \ldots, n$. For all $k > l$ there is a type II move that pushes strand k over strand l. The order in which these moves occur is as follows. If $k < i$ then k crosses over l before i crosses over any strand. If $l < j < k$ then k crosses over l before k crosses over j. The notation $(k, l) \prec (i, j)$ denotes that k crosses over l before i crosses over j. This notation is due to [36].

The crossings of the dip D are divided into two sets. The *a-lattice* A is

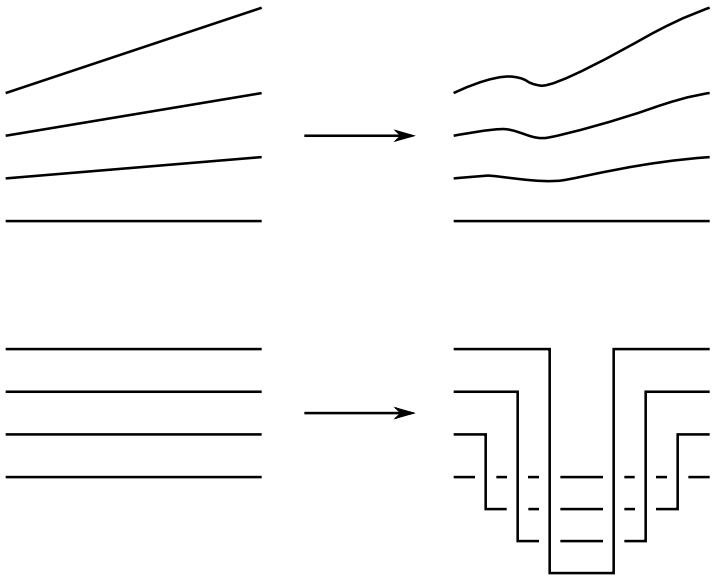

Figure 5.1: The process of adding a dip to L_Σ. The top row indicates the isotopy in Σ' and the bottom row indicates the result in L_Σ.

comprised of all crossings to the right of the vertical line of symmetry and the *b-lattice* B is comprised of all crossings to the left of the vertical line of symmetry. We assign a label to each crossing in A and B as follows. The label $a^{k,l}$ denotes the crossing in the a-lattice of strand k over strand l where $k > l$. The label $b^{k,l}$ is similarly defined; see Figure 5.2. The gradings of the crossings in a dip may be easily computed using a Maslov potential μ on the strands of Σ. In particular, $|b^{k,l}| = \mu(l) - \mu(k)$ and $|a^{k,l}| = |b^{k,l}| - 1$.

Recall that the isotopy in the Ng resolution procedure is arranged so that the heights of the crossings in L_Σ are strictly increasing as we move from left to right along the x-axis. In a similar fashion, we have control over the heights of the crossings in the A and B lattice of a dip. The indentations

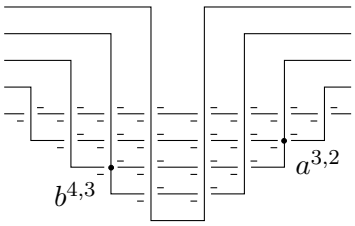

Figure 5.2: The dip D in a Lagrangian projection. Negative signs indicate the negative corners used to compute ∂. Positive signs are left out to prevent clutter.

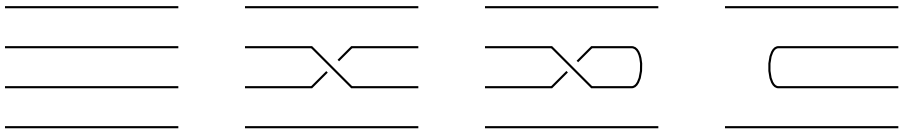

Figure 5.3: The four possible inserts in a sufficiently dipped diagram L_Σ^d; (1) parallel lines, (2) a single crossing, (3) a resolved right cusp, and (4) a resolved left cusp. In each case, any number of horizontal strands may exist.

in Σ' that create D may be arranged so that given a crossing $b^{k,l}$ in the B lattice of D, a crossing q has height less than $b^{k,l}$ if and only if q is to the left of the dip D, or $q = b^{r,s}$ or $q = a^{r,s}$ where $r - s \leq k - l$. Similarly, a crossing q has height less than $a^{k,l}$ if and only if q is to the left of the dip D, or $q = b^{r,s}$ or $q = a^{r,s}$ where $r - s \leq k - l$.

Definition 5.1.1. Given a Legendrian knot K with front projection Σ and Ng resolution L_Σ. A *dipped diagram* for K is the result of adding some number of dips to L_Σ. We require that during the process of adding dips, we not allow a dip to be added between the crossings of an existing dip. We denote a dipped diagram by L_Σ^d.

We let $D_1, \ldots, D_m$ denote the m dips of L_Σ^d, ordered from left to right

with respect to the x-axis. For consecutive dips D_{j-1} and D_j we let I_j denote the region of L_Σ^d between D_{j-1} and D_j. We define I_1 to be the region of L_Σ^d to the left of D_1 and define I_{m+1} to be the region of L_Σ^d to the right of D_m. We call $I_1, \ldots, I_{m+1}$ the *inserts* of L_Σ^d.

Definition 5.1.2. We say a dipped diagram L_Σ^d is *sufficiently dipped* if each insert $I_1, \ldots, I_{n+1}$ is isotopic to one of those in Figure 5.3.

One way to create a sufficiently dipped diagram L_Σ^d is to add a dip to the left of every resolved left cusp, right cusp and crossing in L_Σ. We will primarily concern ourselves with sufficiently dipped diagrams. As noted by Fuchs and Rutherford in [19], these are the Lagrangian projections on which it is easy to understand the boundary map of the CE-DGA.

Warning: As we will see, working with a specific dip D_j often involves working with I_j and D_{j-1} as well. When calculating ∂B_j, it will make our computations clearer and cleaner if we change slightly the labeling we use for the strands in D_{j-1} and D_j. If I_j is of type (3) and the right cusp occurs between strands $i+1$ and i, then we will label the strands of D_{j-1} by $1, \ldots, n$ and the strands of D_j by $1, \ldots, i-1, i+2, \ldots, n$. If I_j is of type (4) and the left cusp occurs between strands $i+1$ and i, then we will label the strands of D_{j-1} by $1, \ldots, i-1, i+2, \ldots, n$ and the strands of D_j by $1, \ldots, n$. If I_j is of type (1) or (2), we will make no changes to the labeling. These labeling changes are local. In particular, the labeling of the strands in D_j may vary depending on whether we are calculating ∂B_j or ∂B_{j+1}

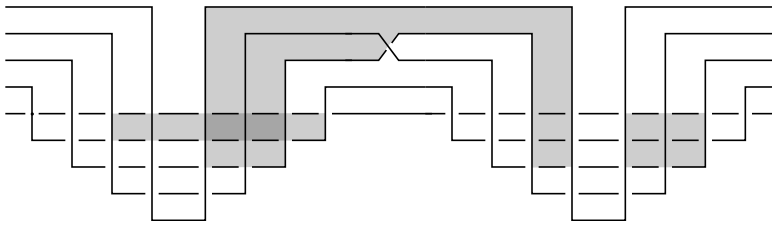

Figure 5.4: Three disks contributing to ∂ in a dipped diagram.

5.2 The CE-DGA on a sufficiently dipped diagram

The importance of adding dips to L_Σ is that they restrict the path that convex immersed polygons can take through the Lagrangian projection. In particular, the map defining a convex immersed polygon is orientation preserving, so the image of the map can not pass completely through a dip. In a sufficiently dipped diagram, calculating the boundary map of $\mathcal{A}(L_\Sigma^d)$ reduces to classifying convex immersed polygons between consecutive dips and convex immersed polygons that sit entirely within a single dip. The classification is aided by the fact that we understand the heights of the crossings in L_Σ^d; see Figure 5.4 for examples of disks contributing to ∂. Using this local description of ∂ we can reformulate $\epsilon \circ \partial = 0$ and $\epsilon_1 - \epsilon_2 = H \circ \partial$ as a system of matrix equations. In [19], Fuchs and Rutherford undertake this classification in the case of splashed diagrams. The situation is essentially identical in the case of sufficiently dipped diagrams.

Let L_Σ^d be a sufficiently dipped diagram of L_Σ with dips $D_1, \ldots, D_m$ and inserts $I_1, \ldots, I_{m+1}$. Let $q_i, \ldots, q_M$ denote the crossings found in the inserts of

type (2), where the subscript on q refers to the subscript of the insert in which the crossing appears. Note that these crossings correspond to the crossings of the front projection Σ. Similarly, let $z_j, \ldots, z_N$ denote the crossings found in the inserts of type (3), where the subscript on z refers to the subscript of the insert in which the crossing appears. These crossings correspond to right cusps in Σ. For each dip D_j, let A_j and B_j be the strictly lower triangular matrices defined by:

$$(A_j)_{k,l} = \begin{cases} a_j^{k,l} & k > l \\ 0 & k \leq l \end{cases}$$

$$(B_j)_{k,l} = \begin{cases} b_j^{k,l} & k > l \\ 0 & k \leq l \end{cases}$$

Before giving equations for the boundary map of $(\mathcal{A}(L_\Sigma^d), \partial)$, we need to define more matrix notation. For each insert I_j, $j \notin \{1, m+1\}$, we define a matrix $\widetilde{A}_{j-1}$ using the entries of A_{j-1} and the original crossings of L_Σ. In the following formulae we have left off the subscript $j-1$ on the a's to make the text more readable.

1. Suppose I_j is of type (1). Then $\widetilde{A}_{j-1} = A_{j-1}$.

2. Suppose I_j is of type (2), A_j has dimension m and the crossing q_j

involves strands $i+1$ and i. Then $\widetilde{A}_{j-1}$ is the $m \times m$ matrix with (u, v) entry $\widetilde{a}_{j-1}^{u,v}$ defined by:

$$\widetilde{a}^{u,v} = \begin{cases} a^{u,v} & u, v \notin \{i, i+1\} \\ 0 & u = i+1, v = i \end{cases}$$
$$\widetilde{a}^{i+1,v} = a^{i,v}$$
$$\widetilde{a}^{i,v} = a^{i+1,v} + q_j a^{i,v}$$
$$\widetilde{a}^{u,i} = a^{u,i+1}$$
$$\widetilde{a}^{u,i+1} = a^{u,i} + a^{u,i+1} q_j$$

3. Suppose I_j is of type (3), A_j has dimension m, and the resolved right cusp crossing z_j involves strands $i+1$ and i. Then $\widetilde{A}_{j-1}$ is an $m \times m$ matrix with rows and columns numbered $1, \ldots, i-1, i+2, \ldots, m+2$ and (u, v) entry $\widetilde{a}_{j-1}^{u,v}$ defined by:

$$\widetilde{a}^{u,v} = \begin{cases} a^{u,v} & u < i \text{ or } v > i+1 \\ a^{u,v} + a^{u,i} a^{i+1,v} + a^{u,i+1} z_j a^{i+1,v} & u > i+1 > i > v \\ \qquad + a^{u,i} z_j a^{i,v} + a^{u,i+1} z_j z_j a^{i,v} & \end{cases}$$

4. Suppose I_j is of type (4), A_j has dimension m and the resolved left cusp strands are $i+1$ and i. Then $\widetilde{A}_{j-1}$ is the $m \times m$ matrix with (u, v)

entry $\widetilde{a}_{j-1}^{u,v}$ defined by:

$$\widetilde{a}^{u,v} = \begin{cases} a^{u,v} & u, v \notin \{i, i+1\} \\ 1 & u = i+1, v = i \\ 0 & \text{otherwise} \end{cases}$$

We calculate the boundary map of the CE-DGA $(\mathcal{A}(L_\Sigma^d), \partial)$ by the following formulae and matrix equations.

Lemma 5.2.1. The CE-DGA boundary map ∂ of a sufficiently dipped diagram of a Ng resolution L_Σ is computed by:

1. For all crossings q_s between strands $i+1$ and i, $\partial q_s = a_{s-1}^{i+1,i}$;
2. For all crossings z_r between strands $i+1$ and i, $\partial z_r = 1 + a_{r-1}^{i+1,i}$, where z_r is a crossing between strands $i+1$ and i;
3. $\partial A_j = A_j^2$; and
4. $\partial B_j = (I + B_j)A_j + \widetilde{A}_{j-1}(I + B_j)$.

where I is the identity matrix of appropriate dimension and the matrices ∂A_j and ∂B_j are the result of applying ∂ to A_j and B_j entry-by-entry.

This result appears in [19] in the language of "splashed diagrams" instead of dipped diagrams. In the next three sections we justify these formulae. In

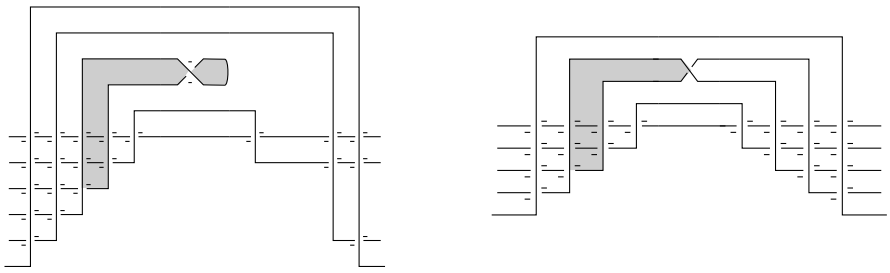

Figure 5.5: Disks contributing to ∂q_s and ∂z_r.

the figures that follow, we have included the negative signs coming from the Reeb decorations of the crossings. We have left off the plus signs to prevent clutter. Recall that a convex immersed polygon contributing to ∂ has exactly one positive convex corner and possibly other negative convex corners.

Computing ∂ on q_s and z_r

Given a crossing q_s, we note that all of the crossings of height less than $h(q_s)$ sit to the left of q_s. Thus q_s must be the right-most convex corner of any non-trivial disk in ∂q_s. The disks with positive corner at q_s can not move through the dip D_{s-1}, thus the disk in Figure 5.5 is the only disk contributing to ∂q_s. The case of ∂z_r is similar.

Computing ∂ on the A_j lattice

The combinatorics of the dip D_j along with the height ordering on the crossings of L^d_Σ require that disks in $\partial a_j^{k,l}$ sit within the A_j lattice. In addition, a convex immersed polygon sitting within the A_j lattice must have exactly two negative convex corners; see Figure 5.6. From this we compute:

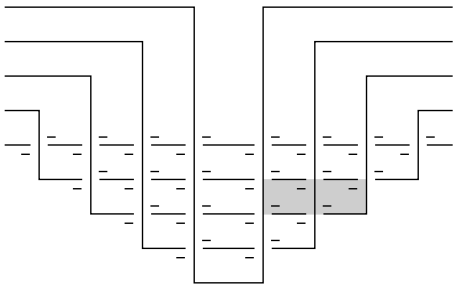

Figure 5.6: The disk $a_j^{5,3}a_j^{3,2}$ appearing in $\partial a_j^{5,2}$.

$$\partial a_j^{k,l} = \sum_{l<i<k} a_j^{k,i} a_j^{i,l} \tag{5.1}$$

Thus $\partial a_j^{k,l}$ is the (k,l)-entry in the matrix A_j^2 and so $\partial A_j = A_j^2$.

Computing ∂ on the B_j lattice

The combinatorics of the dip D_j along with the height ordering on the crossings of L_Σ^d require that disks in $\partial b_j^{k,l}$ are of two types. The first sits within the dip D_j and has a convex corner in the A_j lattice. We denote these disks by $R(\partial b_j^{k,l})$ and note that they all include the lower right corner of $b_j^{k,l}$ as their positive convex corner. The second type of disk in $\partial b_j^{k,l}$ includes the upper left corner of $b_j^{k,l}$ as its right-most convex corner. Thus these disks all sit between the B_j lattice and the A_{j-1} lattice. We let $L(\partial b_j^{k,l})$ denote these disks. So $\partial b_j^{k,l} = R(\partial b_j^{k,l}) + L(\partial b_j^{k,l})$.

Since the disks comprising $R(\partial b_j^{k,l})$ are completely contained in the dip D_j, they are easy to classify. In fact, Figure 5.7 shows the two types of

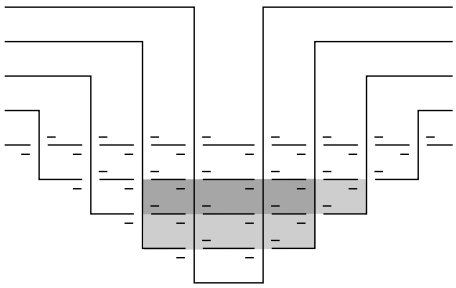

Figure 5.7: The disks $b_j^{4,3}a_j^{3,2}$ and $a_j^{4,2}$ appearing in $R(\partial b_j^{4,2})$.

convex immersed polygons found in $R(\partial b_j^{k,l})$. From this, we compute:

$$R(\partial b_j^{k,l}) = a_j^{k,l} + \sum_{l<i<k} b_j^{k,i} a_j^{i,l}$$

Note that $R(\partial b_j^{k,l})$ is the (k,l)-entry in the matrix $(I + B_j)A_j$.

In order to compute $L(\partial b_j^{k,l})$, we classify all of the convex immersed polygons sitting between two dips. If I_j is of type (1), then there are 2 types of disks; see Figure 5.8(a). If I_j is of type (2), then there are 14 types of disks. Twelve types are shown in Figure 5.9 and the other two types are those appearing in Figure 5.8(a). If I_j is of type (3), then there are 10 types of disks. Eight types are shown in Figure 5.10 and the other two types are those appearing in Figure 5.8(a). If I_j is of type (4), then there are 4 types of disks. Two types are shown in Figure 5.8(b) and the other two types are those appearing in Figure 5.8(a). Computing $L(\partial b_j^{k,l})$ requires understanding which of these disks appear with a positive convex corner at $b_j^{k,l}$. The entries in the matrix $\widetilde{A}_{j-1}$ are defined to encode these disks. In fact, for a fixed $b_j^{k,l}$:

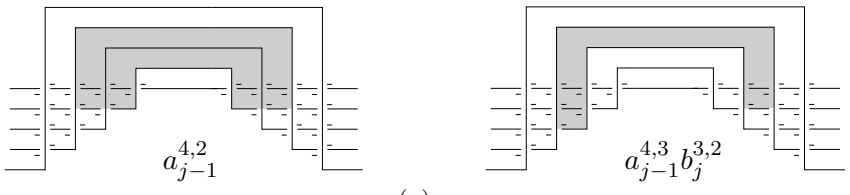

(a)

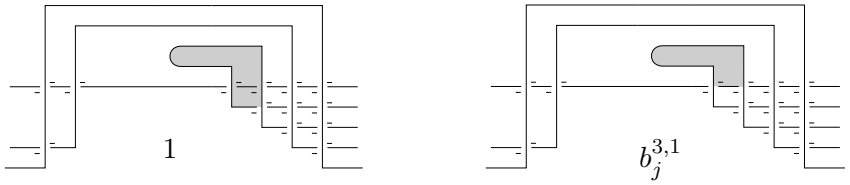

(b) Type (4).

Figure 5.8: Types of disks contributing to $L(\partial b_j^{k,l})$ when I_j is of type (1) or (4). The disks in (a) may occur in an insert of any type.

$$L(\partial b_j^{k,l}) = \widetilde{a}_{j-1}^{k,l} + \sum_{l<i<k} \widetilde{a}_{j-1}^{k,i} b_j^{i,l}$$

Regardless of I_j's type, $L(\partial b_j^{k,l})$ is the (k,l)-entry of the matrix $\widetilde{A}_{j-1}(I + B_j)$. Combining this with the matrix equation for $R(\partial b_j^{k,l})$, we have the matrix equation for ∂B_j:

$$\partial B_j = (I + B_j)A_j + \widetilde{A}_{j-1}(I + B_j) \tag{5.2}$$

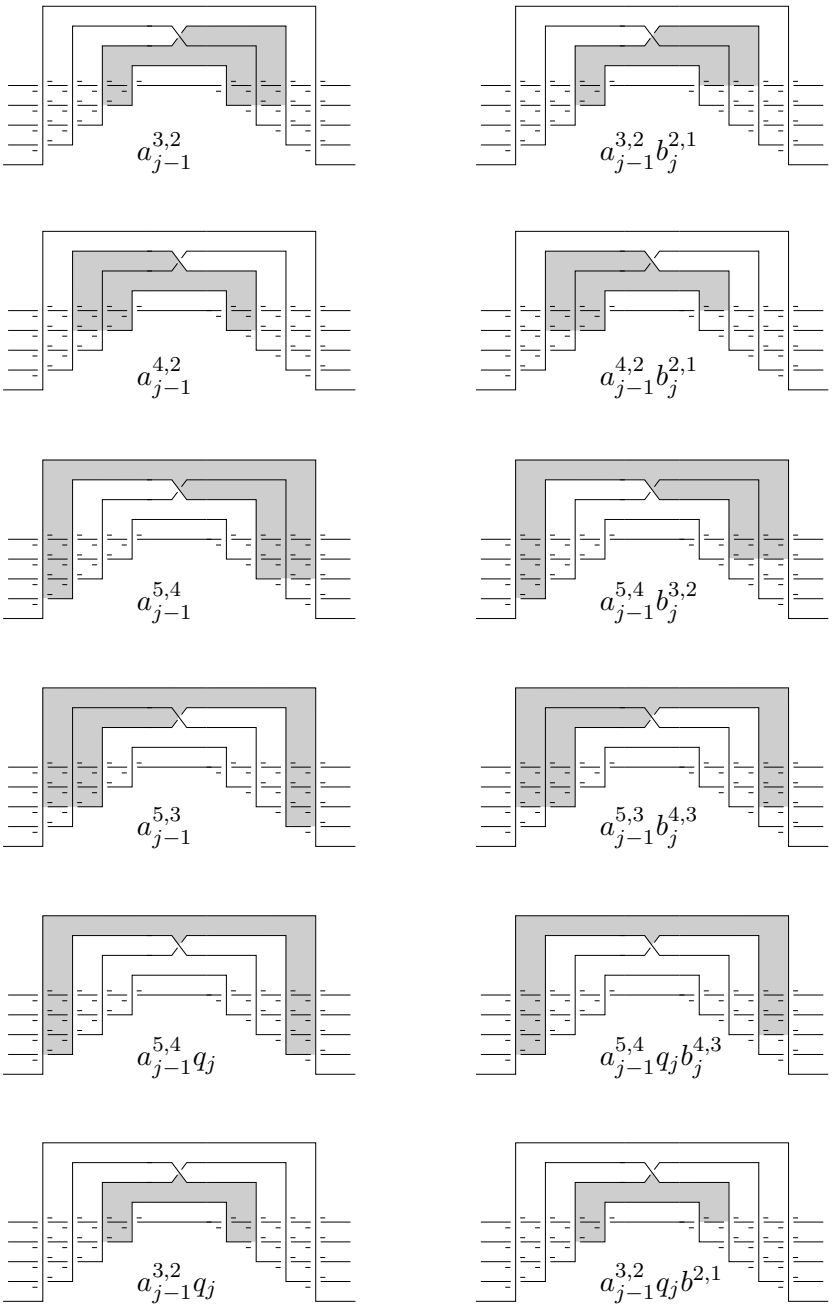

Figure 5.9: Types of disks contributing to $L(\partial B_j)$ when I_j is of type (2). Above each picture we indicate the associated monomial appearing in ∂B_j.

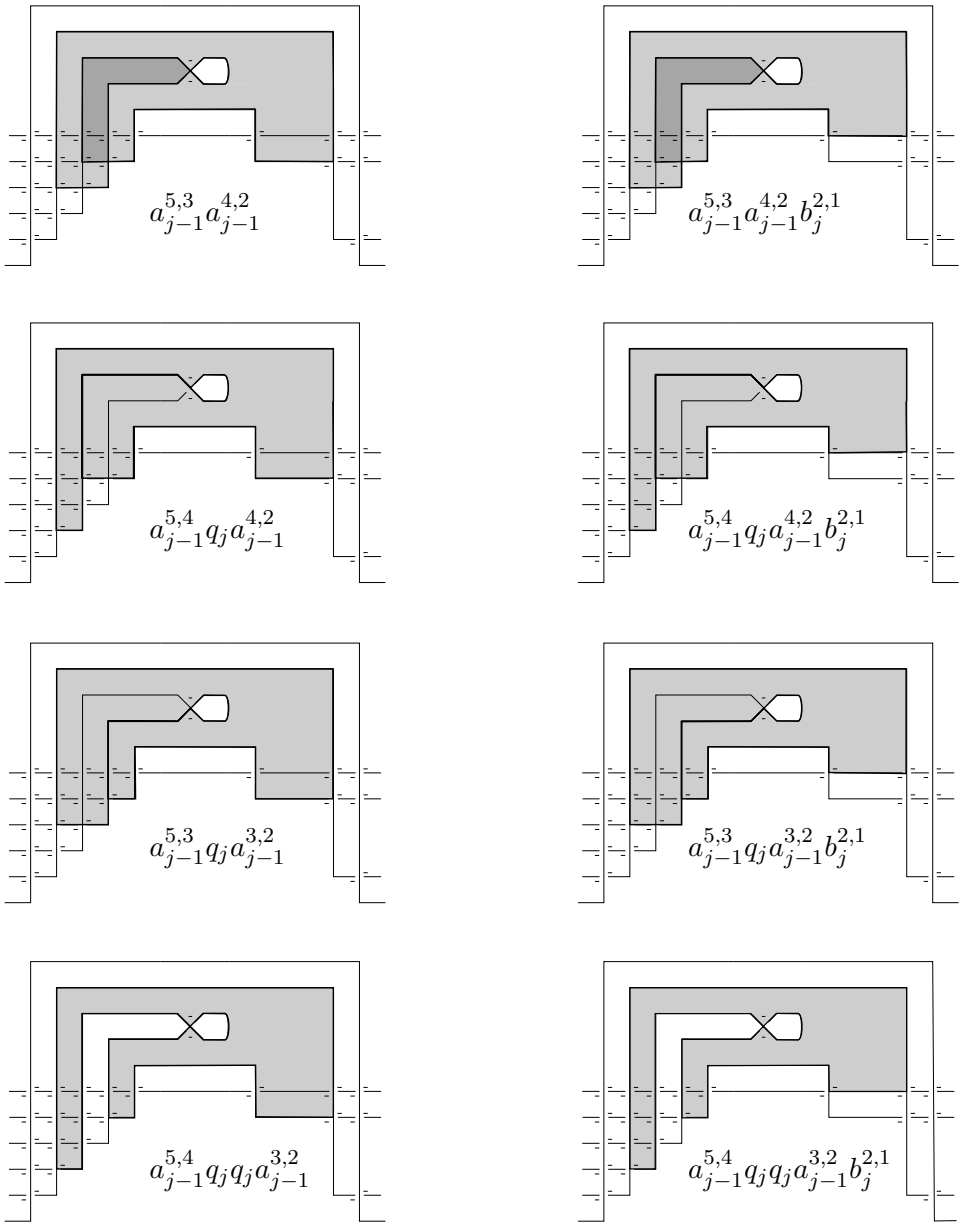

Figure 5.10: Types of disks contributing to $L(\partial B_j)$ when I_j is of type (3). The boundary of each disk is highlighted. Above each picture we indicate the associated monomial appearing in ∂B_j.

5.3 The stable tame isomorphism of a type II move

Suppose the Lagrangian projection L_2 is obtained from L_1 by a single type II move introducing new crossings a and b with $|b| = i$ and $|a| = i - 1$. By Theorem 2.3.19, there exists a stable tame isomorphism from $(\mathcal{A}(L_2), \partial)$ to $(\mathcal{A}(L_1), \partial')$. As we demonstrated in Proposition 4.2.1, such a stable tame isomorphism induces a map from $Aug(L_1)$ to $Aug(L_2)$. We would like to understand this map so that we may keep track of augmentations as we add dips to L_Σ.

The stable tame isomorphism from $(\mathcal{A}(L_2), \partial)$ to $(\mathcal{A}(L_1), \partial')$ was first explicitly written down in [6]. Equivalent isomorphisms appear in [14, 36]. We will use the formulation found in [36]. The stable tame isomorphism is a single stabilization S_i followed by a tame isomorphism ψ. The stabilization $S_i(\mathcal{A}(L_1), \partial')$ adds generators α and β to $(\mathcal{A}(L_1), \partial')$ such that $|\beta| = i$ and $|\alpha| = i - 1$. We extend the differential of $(\mathcal{A}(L_1), \partial')$ to $S_i(\mathcal{A}(L_1), \partial')$ by defining $\partial'\beta = \alpha$ and $\partial'\alpha = 0$

The tame isomorphism $\psi : (\mathcal{A}(L_2), \partial) \to S_i(\mathcal{A}(L_1), \partial')$ is defined as follows. We begin by ordering the generators of $(\mathcal{A}(L_2), \partial)$ by height. Let $\{x_1, \ldots, x_N\}$ denote the generators with height less than $h(a)$ and labeled so that $h(x_1) < \ldots < h(x_N)$. Let $\{y_1, \ldots, y_M\}$ denote the generators with height greater than $h(b)$ and labeled so that $h(y_1) < \ldots < h(y_M)$. Recall that ∂ lowers height, so a generator p does not appear in ∂q if $h(p) > h(q)$.

In particular, y_k does not appear in ∂y_l if $l < k$. This ordering also allows us to write ∂b as $\partial b = a + v$ where v consists of words in the letters $x_1, \ldots, x_N$.

Our formulation of ψ requires a vector space map H defined on $S_i(\mathcal{A}(L_1), \partial')$ by:

$$H(w) = \begin{cases} 0 & w \in \mathcal{A}(L_1) \\ 0 & w = Q\beta R \quad \text{with } Q \in \mathcal{A}(L_1), R \in S_i(\mathcal{A}(L_1)) \\ Q\beta R & w = Q\alpha R \quad \text{with } Q \in \mathcal{A}(L_1), R \in S_i(\mathcal{A}(L_1)). \end{cases}$$

If we read the generators of w from left to right and β appears before α, then H sends w to 0. However, if α appears before β, then H replaces this occurrence of α with β. If w contains no α's or β's, then H sends w to 0.

We build ψ up from a sequence of maps $\psi_i : (\mathcal{A}(L_2), \partial) \to S_i(\mathcal{A}(L_1), \partial')$ for $0 \leq i \leq M$:

$$\psi_0(w) = \begin{cases} \beta & w = b \\ \alpha + v & w = a \\ w & \text{otherwise} \end{cases}$$

and

$$\psi_i(w) = \begin{cases} y_i + H\psi_{i-1}(\partial y_i) & w = y_i \\ \psi_{i-1}(w) & \text{otherwise.} \end{cases}$$

If we extend map ψ_M by linearity from a map on generators to a map on all of $(\mathcal{A}(L_2), \partial)$, then the resulting map $\psi : (\mathcal{A}(L_2), \partial) \to S_i(\mathcal{A}(L_1), \partial')$ is the desired DGA isomorphism; see [6, 36].

5.3.1 Extending augmentations across a type II move

Given the stabilization S_i and tame isomorphism ψ defined above, we would like to understand the induced map from $Aug(L_1)$ to $Aug(L_2)$. The lemmata that follow are motivated by Lemma 3.2 in [36]. We begin by recalling the relationship between $Aug(L_1)$ and $Aug(S_i(L_1))$ noted in Proposition 4.2.1. If $i \neq 0$ then there is a bijection between $Aug(L_1)$ and $Aug(S_i(L_1))$. The bijection extends an augmentation $\epsilon \in Aug(L_1)$ to an augmentation in $Aug(S_i(L_1))$ by sending both β and α to 0. If $i = 0$ then there are two ways to extend $\epsilon \in Aug(L_1)$. The first is to send both β and α to 0 and the second is to send β to 1 and α to 0. As we saw in Proposition 4.2.1, these two extensions are chain homotopic.

The tame isomorphism $\psi : (\mathcal{A}(L_2), \partial) \to S_i(\mathcal{A}(L_1), \partial')$ gives a bijection $\Psi : Aug(S_i(L_1)) \to Aug(L_2)$ by $\epsilon \mapsto \epsilon \circ \psi$. Let $\epsilon' = \epsilon \circ \psi$. From the formulae for ψ we note several facts about ϵ':

1. $\epsilon'(x_i) = \epsilon \circ \psi(x_i) = \epsilon(x_i)$ for all i.

2. $\epsilon'(b) = \epsilon(\beta)$.

3. $\epsilon'(a) = \epsilon(v)$ where $\partial b = a + v$.

Furthermore, we have the following results.

Lemma 5.3.1. If we extend an augmentation $\epsilon \in Aug(L_1)$ to an augmentation $\epsilon \in Aug(S_i(L_1))$ by $\epsilon(\beta) = \epsilon(\alpha) = 0$ then the augmentation $\epsilon' \in Aug(L_2)$ satisfies:

1. $\epsilon'(b) = 0$,

2. $\epsilon'(a) = \epsilon(v)$ where $\partial b = a + v$, and

3. $\epsilon' = \epsilon$ on all other crossings.

Proof. We need only check that $\epsilon' = \epsilon$ on $y_1, \ldots, y_M$ since the other conclusions follow from our discussion above. By the definition of ϵ' and ψ we have,

$$\begin{aligned} \epsilon'(y_j) &= \epsilon \circ \psi(y_j) \\ &= \epsilon(y_j + H \circ \psi(\partial y_j)) \\ &= \epsilon(y_j) + \epsilon \circ H \circ \psi(\partial y_j) \end{aligned} \tag{5.3}$$

Thus we must show $\epsilon \circ H \circ \psi(\partial y_j) = 0$. By the definition of H, every word in $H \circ \psi(\partial y_j)$ contains the generator β. Hence, $\epsilon(\beta) = 0$ implies $\epsilon \circ H \circ \psi(\partial y_j) = 0$. □

In the case of Lemma 5.3.1, extending an augmentation from $Aug(L_1)$ to $Aug(L_2)$ only requires that we understand $\partial b = a + v$ in $(\mathcal{A}(L_2), \partial)$. If the type II move we are considering occurs during the creation of a dip, then we can often determine v explicitly. The next Lemma will be useful in our later discussion of extending augmentations to dipped diagrams.

Lemma 5.3.2. Suppose we extend an augmentation $\epsilon \in Aug(L_1)$ to an augmentation $\epsilon \in Aug(S_i(L_1))$ by $\epsilon(\beta) = 1$ and $\epsilon(\alpha) = 0$. Suppose that in $(\mathcal{A}(L_2), \partial)$ the generator a appears in the boundary of each of the generators $\{y_{j_1}, \ldots, y_{j_l}\}$. Suppose that for $y \in \{y_{j_1}, \ldots, y_{j_l}\}$, each disk contributing a to ∂y has the form QaR where $Q, R \in \mathcal{A}(L_2)$ and Q and R do not contain a or b. Then the augmentation $\epsilon' \in Aug(L_2)$ satisfies:

1. $\epsilon'(b) = 1$;
2. $\epsilon'(a) = \epsilon(v)$ where $\partial b = a + v$;
3. For each $y \in \{y_{j_1}, \ldots, y_{j_l}\}$, $\epsilon'(y) = \epsilon(y)$ if and only if the generator a appears in an even number of terms in ∂y that are of the form QaR with $\epsilon(Q) = \epsilon(R) = 1$; and
4. $\epsilon' = \epsilon$ on all other crossings.

Proof. We need only understand how ϵ' acts on $y_1, \ldots, y_M$ since the other conclusions follow from our discussion above. Let $y \in \{y_1, \ldots, y_M\}$. From Equation 5.3, we have $\epsilon'(y) = \epsilon(y) + \epsilon \circ H \circ \psi(\partial y)$. Suppose a does not appear in ∂y. Then $H \circ \psi(\partial y) = 0$, so $\epsilon'(y) = \epsilon(y)$. Suppose a does appear in ∂y. Then we must show that $\epsilon \circ H \circ \psi(\partial y_j) = 0$ if and only if a appears in an even number of terms in ∂y that are of the form QaR with $\epsilon(Q) = \epsilon(R) = 1$.

By assumption, each disk contributing a to ∂y has the form QaR where $Q, R \in \mathcal{A}(L_2)$ and Q and R do not contain a or b. Thus $H \circ \psi(QaR) = Q\beta R$ for each disk of the form QaR in ∂y and $H \circ \psi$ is 0 on all of the other disks in ∂y. Now $\epsilon \circ H \circ \psi(QaR) = \epsilon(Q)\epsilon(R)$, so $\epsilon \circ H \circ \psi(\partial y) = 0$ if and only if a appears in an even number of terms in ∂y that are of the form QaR with $\epsilon(Q) = \epsilon(R) = 1$. □

These two technical lemmata form the basis of an algorithm that assigns to each augmentations in $Aug(L_\Sigma)$ an MCS in $MCS(\Sigma)$. In the next section, we follow an augmentation through the process of adding a dip to L_Σ. We keep careful track of the stable tame isomorphisms involved in the creation of a dip. This allows us to extend an augmentation to the new crossings in the dip.

5.4 Extending an augmentation across a dip

Suppose L_Σ^d is a dipped diagram of L_Σ with dips $D_1, \ldots, D_m$. L_Σ^d may not be *sufficiently* dipped. We would like to add a new dip D to L_Σ^d away

from $D_1, \ldots, D_m$. We will denote the resulting dipped diagram by $L_\Sigma^{d'}$. D is created by performing a sequence of type II moves on L_Σ^d. Our goal is to understand how an augmentation in $Aug(L_\Sigma^d)$ extends to an augmentation in $Aug(L_\Sigma^{d'})$ using the stable tame isomorphisms defined in the previous section. This work is motivated by the construction defined in Section 3.3 of [36]. In [36], Sabloff restricts to front projections in plat position. Our techniques generalize Sabloff's techniques to σ-generic front projections. The results in the rest of this chapter will form the basis of an algorithm that assigns to $\epsilon \in Aug(L_\Sigma)$ an MCS $\mathcal{C}_\epsilon \in MCS(\Sigma)$.

We set the following notation so that the arguments below are not as cluttered. Let $L = L_\Sigma^d$ and $L' = L_\Sigma^{d'}$. We will assume that, with respect to the ordering on dips coming from the x-axis, D is not the left-most dip in L'. D creates two new inserts. Let I denote the insert in L' bounded on the right by D. Let D_j denote the dip bounding I on the left. The sequence of type II moves that change L to L' are done in the following order. At the location of the dip D, label the strands of L_Σ^d from bottom to top with the integers $1, \ldots, n$. For all $k > l$ there is a type II move that pushes strand k over strand l. The order in which these moves occur was defined in Section 5.1. Recall that the notation $(k, l) \prec (i, j)$ denotes that k crosses over l before i crosses over j. The creation of the dip D gives a sequence of Lagrangian projections $L, L_{2,1}, \ldots, L_{n,n-1} = L'$, where $L_{k,l}$ denotes the result of pushing strand k over strand l. Let $\partial_{k,l}$ denote the boundary map of the CE-DGA of $L_{k,l}$. Let $D_{k,l}$ denote the partial dip in $L_{k,l}$; see Figure 5.11. In each Lagrangian

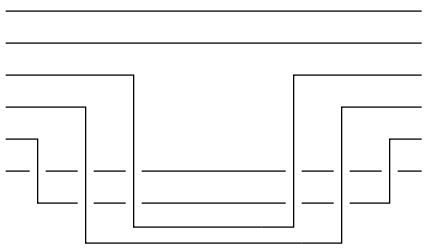

Figure 5.11: The partial dip $D_{4,2}$ in $L_{4,2}$.

projection $L_{k,l}$, the insert I and dip D_j sit to the left of the partial dip $D_{k,l}$.

Suppose (r,s) denotes the type II move immediately preceding the type II move (k,l). So $(r,s) \prec (k,l)$ and if $(x,y) \prec (k,l)$ then $(x,y) \prec (r,s)$. Either $(r,s) = (k,l-1)$ or $(r,s) = (k-1,k-2)$. Then $L_{k,l}$ is the result of pushing strand k over strand l in $L_{r,s}$. Let $\epsilon \in Aug(L_{r,s})$. We would like to understand the extension of ϵ to an augmentation $\epsilon' \in Aug(L_{k,l})$ that results from the stable tame isomorphism defined in the previous section.

If $\mu(l) \neq \mu(k)$ then the new augmentation ϵ' satisfies $\epsilon'(b^{k,l}) = 0$. If $\mu(l) = \mu(k)$ then we have two choices for extending ϵ to ϵ'. The first choice is to extend ϵ so that $\epsilon'(b^{k,l}) = 0$. The second is to extend ϵ so that $\epsilon'(b^{k,l}) = 1$. We begin by considering the first case.

5.4.1 Extending $\epsilon \in Aug(L^d_\Sigma)$ by 0.

Let us suppose that, regardless of $\mu(l)$ and $\mu(k)$, we have extended ϵ so that $\epsilon'(b^{k,l}) = 0$. In this case, Lemma 5.3.1 implies:

1. $\epsilon'(a^{k,l}) = \epsilon(v)$ where $\partial_{k,l} b^{k,l} = a^{k,l} + v$, and

2. $\epsilon' = \epsilon$ on all other crossings.

If we understand the convex immersed polygons in v, then we completely understand the extension of ϵ to ϵ'. Recall that the convex immersed polygons in v involve crossings with height less than $h(b^{k,l})$ and have a positive convex corner at $b^{k,l}$. Suppose q is a crossing appearing in v. As we noted previously, the isotopy of Σ that create L_Σ and add a dip to L_Σ ensure that either q is to the left of $D_{k,l}$, or $q = b^{c,d}$ or $q = a^{c,d}$ where $c - d \leq k - l$. Note that $a^{k,l}$ is the only disk in $\partial_{k,l} b^{k,l}$ with the lower right corner of $b^{k,l}$ as its positive convex corner. So no other crossings in the A lattice appear in $\partial_{k,l} b^{k,l}$ and the disks in v must include the upper left corner of $b^{k,l}$ as their right-most convex corner. Thus the disks in v appear to the left of $D_{k,l}$.

If the insert I is of one of the four types in Figure 5.3, then we can describe the disks in v. In our discussion of Lemma 5.2.1, we let $L(\partial b^{k,l})$ denote the disks in $\partial b^{k,l}$ that include the upper left corner of $b^{k,l}$ as their right-most convex corner. Here $\partial b^{k,l}$ refers to the boundary map in the CE-DGA of $L_\Sigma^{d'}$. The order in which we perform the type II moves that create the dip D ensures that when the crossing $b^{k,l}$ is created, all of the disks in $L(\partial b^{k,l})$ appear in $\partial_{k,l} b^{k,l}$. In fact, the restrictions placed on convex immersed polygons by the height function imply that any disk appearing in $\partial_{k,l} b^{k,l}$ must also appear in $\partial b^{k,l}$. Thus, we have:

$$\begin{aligned} v &= L(\partial b^{k,l}) \\ &= \widetilde{a}_j^{k,l} + \sum_{l<i<k} \widetilde{a}_j^{k,i} b^{i,l} \end{aligned}$$

Since $L(\partial b^{k,l})$ is the (k,l) entry in the matrix $\widetilde{A_j}(I+B)$, we see that $\epsilon'(A) = \epsilon(\widetilde{A}_j(I+B))$. Summarizing we have:

Lemma 5.4.1. Suppose L_Σ^d is a dipped diagram of the Ng resolution L_Σ. Suppose we use the dipping procedure to add a dip D between the existing dips D_j and D_{j+1} and thus create a new dipped diagram $L_\Sigma^{d'}$. Suppose the insert I between D and D_j is of one of the four types in Figure 5.3. Let $\epsilon \in Aug(L_\Sigma^d)$. Then if at every type II move in the creation of the dip D we choose to extend ϵ so that ϵ' is 0 on the new crossing in the B lattice, then the stable tame isomorphism from Section 5.3 maps ϵ to $\epsilon' \in Aug(L_\Sigma^{d'})$ satisfying:

1. $\epsilon'(B) = 0$,
2. $\epsilon'(A) = \epsilon(\widetilde{A}_j)$, and
3. $\epsilon' = \epsilon$ on all other crossings.

Proof. This lemma follows directly from the discussion above and the following computation.

$$\begin{aligned}\epsilon'(A) &= \epsilon(\widetilde{A}_j(I+B)) \\ &= \epsilon(\widetilde{A}_j) + \epsilon(\widetilde{A}_j B) \\ &= \epsilon(\widetilde{A}_j) + \epsilon(\widetilde{A}_j)\epsilon'(B) \\ &= \epsilon(\widetilde{A}_j)\end{aligned}$$

□

Definition 5.4.2. If $\epsilon \in Aug(L^d_\Sigma)$ then we say that ϵ is *extended by 0* if after each type II move in the creation of D, we extend ϵ so that ϵ sends the new crossing of the B lattice of D to 0.

In the next corollary, we consider the specific types of inserts that arise.

Corollary 5.4.3. Suppose we are in the setup of Lemma 5.4.1. Let $\epsilon \in Aug(L^d_\Sigma)$ and let $\epsilon' \in Aug(L^{d'}_\Sigma)$ be the extension of ϵ described in Lemma 5.4.1. Then:

1. If I is of type (1), then $\epsilon'(A) = \epsilon(A_j)$.
2. Suppose I is of type (2) with crossing q between strands $i+1$ and i. If $\epsilon(q) = 0$, then $\epsilon'(A) = P_{i+1,i}\epsilon(A_j)P_{i+1,i}$
3. Suppose I is of type (3) with crossing z between strands $i+1$ and i.
   (a) Let $i+1 < u_1 < u_2 < \ldots < u_s$ denote the strands at dip D_j that satisfy $\epsilon(a_j^{u_1,i}) = \ldots = \epsilon(a_j^{u_s,i}) = 1$;

(b) Let $v_r < \ldots < v_1$ denote the strands at dip D_j that satisfy $\epsilon(a_j^{i+1,v_1}) = \epsilon(a_j^{i+1,v_2}) = \ldots = \epsilon(a_j^{i+1,v_r}) = 1$; and

(c) Let $E = E_{i,v_r} \ldots E_{i,v_1} E_{u_1,i+1} \ldots E_{u_s,i+1}$.

If $\epsilon(z) = 0$ and $\epsilon(a_j^{i+1,i}) = 1$, then, as matrices, $\epsilon'(A) = J_{i-1} E \epsilon(A_j) E^{-1} J_{i-1}^T$

4. Suppose I is of type (4) and the resolved birth is between strands $i+1$ and i. Then, as matrices, $\epsilon'(A)$ is obtained from $\epsilon(A_j)$ by inserting two rows (columns) of zeros after row (column) $i-1$ in $\epsilon(A_j)$ and then changing the $(i+1, i)$ entry to 1.

Proof. In the each of the four cases, we revisit the definition of $\widetilde{A}_j$ from section . The assumptions on $\epsilon(q)$ and $\epsilon(z)$ in cases 2. and 3. simplify the matrices $\epsilon(\widetilde{A}_j)$ considerably.

Case 1 and 4.

Case 1. and 4. follow immediately from Lemma 5.4.1 and the definition of $\widetilde{A}_j$.

Case 2.

If $\epsilon(q) = 0$, then the entry $\epsilon(\widetilde{a}_j^{u,v})$ in $\epsilon(\widetilde{A}_j)$ is defined by:

$$\epsilon(\widetilde{a}^{u,v}) = \begin{cases} \epsilon(a^{u,v}) & u, v \notin \{i, i+1\} \\ 0 & u = i+1, v = i \end{cases}$$

$$\epsilon(\widetilde{a}^{i+1,v}) = \epsilon(a^{i,v})$$

$$\epsilon(\widetilde{a}^{i,v}) = \epsilon(a^{i+1,v})$$

$$\epsilon(\widetilde{a}^{u,i}) = \epsilon(a^{u,i+1})$$

$$\epsilon(\widetilde{a}^{u,i+1}) = \epsilon(a^{u,i})$$

In particular, the terms involving q in $\epsilon(\widetilde{a}^{i,v})$ and $\epsilon(\widetilde{a}^{u,i+1})$ drop out. Thus $\epsilon'(A) = \epsilon(\widetilde{A}_j) = P_{i+1,i}\epsilon(A_j)P_{i+1,i}$

Case 3.

If $\epsilon(z) = 0$, then the entry $\epsilon(\widetilde{a}_j^{u,v})$ in $\epsilon(\widetilde{A}_j)$ is defined by:

$$\epsilon(\widetilde{a}^{u,v}) = \begin{cases} \epsilon(a^{u,v}) & u < i \text{ or } v > i+1 \\ \epsilon(a^{u,v}) + \epsilon(a^{u,i})\epsilon(a^{i+1,v}) & u > i+1 > i > v \end{cases}$$

In particular, the three terms involving z in $\epsilon(\widetilde{a}^{u,v})$ when $u > i+1 > i > v$ all drop out. A slightly tedious matrix calculation verifies that $\epsilon(\widetilde{A}_j) = J_{i-1}E\epsilon(A_j)E^{-1}J_{i-1}^T$.

□

The matrix equations in Corollary 5.4.3 should look familiar. Besides Case 1., these matrix equations appear in the definition of an MCS, Definition 3.2.3. Thus we see the first hint of an explicit connection between MCSs and augmentations. We will explore this connection extensively in the next chapter.

5.4.2 Extending $\epsilon \in Aug(L^d_\Sigma)$ by $\delta_{i+1,i}$.

In the last section, we extended $\epsilon \in Aug(L^d_\Sigma)$ to an augmentation $\epsilon' \in Aug(L^{d'}_\Sigma)$ so that $\epsilon'(B) = 0$. In this section, we consider extending $\epsilon \in Aug(L^d_\Sigma)$ to an augmentation $\epsilon' \in Aug(L^{d'}_\Sigma)$ so that $\epsilon'(B) = \delta_{i+1,i}$. During the type II move that pushes strand $i+1$ over strand i we will choose to extend ϵ so that $\epsilon'(b^{i+1,i}) = 1$. By carefully using Lemma 5.3.2, we are able to keep track of the extended augmentation ϵ'. In Section 6.3, we use the results from the previous section, along with the following lemma, to assign to $\epsilon \in Aug(L_\Sigma)$ an MCS $\mathcal{C}_\epsilon \in MCS(\Sigma)$. In particular, the following lemma will describe the handleslide marks in $\mathcal{C}_\epsilon$.

As we saw in Lemma 5.3.2, understanding ϵ' when $\epsilon'(b^{i+1,i}) = 1$ requires that we understand all of the crossings y such that $a^{i+1,i}$ appears in $\partial_{i+1,i}y$. In general, keeping track of all such y is a global problem, in the sense that the convex immersed polygons containing $a^{i+1,i}$ as a negative convex corner may include convex corners at crossings far away from $a^{i+1,i}$. Thus, we will only extend an augmentation by $\epsilon'(b^{i+1,i}) = 1$ when we have complete control over the disks containing $a^{i+1,i}$ as a negative convex corner. In particular, if

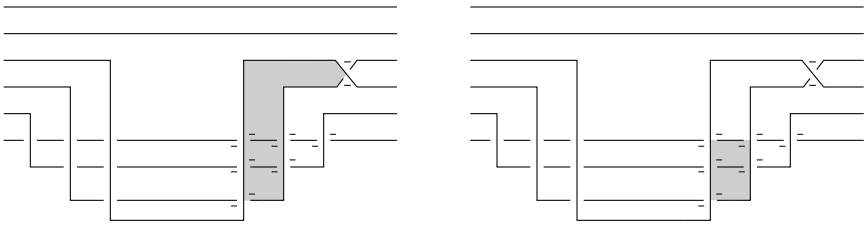

Figure 5.12: Disks appearing in $\partial_{i+1,i}$ with $a^{i+1,i}$ as a negative convex corner.

we add the following restrictions on I, D, and the pair $(i+1, i)$, then we can identify all such disks.

1. $|b^{i+1,i}| = 0$,

2. I is of type (1),

3. D occurs to the immediate left of a crossing q in L_Σ, and

4. q is a resolved crossing of Σ between strands $i+1$ and i.

Given these conditions, we see that the convex immersed polygons in which $a^{i+1,i}$ is a negative convex corner must sit to the left of q. In fact, $a^{i+1,i}$ only appears in $\partial_{i+1,i}q$ and $\partial_{i+1,i}a^{i+1,l}$ for $l < i$; see Figure 5.12. In $\partial_{i+1,i}a^{i+1,l}$, $a^{i+1,i}$ appears in the disk $a^{i+1,i}a^{i,l}$. Thus, the crossings q and $a^{i+1,l}$ have an odd number of disks in their boundary with a negative convex corner at $a^{i+1,i}$. Applying Lemma 5.3.2, we conclude that after the type II move that pushes strand $i+1$ over strand i the augmentation ϵ' satisfies:

1. $\epsilon'(b^{i+1,i}) = 1$,

2. $\epsilon'(a^{i+1,i}) = \epsilon(v)$ where $\partial b = a + v$,

3. $\epsilon'(q) = \epsilon(q) + 1$,

4. For all $l < i$, $\epsilon'(a^{i+1,l}) = \epsilon(a_j^{i+1,l})$ if and only if $\epsilon'(a^{i,l}) = 0$, and

5. $\epsilon' = \epsilon$ on all other crossings.

In Section 5.4.1 we showed that when I is an insert of type (1) - (4), $v = L(\partial b^{i+1,i})$ where ∂ is the boundary in $L_\Sigma^{d'}$; see Equation 5.4. Since I is an insert of type (1), we conclude $\epsilon(a^{i+1,i}) = \epsilon(L(\partial b^{i+1,i})) = \epsilon(a_j^{i+1,i})$.

Suppose we continue creating the dip D and with each new type II move we extend the augmentation so that it sends the new crossing in the B lattice to 0. By Lemma 5.4.1, the augmentation extends so that it takes the same value on the crossings that existed before the type II move. We need only compute the value of the extended augmentation on the new crossing in the A lattice. In particular, suppose we are considering the type II move pushing strand k over l where $(i+1, i) \prec (k, l)$. Then we extend ϵ over $b^{k,l}$ by $\epsilon'(b^{k,l}) = 0$ and by Lemma 5.4.1 and Equation 5.4, we have

$$\begin{aligned}
\epsilon'(a^{k,l}) &= \epsilon(v) \\
&= \epsilon(L(\partial b^{k,l})) \\
&= \epsilon(a_j^{k,l}) + \sum_{l<p<k} \epsilon(a_j^{k,p})\epsilon'(b^{p,l})
\end{aligned}$$

Since $\epsilon'(b^{p,l}) = 1$ if and only if $(p, l) = (i+1, i)$, we know that $\epsilon'(a^{k,l}) =$

$\epsilon(a_j^{k,l})$ if and only if $l \neq i$ or $\epsilon(a_j^{k,i+1}) = 0$.

Pulling this all together, we see that if we extend $\epsilon \in Aug(L_\Sigma^d)$ to $\epsilon' \in Aug(L_\Sigma^{d'})$ so that $\epsilon'(B) = \delta_{i+1,i}$ then ϵ' satisfies:

1. $\epsilon'(B) = \delta_{i+1,i}$,

2. $\epsilon'(q) = \epsilon(q) + 1$,

3. $\epsilon'(a^{i+1,i}) = \epsilon(a_j^{i+1,i})$,

4.

$$\epsilon'(a^{k,l}) = \begin{cases} \epsilon(a_j^{i+1,l}) + \epsilon'(a^{i,l}) & k = i+1, \text{ and } l < i \\ \epsilon(a_j^{k,i}) + \epsilon(a_j^{k,i+1}) & k > i+1, \text{ and } l = i \\ \epsilon(a_j^{k,l}) & \text{otherwise.} \end{cases} \tag{5.4}$$

5. $\epsilon' = \epsilon$ the all other crossings of L_Σ^d.

Note that Equation 5.4 is equivalent to $\epsilon'(A) = E_{i+1,i}\epsilon(A_j)E_{i+1,i}^{-1}$.

Definition 5.4.4. Let $\epsilon \in Aug(L_\Sigma^d)$. We say that ϵ is *extended by* $\delta_{i+1,i}$ if $\mu(i+1) = \mu(i)$ and after each type II move in the creation of a new dip D, we extend ϵ so that the extended augmentation $\epsilon' \in Aug(L_\Sigma^{d'})$ satisfies $\epsilon'(B) = \delta_{i+1,i}$.

The culmination of our work in this section is the following Lemma.

Lemma 5.4.5. Suppose L^d_Σ is a dipped diagram of the Ng resolution L_Σ. Let q be a crossing in L^d_Σ corresponding to a resolved crossing of Σ and with $|q| = 0$. Suppose we add a dip D to the right of the existing dip D_j and just to the left of q, thus creating a new dipped diagram $L^{d'}_\Sigma$. Suppose the insert I between D and D_j is of type (1). Let $\epsilon \in Aug(L^d_\Sigma)$. If ϵ is extended by $\delta_{i+1,i}$, then the stable tame isomorphism from Section 5.3 maps ϵ to $\epsilon' \in Aug(L^{d'}_\Sigma)$ where ϵ' satisfies:

1. $\epsilon'(B) = \delta_{i+1,i}$
2. $\epsilon'(A) = E_{i+1,i}\epsilon(A_j)E^{-1}_{i+1,i}$
3. $\epsilon'(q) = \epsilon(q) + 1$
4. $\epsilon' = \epsilon$ on all other crossings

The reader who has successfully made it through these somewhat tedious lemmata may wonder what the payoff is to all their diligence. The payoff is an algorithm that assigns to each augmentation in $Aug(L_\Sigma)$ an MCS in $MCS(\Sigma)$. The algorithm is easy because of the work we did building Lemma 5.4.5 and Corollary 5.4.3. We will put this algorithm on hold until Section 6.3.

We now have all of the necessary tools to start connecting MCSs and augmentations.

Chapter 6

Relating MCSs and Augmentations

In this chapter we detail connections between MCSs and augmentations. In particular, we show the existence of a surjective map $\widehat{\Psi} : \widehat{MCS}(\Sigma) \to Aug^{ch}(L_\Sigma)$. We also define a simple algorithm that associates an MCS $\mathcal{C}$ to an augmentation $\epsilon \in Aug(L_\Sigma)$ so that $\widehat{\Psi}([\mathcal{C}]) = [\epsilon]$. The last section details two algorithms that use MCS moves to place an arbitrary MCS in one of two standard forms. In addition, the many-to-one map between augmentations and graded normal rulings defined in [29] may be restated using the $S\bar{R}$-form of MCSs. The starting point for all of these connections is Lemma 5.2.1.

6.1 Augmentations on sufficiently dipped diagrams

Lemma 5.2.1 gives local formulae for the boundary map of a sufficiently dipped diagram L^d_Σ. From these formulae, we can write the system of equations $\epsilon \circ \partial$ as a system of local equations involving the dips and inserts of L^d_Σ.

Lemma 6.1.1. An algebra homomorphism $\epsilon : \mathcal{A}(L^d_\Sigma) \to \mathbb{Z}_2$ on a sufficiently dipped diagram L^d_Σ of a Ng resolution L_Σ with $\epsilon(1) = 1$ satisfies $\epsilon \circ \partial = 0$ if and only if:

1. $\epsilon(a_{s-1}^{i+1,i}) = 0$, where q_s is a crossing between strands $i+1$ and i,
2. $\epsilon(a_{r-1}^{k+1,k}) = 1$, where z_r is a crossing between strands $i+1$ and i,
3. $\epsilon(A_j)^2 = 0$, and
4. $\epsilon(A_j) = (I + \epsilon(B_j))\epsilon(\widetilde{A}_{j-1})(I + \epsilon(B_j))^{-1}$.

Proof. Let L^d_Σ be a sufficiently dipped diagram of L_Σ with dips $D_1, \ldots, D_m$ and inserts $I_1, \ldots, I_{m+1}$. Let q_i, ..., q_M denote the crossings found in the inserts of type (2), where the subscript on q refers to the subscript of the insert in which the crossing appears. Similarly, let z_j, ..., z_N denote the crossings found in the inserts of type (3), where the subscript on z refers to the subscript of the insert in which the crossing appears.

Recall from Theorem 5.2.1 that ∂ on a sufficiently dipped diagram is calculated as follows.

1. For all crossings q_s between strands $i+1$ and i, $\partial q_s = a_{s-1}^{i+1,i}$;
2. For all crossings z_r between strands $i+1$ and i, $\partial z_r = 1 + a_{r-1}^{k+1,k}$, where z_r is a crossing between strands $i+1$ and i;
3. $\partial A_j = A_j^2$; and
4. $\partial B_j = (I + B_j)A_j + \widetilde{A}_{j-1}(I + B_j)$.

Thus, given an algebra homomorphism $\epsilon : \mathcal{A}(L_\Sigma^d) \to \mathbb{Z}_2$ with $\epsilon(1) = 1$, $\epsilon \circ \partial = 0$ if and only if:

1. $\epsilon(\partial q_s) = a_{s-1}^{i+1,i} = 0$,
2. $\epsilon(\partial z_r) = 1 + \epsilon(a_{r-1}^{k+1,k}) = 0$,
3. $\epsilon(\partial A_j) = \epsilon(A_j^2) = 0$, and
4. $\epsilon(\partial B_j) = (I + \epsilon(B_j))\epsilon(A_j) + \epsilon(\widetilde{A}_{j-1})(I + \epsilon(B_j)) = 0$.

By rearranging terms, we see that the last equation is equivalent to:

$$\epsilon(A_j) = (I + \epsilon(B_j))\epsilon(\widetilde{A}_{j-1})(I + \epsilon(B_j))^{-1} \tag{6.1}$$

□

We will primarily concern ourselves with the set $Aug_{occ}(L^d_\Sigma) \subset Aug(L^d_\Sigma)$ containing the following type of augmentations.

Definition 6.1.2. Given a sufficiently dipped diagram L^d_Σ, we say an augmentation $\epsilon \in Aug(L^d_\Sigma)$ is *occ-simple* if:

1. ϵ sends all of the crossings of type q_s and z_r to 0,
2. For I_j of type (1), either $\epsilon(B_j) = 0$ or $\epsilon(B_j) = \delta_{k,l}$ for some $k > l$, and
3. For I_j of type (2), (3), or (4), $\epsilon(B_j) = 0$.

$Aug_{occ}(L^d_\Sigma)$ denotes the set of all such augmentations in $Aug(L^d_\Sigma)$. In addition, we say $\epsilon \in Aug_{occ}(L^d_\Sigma)$ is *minimal occ-simple* if for all I_j of type (1), $\epsilon(B_j) = \delta_{k,l}$ for some $k > l$. We let $Aug^m_{occ}(L_\Sigma)$ denote the set of all minimal occ-simple augmentations over all sufficiently dipped diagrams of L_Σ.

Remark 6.1.3. Suppose L^d_Σ is a sufficiently dipped diagram. If we slide the dips of L^d_Σ left and right without passing them by crossings, cusps or other dips, then the resulting sufficiently dipped diagram is topologically identical to the original. In particular, they both determine the same CE-DGA. Thus, we will not distinguish between two sufficiently dipped diagrams that differ by such a change. Note that this is similar in spirit to MCS move 0, which allows us to slide handleslide marks left and right as long as we do not slide them past crossings, cusps, or other handleslide marks.

Remark 6.1.4. The name *occ-simple* refers to the fact that the matrices $\epsilon(A_1), \ldots, \epsilon(A_m)$ of an occ-simple augmentation determine a sequence of ordered chain complexes $(C_1, \partial_1), \ldots, (C_m, \partial_m)$ on L^d_Σ. For each dip D_j, we form an ordered chain complex (C_j, ∂_j) as follows. Let t_j denote the x-coordinate of the vertical lines of symmetry of D_j in L^d_Σ. Label the m_j points of intersection in $L^d_\Sigma \cap (\{t_j\} \times \mathbb{R})$ by $y^j_1, \ldots, y^j_{m_j}$ and let C_j be a $\mathbb{Z}_2$ vector space generated by $y^j_1, \ldots, y^j_{m_j}$. We label the generators $y^j_1, \ldots, y^j_{m_j}$ based on their y-coordinate so that $y^j_1 > \ldots > y^j_{m_j}$. Each generator is graded by $|y^j_i| = \mu(i)$ where $\mu(i)$ is the Maslov potential of the strand in Σ corresponding to the strand y^j_i sits on in L^d_Σ. In this manner, C_j is a graded vector space with ordered generating set. Then the grading condition on ϵ and the fact that $\epsilon(A_j)^2 = 0$ implies that $\epsilon(A_j)$ is the matrix of a differential on C_j. Thus (C_j, ∂_j) is an ordered chain complex where $\partial_j = \epsilon(A_j)$.

The matrices $\epsilon(B_1), \ldots, \epsilon(B_n)$, along with the inserts $I_1, \ldots, I_n$, determine the relationship between consecutive ordered chain complexes $(C_{j-1}, \partial_{j-1})$ and (C_j, ∂_j). The following results describe the relationship between consecutive matrices $\epsilon(A_{j-1})$ and $\epsilon(A_j)$ in an occ-simple augmentation. Recall that the matrices $E_{k,l}$, $P_{i+1,i}$, J_i, and $\delta_{k,l}$ were defined in Section 3.1.1.

The following result is an immediate consequence of Lemma 6.1.1 and Definition 6.1.2.

Corollary 6.1.5. If L^d_Σ is a sufficiently dipped diagram and $\epsilon \in Aug_{occ}(L^d_\Sigma)$, then for each insert I_j:

1. If I_j is of type (1), then either $\epsilon(A_j) = \epsilon(\widetilde{A}_{j-1})$ or $\epsilon(A_j) = E_{k,l}\epsilon(\widetilde{A}_{j-1})E_{k,l}^{-1}$; and

2. If I_j of type (2), (3), or (4), then $\epsilon(A_j) = \epsilon(\widetilde{A}_{j-1})$.

We can further relate $\epsilon(A_j)$ and $\epsilon(A_{j-1})$ using the definition of $\widetilde{A}_{j-1}$ given in Section 5.2. The proof of Lemma 6.1.6 is essentially identical to the proof of Corollary 5.4.3.

Lemma 6.1.6. If L_Σ^d is a sufficiently dipped diagram and $\epsilon \in Aug_{occ}(L_\Sigma^d)$, then for each insert I_j:

1. If I is of type (1), then either

$$\epsilon(A_j) = \epsilon(A_{j-1}) \tag{6.2}$$

or

$$\epsilon(A_j) = E_{k,l}\epsilon(A_{j-1})E_{k,l}^{-1} \tag{6.3}$$

2. Suppose I_j is of type (2) with crossing q between strands $i+1$ and i. If $\epsilon(q) = 0$, then:

$$\epsilon(A_j) = P_{i+1,i}\epsilon(A_{j-1})P_{i+1,i}^{-1} \tag{6.4}$$

3. Suppose I is of type (3) with crossing z between strands $i+1$ and i.

   (a) Let $i+1 < u_1 < u_2 < \ldots < u_s$ denote the strands at dip D_{j-1} that satisfy $\epsilon(a_{j-1}^{u_1,i}) = \ldots = \epsilon(a_{j-1}^{u_s,i}) = 1$;

   (b) Let $v_r < \ldots < v_1$ denote the strands at dip D_{j-1} that satisfy $\epsilon(a_{j-1}^{i+1,v_1}) = \epsilon(a_{j-1}^{i+1,v_2}) = \ldots = \epsilon(a_{j-1}^{i+1,v_r}) = 1$; and

   (c) Let $E = E_{i,v_r} \ldots E_{i,v_1} E_{u_1,i+1} \ldots E_{u_s,i+1}$.

   Then, as matrices,:

$$\epsilon(A_j) = J_{i-1} E \epsilon(A_{j-1}) E^{-1} J_{i-1}^T \tag{6.5}$$

4. Suppose I is of type (4) and the resolved birth is between strands $i+1$ and i. Then, as matrices, $\epsilon(A_j)$ is obtained from $\epsilon(A_{j-1})$ by inserting two rows (columns) of zeros after row (column) $i-1$ in $\epsilon(A_{j-1})$ and then changing the $(i+1, i)$ entry to 1.

The matrix equations in Lemma 6.1.6 should look familiar. In fact, except in the first case of a type (1) insert, the equations are identical to the equations found in Definition 3.2.3. This connection allows us to assign an occ-simple augmentation to a Morse complex sequence.

6.1.1 Notation for keeping track of singularities.

We pause momentarily to define notation that will be used in the rest of this chapter to keep track of the resolved crossings and cusps that appear in L_Σ. Let $Q = \{q_1, \ldots, q_u\}$ denote the crossings in L_Σ that correspond to the resolved crossings of the front projection Σ. Similarly, let $Z = \{z_1, \ldots, z_n\}$ denote the crossings in L_Σ that correspond to the resolved right cusps in Σ. Let $Z' = \{z'_1, \ldots, z'_n\}$ denote the local maxima of L_Σ with respect to the x-axis. The local maximum z'_i corresponds to the local maximum created by a resolved right cusp of Σ, thus each z'_i pairs with the crossing z_i. Let $W = \{w_1, \ldots, w_p\}$ denote the local minima of L_Σ with respect to the x-axis. The local minima correspond to the resolved left cusps of Σ. We allow q_i, z_i, z'_i, and w_i to denote both the point on L_Σ and its x-coordinate. We also require that for each of the sets Q, Z, Z', and W, the indices on the elements correspond to the ordering from the x-axis. For example, $q_i < q_j$ as x-coordinates if and only if $i < j$; see Figure 6.1. Let

$$\widetilde{Z} = \bigcup_{i=1}^{n} [z_i, z'_i] \cup (-\infty, w_1] \cup [z'_n, \infty), \text{ and}$$
$$T = \mathbb{R} \setminus (Q \cup W \cup \widetilde{Z}).$$

T is the finite union of open intervals. We denote these open intervals by:

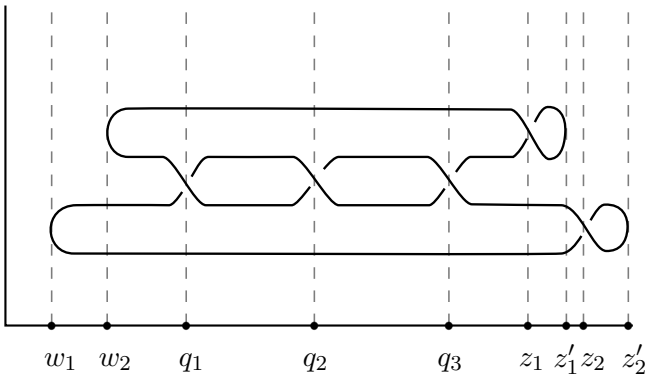

Figure 6.1: Labeling points in L_Σ.

$$T = \bigcup_{i=1}^{k} (a_i, b_i) \tag{6.6}$$

where $a_1 < \ldots < a_k$. In the following sections, we will often select points from the T and add dips to L_Σ in small neighborhoods of the selected points. We have constructed T so that the points chosen from T will correspond nicely to points in Σ.

6.1.2 Assigning $\epsilon_\mathcal{C} \in Aug(L_\Sigma^d)$ to an MCS $\mathcal{C}$

Given a front diagram Σ with resolution L_Σ, we show that MCSs correspond to minimal occ-simple augmentations of L_Σ. We will assign a minimal occ-simple augmentation $\epsilon_\mathcal{C}$ to an MCS $\mathcal{C}$ using an argument of Fuchs and Rutherford from [19].

Lemma 6.1.7. The set of MCSs of Σ, modulo MCS move 0, are in bijection

with minimal occ-simple augmentations in $Aug^m_{occ}(L_\Sigma)$.

Proof. Throughout this proof, we will use the notation defined in Section 6.1.1.

We begin by assigning an MCS to a minimal occ-simple augmentation $\epsilon \in Aug(L^d_\Sigma)$, where L^d_Σ is a sufficiently dipped diagram of L_Σ. Let t_j denote the x-coordinate of the vertical line of symmetry of the dip D_j of L^d_Σ. In a slight abuse of notation, we also let t_j denote the corresponding point on the x-axis of the front projection Σ. This correspondence comes from the Ng resolution procedure. Let $\epsilon \in Aug^m_{occ}(L_\Sigma)$ and let $(C_1, \partial_1), \ldots, (C_m, \partial_m)$ denote the sequence of ordered chain complexes constructed from ϵ in Remark 6.1.4. The relationship between consecutive differentials ∂_{j-1} and ∂_j is defined in Lemma 6.1.6. Since ϵ is minimal occ-simple, each insert I_j of type (1) satisfies $\partial_j = E_{k,l}\partial_{j-1}E^{-1}_{k,l}$ where $\epsilon(B_j) = \delta_{k,l}$ and $k > l$. In this case, place a handleslide mark between strands k and l in Σ just to the left of the point t_j. Then the matrix equations in Lemma 6.1.6 satisfied by ϵ are equivalent to the matrix equations in Definition 3.2.3. Thus the marked front projection we have constructed and the sequence $(C_1, \partial_1), \ldots, (C_m, \partial_m)$ form an MCS $\mathcal{C}$ on Σ. Note that if we slide the dips of L^d_Σ left and right without passing them by crossings, cusps or other dips, then the resulting augmentation on the new Lagrangian projection would map to an MCS $\mathcal{C}'$ that differs from $\mathcal{C}$ by MCS move 0.

This process is invertible. Let $\mathcal{C} \in MCS(\Sigma)$ be a Morse complex sequence of the front projection Σ with chain complexes $(C_1, \partial_1) \ldots (C_m, \partial_m)$. We begin by defining the placement of dips creating L^d_Σ. Afterwards, we

define an algebra homomorphism $\epsilon_{\mathcal{C}} : \mathcal{A}(L_\Sigma) \to \mathbb{Z}_2$ and show that it is an augmentation. Figure 6.2 gives an example of this process.

Let X denote the set of x-coordinates of the handleslide marks of $\mathcal{C}$. In a slight abuse of notation, we also let X denote the set of x-coordinates in the xy-plane that correspond by the Ng resolution procedure to the handleslide marks in $\mathcal{C}$. Choose a single point t_i from each connected component of $T \setminus X$ and label them so that $t_i < t_j$ if and only if $i < j$. The number of connected components in $T \setminus X$ is equal to the number of ordered chain complexes in $\mathcal{C}$, hence we have a t_i for each (C_i, ∂_i). For each t_j, add a dip D_j to the Ng resolution L_Σ in a small neighborhood of the point t_j. The resulting dipped diagram L_Σ^d is sufficiently dipped with m dips.

We define a $\mathbb{Z}_2$-valued map $\epsilon_{\mathcal{C}}$ on the crossings of L_Σ^d by:

1. $\epsilon_{\mathcal{C}}(q_s) = 0$ for all crossings q_s coming from a resolved crossing of Σ;
2. $\epsilon_{\mathcal{C}}(z_r) = 0$ for all crossings z_r coming from a resolved right cusp;
3. $\epsilon_{\mathcal{C}}(A_j) = \partial_j$ for all j;
4. If I_j is of type (1), then x_{j-1} denotes a handleslide mark between strands k and l. Let $\epsilon_{\mathcal{C}}(B_j) = \delta_{k,l}$; and
5. If I_j is of type (2), (3), or (4), then let $\epsilon_{\mathcal{C}}(B_j) = 0$.

We define $\epsilon_{\mathcal{C}}(1) = 1$ and extend $\epsilon_{\mathcal{C}}$ by linearity to an algebra homomorphism on $\mathcal{A}(L_\Sigma^d)$. We now show that $\epsilon_{\mathcal{C}}$ is an augmentation. If $\epsilon_{\mathcal{C}}$ is an

augmentation, then it is minimal occ-simple by construction. We must show $\epsilon_{\mathcal{C}} \circ \partial = 0$ and, for all crossings q of L^d_Σ, $\epsilon_{\mathcal{C}}(q) = 1$ implies $|q| = 0$.

Since $\epsilon_{\mathcal{C}}(q_r) = \epsilon_{\mathcal{C}}(z_s) = 0$ for all r and s, we only need to check the grading condition on the crossings in A_j and B_j. Suppose $\epsilon_{\mathcal{C}}(a_j^{k,l}) = 1$. Now $\epsilon_{\mathcal{C}}(a_j^{k,l}) = 1$ implies that in the ordered chain complex (C_j, ∂_j), the generator y_l^j appears in $\partial_j y_k^j$. The notation for the generators in (C_j, ∂_j) corresponds to the notation in Definition 3.2.3. Thus $\mu(y_k^j) = \mu(y_l^j) + 1$, where $\mu(y_i^j)$ denotes the Maslov potential of the strand in Σ corresponding to the generator y_i^j. Recall $|a_j^{k,l}| = \mu(l) - \mu(k) - 1$ where $\mu(i)$ denotes the Maslov potential of the corresponding strand i in Σ. Thus $\mu(y_k^j) = \mu(y_l^j) + 1$ implies $\mu(l) - \mu(k) - 1 = 0$ which implies $|a_j^{k,l}| = 0$.

If $\epsilon_{\mathcal{C}}(b_j^{k,l}) = 1$, then in the marked front projection of $\mathcal{C}$, a handleslide mark occurs in I_j between strands k and l. Thus $\mu(k) = \mu(l)$. Recall $|b_j^{k,l}| = \mu(l) - \mu(k)$. So $\mu(k) = \mu(l)$ implies $|b_j^{k,l}| = 0$.

It remains to show that $\epsilon_{\mathcal{C}} \circ \partial = 0$. We begin with crossing of the form q_r and z_s:

Let q_r denote a crossing corresponding to a resolved crossing of Σ between strands $i+1$ and i. Then by Remark 3.2.4 part 2, the $(i+1, i)$ entry of the matrix ∂_{r-1} is 0, hence $\epsilon_{\mathcal{C}}(a_{r-1}^{i+1,i}) = 0$. Thus we have:

$$\begin{aligned} \epsilon_{\mathcal{C}}(\partial q_r) &= \epsilon_{\mathcal{C}}(a_{r-1}^{i+1,i}) \\ &= 0 \end{aligned}$$

Let z_s denote a crossing corresponding to a resolved right cusp of Σ between strands $i+1$ and i. Then by Remark 3.2.4 part 2, the $(i+1,i)$ entry of the matrix ∂_{s-1} is 1, hence $\epsilon_{\mathcal{C}}(a_{s-1}^{i+1,i}) = 1$. Thus we have:

$$\begin{aligned}
\epsilon_{\mathcal{C}}(\partial z_s) &= \epsilon_{\mathcal{C}}(1 + a_{s-1}^{i+1,i}) \\
&= 1 + \epsilon_{\mathcal{C}}(a_{s-1}^{i+1,i}) \\
&= 0
\end{aligned}$$

For each a-lattice A_j, we have:

$$\begin{aligned}
\epsilon_{\mathcal{C}}(\partial A_j) &= \epsilon_{\mathcal{C}}(A_j)^2 \\
&= \partial_j^2 \\
&= 0
\end{aligned}$$

For each b-lattice B_j, Lemma 6.1.6 gives equivalent conditions for checking that $\epsilon_{\mathcal{C}}(\partial B_j) = 0$. In particular, for inserts of type (1), (2), and (3), we must show Equations 6.3, 6.4, and 6.3 hold for $\epsilon_{\mathcal{C}}$. By our construction, Equations 6.3, 6.4, and 6.3 are equivalent to Equations 3.2, 3.4, and 3.5. These last three equations hold because $\mathcal{C}_1$ is assumed to be an MCS. In the case of an insert of type (4), we must show that $\epsilon(A_j)$ is obtained from $\epsilon(A_{j-1})$ by inserting two rows (columns) of zeros after row (column) $i-1$ in $\epsilon(A_{j-1})$ and then changing the $(i+1,i)$ entry to 1. This follows from our

construction and part 3(c) of Definition 3.2.3. Thus $\epsilon_{\mathcal{C}}(\partial B_j) = 0$ for all j and so $\epsilon_{\mathcal{C}}$ is a minimal occ-simple augmentation on L^d_Σ.

Suppose we had chosen a different set of points $\{t'_1, \ldots, t'_m\}$ or we modified $\mathcal{C}$ by MCS move 0. Then the resulting dipped diagram $L^{d'}_\Sigma$ would differ from L^d_Σ by an isotopy of the Lagrangian projection that slides the dips left and right. By Remark 6.1.3, we consider the constructed augmentation $\epsilon'_{\mathcal{C}}$ to be equivalent to $\epsilon_{\mathcal{C}}$ in $Aug^m_{occ}(L_\Sigma)$. □

6.2 Defining $\Psi : MCS(\Sigma) \to Aug^{ch}(L_\Sigma)$

Lemma 6.1.7 gives an explicit construction of an augmentation $\epsilon_{\mathcal{C}}$ on a sufficiently dipped diagram L^d_Σ from an MCS $\mathcal{C} \in MCS(\Sigma)$. In this section, we will use this construction to build a map $\Psi : MCS(\Sigma) \to Aug^{ch}(L_\Sigma)$.

We begin with a brief discussion concerning the possible sequences of Lagrangian Reidemeister moves relating two Lagrangian projections. Two Legendrian isotopic knots K_1 and K_2 with Lagrangian projections L_1 and L_2 are related by a finite sequence of Lagrangian Reidemeister moves and have stable tame isomorphic CE-DGAs. In [6], Chekanov gives formulae for the stable tame isomorphisms of each of the Lagrangian Reidemeister moves. In Chapter 5, we used the tame isomorphism, $\psi : (\mathcal{A}(L_2), \partial) \to S_i(\mathcal{A}(L_1), \partial)$, of a type II move to keep track of the induced map $\Psi : Aug(L_1) \to Aug(L_2)$ and the subsequent bijection $\Psi_* : Aug^{ch}(L_1) \to Aug^{ch}(L_2)$.

In [22], Kalman proves that different sequences of Lagrangian Reidemeis-

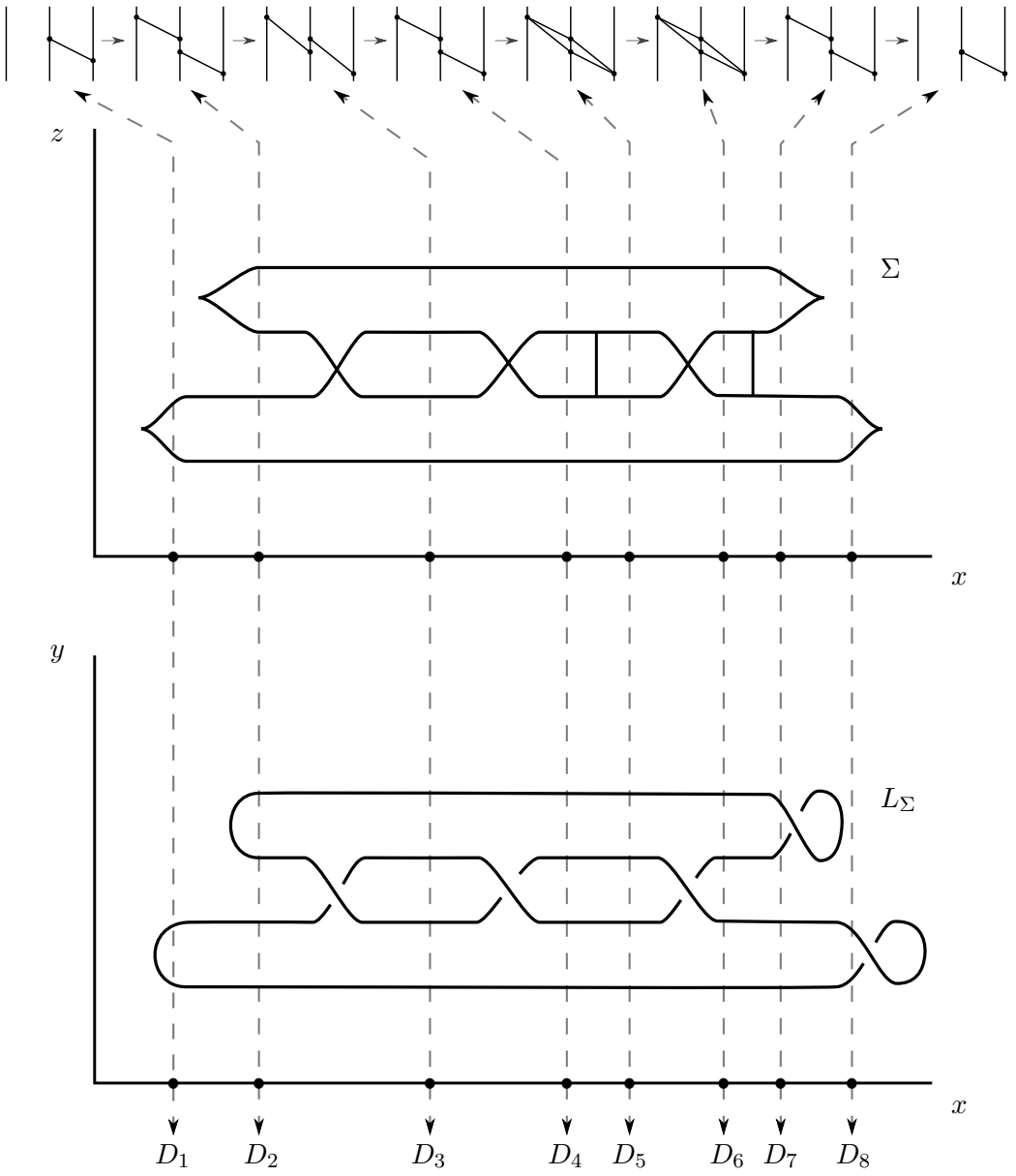

Figure 6.2: Assigning an augmentation to an MCS.

ter moves relating L_1 and L_2 may induce inequivalent maps between the contact homologies $H(L_1)$ and $H(L_2)$. We can think of two sequences of Reidemeister moves as giving two paths from K_1 to K_2 in the space of all knots Legendrian isotopic to K_1. If these two paths are homotopic in an appropriate sense, then Kalman proves that they induce equivalent maps between $H(L_1)$ and $H(L_2)$; see Theorem 3.7 in [22]. The proof of this theorem provide us with the tools necessary to construct the map $\Psi : MCS(\Sigma) \to Aug^{ch}(L_\Sigma)$. These tools show that $\Psi : MCS(\Sigma) \to Aug^{ch}(L_\Sigma)$ is well-defined in an appropriate sense.

The dipped diagram L^d_Σ from Lemma 6.1.7 and the Ng resolution L_Σ represent Legendrian isotopic Legendrian knots. Hence, there exists a stable tame isomorphism ϕ between $\mathcal{A}(L^d_\Sigma)$ and $\mathcal{A}(L_\Sigma)$. By Proposition 4.2.1, ϕ induces a bijection $\Phi : Aug^{ch}(L^d_\Sigma) \to Aug^{ch}(L_\Sigma)$. In this manner, we may assign an element of $Aug^{ch}(L_\Sigma)$ to $\mathcal{C}$ by looking at the image of $[\epsilon_\mathcal{C}]$ under Φ. However, a different stable tame isomorphism between $\mathcal{A}(L^d_\Sigma)$ and $\mathcal{A}(L_\Sigma)$ may determine a different bijection from $Aug^{ch}(L^d_\Sigma)$ to $Aug^{ch}(L_\Sigma)$. In the definition of $\Psi : MCS(\Sigma) \to Aug^{ch}(L_\Sigma)$, we choose to restrict our attention to a certain class of stable tame isomorphisms coming from type II and II^{-1} moves on L^d_Σ. We will use results from [22] to show that our definition of $\Psi : MCS(\Sigma) \to Aug^{ch}(L_\Sigma)$ is well-defined up to certain paths of Lagrangian Reidemeister moves.

The following results from [22] allow us to modify paths of Lagrangian Reidemeister moves by removing canceling pairs and commuting pairs of

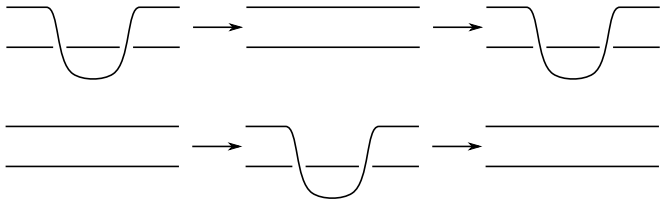

Figure 6.3: The top row is a type II^{-1} move followed by a type II move. The bottom row is a type II move followed by a type II^{-1} move.

moves that are far away from each other. Let L be a Lagrangian projection with CE-DGA $(\mathcal{A}(L), \partial)$. Suppose we perform a type II^{-1} move and thus create a new Lagrangian projection L' with two fewer crossings. In the following results, τ denotes the tame isomophism from $(\mathcal{A}(L), \partial)$ to the stabilization $S_i(\mathcal{A}(L'), \partial')$ defined in [6].

Proposition 6.2.1 ([22])**.** Suppose we perform a type II move on L creating crossings b and a and then perform a type II^{-1} move removing crossings b and a; see the bottom row of Figure 6.3. Then the composition of DGA morphisms $\tau \circ \psi^{-1} : (\mathcal{A}(L), \partial) \to (\mathcal{A}(L), \partial)$ is equal to the identity.

Suppose we perform a type II^{-1} move on L removing crossings b and a and then perform a type II move reintroducing crossings b and a; see the top row of Figure 6.3. Then the composition of DGA morphisms $\psi^{-1} \circ \tau : (\mathcal{A}(L), \partial) \to (\mathcal{A}(L), \partial)$ is chain homotopic to the identity.

Proposition 6.2.2 ([22])**.** Suppose L_1 and L_2 are related by two consecutive moves of type II or II^{-1}. We will call these moves A and B. Suppose the crossings involved in A and B form disjoint sets. Then the composition of DGA morphisms constructed by performing move A and then move B is chain

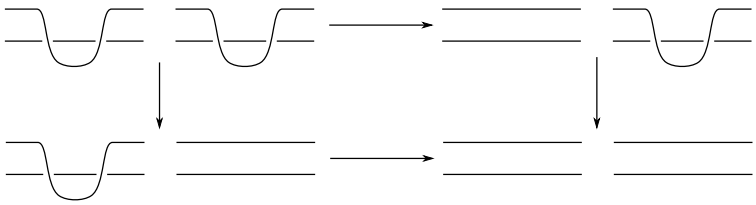

Figure 6.4: Two "far away" type II^{-1} moves.

homotopic to the composition of DGA morphisms constructed by performing move B and then move A; see Figure 6.4.

Proposition 6.2.2 follows from Case 1 of Theorem 3.7 in [22].

Corollary 6.2.3. In Proposition 6.2.1, the compositions $\tau \circ \psi^{-1}$ and $\psi^{-1} \circ \tau$ are both chain homotopic to the identity. By Lemma 4.2.3, both maps induce the identity map on $Aug^{ch}(\mathcal{A}(L))$. Thus, removing these pairs of moves from a sequence of Lagrangian Reidemeister moves does not change the resulting bijection on augmentation chain homotopy classes.

In Proposition 6.2.2, the order in which we perform moves A and B does not effect the chain homotopy class of the resulting DGA morphism. By Lemma 4.2.3, in a sequence of Lagrangian Reidemeister moves, we can commute these moves without changing the resulting bijection on augmentation chain homotopy classes.

6.2.1 Dipping/undipping paths for L^d_Σ

Suppose L^d_Σ has dips $D_1, \ldots, D_m$. Let $t_1, \ldots, t_m$ denote the x-coordinates of the vertical lines of symmetry of the dips $D_1, \ldots, D_m$ in L^d_Σ.

Definition 6.2.4. A *dipping/undipping path for* L_Σ^d is a finite-length monomial w in the elements of the set $G = \{s_1^\pm, \ldots, s_n^\pm, t_1^\pm, \ldots, t_m^\pm\}$. We require that w satisfies:

1. Each s_i in w denotes a point on the x-axis in T away from the dips $D_1, \ldots, D_m$, where T is as defined in Section 6.1.1; and

2. As we read w from left to right, the appearances of s_i alternate between s_i^+ and s_i^-, beginning with s_i^+ and ending with s_i^-. The appearances of t_i alternate between t_i^- and t_i^+, beginning with t_i^- and ending with t_i^- and each t_i is required to appear at least once.

Each dipping/undipping path w is a prescription for adding and removing dips from L_Σ^d. In particular, s_i^+ tells us to perform the sequence of type II moves that introduce a dip in a small neighborhood of s_i. The order in which these type II moves occur is the same as the order used in the definition of a dip in Section 5.1. The letter s_i^- tells us to perform a sequence of type II^{-1} so as to remove the dip that sits in a small neighborhood of s_i. The order in which these type II^{-1} moves occurs is the opposite of the order used in s_i^+. The elements t_i^+ and t_i^- work similarly. We perform these moves on L_Σ^d by reading w from left to right. The conditions we have placed on w ensure that we are left with L_Σ after performing all of the prescribed dips and undips.

Let $w_0 = t_m^- t_{m-1}^- \ldots t_1^-$. Then w_0 tells us to undip $D_1, \ldots, D_m$ beginning with D_m and working to D_1. Each w also determines a stable

tame isomorphism ψ_w from $\mathcal{A}(L^d_\Sigma)$ to $\mathcal{A}(L_\Sigma)$ which determines a bijection $\Psi_w : Aug^{ch}(L^d_\Sigma) \to Aug^{ch}(L_\Sigma)$.

We are now in a position to define the map Ψ from Lemma 1.2.2 in Chapter 1.

Definition 6.2.5. We define $\Psi : MCS(\Sigma) \to Aug^{ch}(L_\Sigma)$ by $\Psi(\mathcal{C}) = \Psi_{w_0}([\epsilon_\mathcal{C}])$.

As we will see, dipping/undipping paths play an integral part in extending $\Psi : MCS(\Sigma) \to Aug^{ch}(L_\Sigma)$ to a map $\widehat{\Psi} : \widehat{MCS}(\Sigma) \to Aug^{ch}(L_\Sigma)$. The following result implies that the definition of Ψ is independent of dipping/undipping paths.

Lemma 6.2.6. If w and v are dipping/undipping paths for L^d_Σ, then $\Psi_w = \Psi_v$.

Proof. We may assume $v = w_0$. The path w determines a sequence of type II and II^{-1} moves on L^d_Σ. By part 2 of Corollary 6.2.3, we may reorder type II and II^{-1} moves that are "far apart" without changing the chain homotopy type of the resulting map from $\mathcal{A}(L^d_\Sigma)$ and $\mathcal{A}(L_\Sigma)$. If s_i^+ appears in w, then the next appearance of s_i is the letter s_i^- to the right of s_i^+. The letters between s_i^- and s_i^+ represent type II and II^{-1} moves that are far away from s_i^- and s_i^+. Thus, by repeated applications of part 2 of Corollary 6.2.3, we may commute s_i^- past the other letters so that s_i^- is the letter immediately following s_i^+. This does not change the chain homotopy type of the resulting map from $\mathcal{A}(L^d_\Sigma)$ and $\mathcal{A}(L_\Sigma)$.

By our ordering of the type II moves in s_i^+ and the type II^{-1} moves in s_i^-, the last type II move in s_i^+ creates two new crossings which are removed by the first type II^{-1} move in s_i^-. Since these two moves occur in succession, we may remove them, using Corollary 6.2.3, without changing the chain homotopy type of the resulting map from $\mathcal{A}(L_\Sigma^d)$ and $\mathcal{A}(L_\Sigma)$. In this manner, we remove all of the type II and II^{-1} in s_i^+ and s_i^- and, hence, we remove the letters s_i^+ and s_i^- from w.

In this manner, we remove all of the pairs of s_i^+, s_i^- from w. By the same argument we remove pairs of letters t_i^+, t_i^-. The resulting dipping/undipping path, which we denote w', only contains the letters $t_1^-, \ldots, t_m^-$. We may rearrange these letters using part 2 of Corollary 6.2.3 so that $w' = w_0$. These moves do not change the chain homotopy type of the resulting map from $\mathcal{A}(L_\Sigma^d)$ and $\mathcal{A}(L_\Sigma)$, thus, by Lemma 4.2.3, $\Psi_w = \Psi_{w_0}$. □

Corollary 6.2.7. The map $\Psi : MCS(\Sigma) \to Aug^{ch}(L_\Sigma)$ is independent of dipping/undipping paths. If w is a dipping/undipping path for L_Σ^d, then $\Psi_w([\epsilon_\mathcal{C}]) = \Psi_{w_0}([\epsilon_\mathcal{C}]) = \Psi(\mathcal{C})$.

6.3 Algorithm 1: Associating an MCS to $\epsilon \in Aug(L_\Sigma)$

In this section, we prove that $\Psi : MCS(\Sigma) \to Aug^{ch}(L_\Sigma)$ is surjective. We do so by giving an explicit algorithm that assigns to each augmentation

in $Aug(L_\Sigma)$ an MCS in $MCS(\Sigma)$. The algorithm follows from our work in Lemma 5.4.5 and Corollary 5.4.3. In particular, this algorithm proves Lemma 1.2.3 from Chapter 1.

Theorem 6.3.1. $\Psi : MCS(\Sigma) \to Aug^{ch}(L_\Sigma)$ is surjective.

Proof. We will prove this theorem using the following algorithm. Recall the notation established in Section 6.1.1. We will select points from each connected component (a_i, b_i) in T. These points will indicate the locations of the dips that we will add to L_Σ. Let $\epsilon \in Aug(L_\Sigma)$. We select elements from the open intervals of T as follows. Let (a_i, b_i) be an open interval of T. If $b_i \in Q$ and $\epsilon(b_i) = 1$ then choose two elements of (a_i, b_i). Otherwise choose a single element in (a_i, b_i). Label all of the elements picked from T by $t_1, \ldots, t_n$ and order them so that $t_i < t_j$ if and only if $i < j$. We have chosen the t_i so that, for each $1 < i \leq n$, $L_\Sigma \cap ((t_{i-1}, t_i) \times \mathbb{R})$ is isotopic to one of the inserts in Figure 5.3. Thus if we add a dip to L_Σ in a small neighborhood of each t_i, the resulting dipped diagram L_Σ^d will be sufficiently dipped. Our algorithm will add the dips one at a time from t_1 to t_n. As we add dips from left to right in L_Σ, we will extend the augmentation ϵ so that the resulting augmentation on L_Σ^d is occ-simple. Along the way we will abuse notation by letting ϵ denote the result of extending the augmentation over each dip. The algorithm is inductive in the sense that we add dips one at a time from t_1 to t_n and, at each t_j, we extend ϵ to the crossings of D_j.

We comment briefly on the set $\{t_1, \ldots, t_m\}$. Suppose we had chosen a different set of points $\{t'_1, \ldots, t'_m\}$. Then the resulting dipped diagram $L_\Sigma^{d'}$

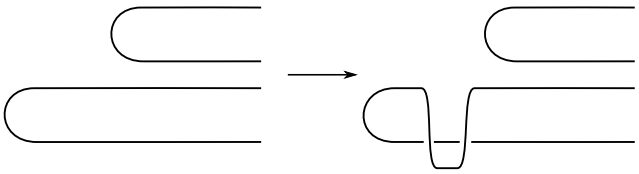

Figure 6.5: The first dip created by Algorithm 1.

would differ from L_Σ^d by an isotopy of the Lagrangian projection that slides the dips left and right. The CE-DGA does not detect this difference and, thus, we will not keep track of the difference.

The process of adding dips to L_Σ proceeds as follows. We begin with t_1. Note that t_1 occurs between the two local minima w_1 and w_2; see Figure 6.5. We add the dip D_1 in a small neighborhood of t_1. This requires a single type II move. Let $L_\Sigma^{d_1}$ denote the projection resulting from adding the first dip. We extend ϵ by requiring $\epsilon(b_1^{2,1}) = 0$. In the dipped projection, $\partial_1(b_1^{2,1}) = 1 + a_1^{2,1}$. Hence, $\epsilon(a_1^{2,1}) = 1$. Suppose we have added dips to L_Σ for all t_i with $i < j$. We now add a dip in a small neighborhood of t_j and indicate how to extend the augmentation ϵ over the new crossings in D_j. Recall that t_j sits in some connected component (a, b) of T. How we extend ϵ over D_j depends on t_j, the set $\{t_1, \ldots, t_n\}$, and the open interval (a, b):

1. If $\{t_1, \ldots t_n\} \cap (a, b) = t_j$, then we extend ϵ by 0 as in Definition 5.4.2, i.e. $\epsilon(B_j) = 0$. The resulting relationship between $\epsilon(A_j)$ and $\epsilon(A_{j-1})$ depends on the insert I_j and is detailed in Corollary 5.4.3.

2. If $\{t_1, \ldots t_n\} \cap (a, b) = \{t_j, t_{j+1}\}$, then we extend ϵ by 0 as in Definition 5.4.2. The resulting relationship between $\epsilon(A_j)$ and $\epsilon(A_{j-1})$

depends on the insert I_j and is detailed in Corollary 5.4.3.

3. If $\{t_1, \dots t_n\} \cap (a, b) = \{t_{j-1}, t_j\}$, then by the way we constructed $\{t_1, \dots t_n\}$ we know $b \in Q$ and $\epsilon(b) = 1$. Suppose b represents a crossings between strands $i+1$ and i. We extend ϵ by $\delta_{i+1,i}$ as in Definition 5.4.4, i.e. $\epsilon(B_j) = \delta_{i+1,i}$. Note that after the extension $\epsilon(b) = 0$. The resulting relationship between $\epsilon(A_j)$ and $\epsilon(A_{j-1})$ is detailed in Lemma 5.4.5.

The resulting augmentation is minimal occ-simple by construction. Let $\widetilde{\epsilon}$ denote the resulting augmentation on L^d_Σ. By Lemma 6.1.7, $\widetilde{\epsilon}$ has an associated MCS $\mathcal{C}$ such that $\epsilon_\mathcal{C} = \widetilde{\epsilon}$. By definition, $\Psi(\mathcal{C}) = \Psi_{w_0}([\epsilon_\mathcal{C}])$. The dipping/undipping path w_0 tells us to undip $t_1, \dots, t_n$ in reverse order. In particular, this is the inverse of the process we used to create $\widetilde{\epsilon}$ on L^d_Σ. Thus $\Psi(\mathcal{C}) = \Psi_{w_0}([\widetilde{\epsilon}]) = [\epsilon]$ and so $\Psi : MCS(\Sigma) \to Aug^{ch}(L_\Sigma)$ is surjective.

□

Remark 6.3.2. We can explicitly describe the MCS $\mathcal{C}$ associated to $\widetilde{\epsilon}$ in Theorem 6.3.1. Let $q_{j_1}, \dots, q_{j_l}$ denote the resolved crossings of L_Σ on which $\epsilon = 1$. Define the marked front projection $\mathcal{C}$ on Σ to have a handleslide mark just to the left of each of the crossings $q_{j_1}, \dots, q_{j_l}$; see Figure 6.6. Each handleslide mark begins and ends on the two strands involved in the crossing. The resulting marked front diagram is the MCS defined by the bijection in Lemma 6.1.7.

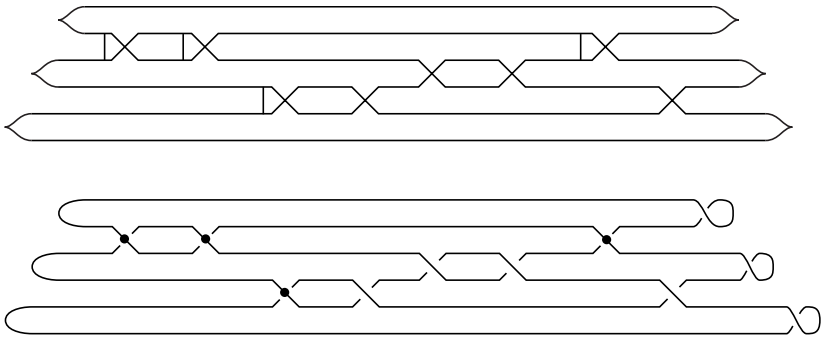

Figure 6.6: The dots in the bottom figure indicate the augmented crossings of $\epsilon \in Aug(L_\Sigma)$. The top figure shows the resulting MCS $\mathcal{C}_\epsilon$ from Algorithm 1.

6.4 Defining $\widehat{\Psi} : \widehat{MCS}(\Sigma) \to Aug^{ch}(L_\Sigma)$

In this section, we prove Theorem 1.2.1 from Chapter 1. In particular,

Theorem 6.4.1. The map $\widehat{\Psi} : \widehat{MCS}(\Sigma) \to Aug^{ch}(L_\Sigma)$ defined by $\widehat{\Psi}([\mathcal{C}]) = \Psi(\mathcal{C})$ is a well-defined, surjective map.

We prove this theorem by constructing explicit chain homotopies between $\Psi(\mathcal{C}_1)$ and $\Psi(\mathcal{C}_2)$ when $\mathcal{C}_1 \sim \mathcal{C}_2$. We begin this section by discussing chain homotopies on sufficiently dipped diagrams.

6.4.1 Chain homotopies on sufficiently dipped diagrams

In Section 6.1, we used the formulae from Lemma 5.2.1 to restate the augmentation property $\epsilon \circ \partial = 0$ as a system of local equations involving the dips and inserts of L_Σ^d. In this section, we will follow a similar line of thought to restate the chain homotopy property $\epsilon_1 - \epsilon_2 = H \circ \partial$ as a system of local

equations.

Let $\epsilon_1, \epsilon_2 \in Aug(L^d_\Sigma)$ where L^d_Σ is a sufficiently dipped diagram of the Ng resolution L_Σ. Let $\widetilde{Q}$ denote the set of crossings of L^d_Σ. $\widetilde{Q}$ includes the crossings in Q and Z from the resolution of Σ along with the crossings in the dips. By Corollary 4.1.4, a map $H : \widetilde{Q} \to \mathbb{Z}_2$ that has support on the crossings of grading -1 may be extended by linearity and the derivation product property to a map $H : (\mathcal{A}(L^d_\Sigma), \partial) \to \mathbb{Z}_2$ with support on $\mathcal{A}_{-1}(L^d_\Sigma)$. Then H is a chain homotopy between ϵ_1 and ϵ_2 if and only if $\epsilon_1 - \epsilon_2 = H \circ \partial$ on $\widetilde{Q}$.

Lemma 6.4.2. Let $\epsilon_1, \epsilon_2 \in Aug(L^d_\Sigma)$ where L^d_Σ is a sufficiently dipped diagram of the Ng resolution L_Σ. Suppose the linear map $H : (\mathcal{A}(L^d_\Sigma), \partial) \to \mathbb{Z}_2$ satisfies the derivation product property and has support on crossings of grading -1. Then H is a chain homotopy between ϵ_1 and ϵ_2 if and only if:

1. For all q_r and z_s, $\epsilon_1 - \epsilon_2 = H \circ \partial$;

2. For all A_j,

$$\epsilon_1(A_j) = (I + H(A_j))\epsilon_2(A_j)(I + H(A_j))^{-1} \tag{6.7}$$

3. For all B_j,

$$\begin{aligned} H(B_j)\epsilon_2(A_j) + \epsilon_1(A_{j-1})H(B_j) &= (I + \epsilon_1(B_j))(I + H(A_j)) \\ &+ (I + H(\widetilde{A}_{j-1}))(I + \epsilon_2(B_j)) \end{aligned}$$

Proof. For each A_j, $\epsilon_1 - \epsilon_2(A_j) = H \circ \partial(A_j)$ is equivalent to:

$$\begin{aligned}
\epsilon_1 - \epsilon_2(A_j) &= H \circ \partial(A_j) \\
&= H(A_j A_j) \\
&= H(A_j)\epsilon_2(A_j) + \epsilon_1(A_j)H(A_j)
\end{aligned}$$

Note that the third equality follows from the derivation property of H. By rearranging terms, we see that $\epsilon_1 - \epsilon_2(A_j) = H \circ \partial(A_j)$ is equivalent to:

$$\epsilon_1(A_j) = (I + H(A_j))\epsilon_2(A_j)(I + H(A_j))^{-1}$$

For each B_j, $\epsilon_1 - \epsilon_2(B_j) = H \circ \partial(B_j)$ is equivalent to:

$$\begin{aligned}
\epsilon_1 - \epsilon_2(B_j) &= H \circ \partial(B_j) \\
&= H((I + B_j)A_j + \widetilde{A}_{j-1}(I + B_j)) \\
&= H(A_j + B_j A_j + \widetilde{A}_{j-1} + \widetilde{A}_{j-1}B_j)) \\
&= H(A_j) + H(B_j)\epsilon_2(A_j) + \epsilon_1(B_j)H(A_j) + \\
&+ H(\widetilde{A}_{j-1}) + H(\widetilde{A}_{j-1})\epsilon_2(B_j) + \epsilon_1(\widetilde{A}_{j-1})H(B_j) \\
&= (I + \epsilon_1(B_j))H(A_j) + H(\widetilde{A}_{j-1})(I + \epsilon_2(B_j)) + \\
&+ H(B_j)\epsilon_2(A_j) + \epsilon_1(\widetilde{A}_{j-1})H(B_j)
\end{aligned}$$

We rewrite this formula to emphasize the role of $H(B_j)$.

$$\begin{aligned} H(B_j)\epsilon_2(A_j) + \epsilon_1(A_{j-1})H(B_j) &= \epsilon_1(B_j) + (I + \epsilon_1(B_j))H(A_j) \\ &+ H(\widetilde{A}_{j-1})(I + \epsilon_2(B_j)) + \epsilon_2(B_j) \end{aligned}$$

Since we are working over $\mathbb{Z}_2$, we can rewrite the right hand side so that:

$$\begin{aligned} H(B_j)\epsilon_2(A_j) + \epsilon_1(A_{j-1})H(B_j) &= (I + \epsilon_1(B_j))(I + H(A_j)) \\ &+ (I + H(\widetilde{A}_{j-1}))(I + \epsilon_2(B_j)) \end{aligned}$$

□

We will use the matrix equations of Lemma 6.4.2 to construct explicit chain homotopies showing that Ψ maps equivalent MCSs to chain homotopic augmentations. We will restrict our attention to occ-simple augmentations and in nearly every situation build chain homotopies that satisfy $H(B_j) = 0$ for all j. These added assumptions simplify the task of constructing chain homotopies. The next Corollary follows immediately from Lemma 6.4.2 and Definition 6.1.2.

Corollary 6.4.3. Let $\epsilon_1, \epsilon_2 \in Aug_{occ}(L^d_\Sigma)$ where L^d_Σ is a sufficiently dipped diagram of the Ng resolution L_Σ. Suppose the linear map $H : (\mathcal{A}(L^d_\Sigma), \partial) \to \mathbb{Z}_2$ satisfies the derivation product property, has support on crossings of grading

-1, and satisfies $H(B_j) = 0$ for all j. Then H is a chain homotopy between ϵ_1 and ϵ_2 if and only if:

1. For all q_r and z_s, $\epsilon_1 - \epsilon_2 = H \circ \partial$;

2. For all A_j,

$$\epsilon_1(A_j) = (I + H(A_j))\epsilon_2(A_j)(I + H(A_j))^{-1} \tag{6.8}$$

3. For B_j with I_j of type (1),

$$\epsilon_1(B_j) + (I + \epsilon_1(B_j))H(A_j) = H(A_{j-1})(I + \epsilon_2(B_j)) + \epsilon_2(B_j) \tag{6.9}$$

4. For B_j with I_j of type (2), (3), or (4),

$$H(A_j) = H(\widetilde{A}_{j-1}) \tag{6.10}$$

6.4.2 $\mathcal{C}_1 \sim \mathcal{C}_2$ implies $\Psi(\mathcal{C}_1) = \Psi(\mathcal{C}_2)$

In this section we prove Lemma 1.2.4 from Chapter 1. In particular,

Lemma 6.4.4. $\mathcal{C}_1 \sim \mathcal{C}_2$ implies $\Psi(\mathcal{C}_1) = \Psi(\mathcal{C}_2)$

Proof. It is sufficient to consider the case when $\mathcal{C}_1$ and $\mathcal{C}_2$ differ by a single MCS move.

Let $\epsilon_{\mathcal{C}_1} \in Aug(L_\Sigma^{d_1})$ and $\epsilon_{\mathcal{C}_2} \in Aug(L_\Sigma^{d_2})$ be as defined in Lemma 6.1.7. Since each MCS move is local, we may assume $L_\Sigma^{d_1}$ and $L_\Sigma^{d_2}$ have identical

dips outside of the region in which the MCS move takes place. The dotted lines in Figures 6.7 and 6.8 indicate the locations of dips in dipped resolutions $L_\Sigma^{d_1}$ and $L_\Sigma^{d_2}$. The index j in Figures 6.7 and 6.8 denotes the dip D_j. This provides us with a point of reference so that we can talk about the dips and inserts in the local region of the MCS move.

We would like to compare the chain homotopy classes of $\epsilon_{\mathcal{C}_1}$ and $\epsilon_{\mathcal{C}_2}$. In order to do so, $\epsilon_{\mathcal{C}_1}$ and $\epsilon_{\mathcal{C}_2}$ must be augmentations on the same dipped diagram. In the case of MCS moves 1-21, we add 0, 1, or 2 additional dips to $L_\Sigma^{d_1}$ and $L_\Sigma^{d_2}$, so that the resulting dipped diagrams are identical. In the case of the Explosion move, we may have to add many more dips. Table 6.2 indicates which dotted lines in Figures 6.7 and 6.8 represent dips that are added to $L_\Sigma^{d_1}$ and $L_\Sigma^{d_2}$. We let L_Σ^{d} denote the resulting dipped diagram.

As we add dips to $L_\Sigma^{d_1}$ and $L_\Sigma^{d_2}$, we extend $\epsilon_{\mathcal{C}_1}$ and $\epsilon_{\mathcal{C}_2}$ by 0. By Corollary 5.4.1 we can keep track of the extensions of $\epsilon_{\mathcal{C}_1}$ and $\epsilon_{\mathcal{C}_2}$ after each dip. In fact, the extensions will be occ-simple. We let $\widetilde{\epsilon}_{\mathcal{C}_1}$ and $\widetilde{\epsilon}_{\mathcal{C}_2}$ denote the extensions of $\epsilon_{\mathcal{C}_1}$ and $\epsilon_{\mathcal{C}_2}$ in $Aug(L_\Sigma^d)$. For each MCS move, we show that $\widetilde{\epsilon}_{\mathcal{C}_1}$ and $\widetilde{\epsilon}_{\mathcal{C}_2}$ are chain homotopic by giving explicit chain homotopies. Since $\widetilde{\epsilon}_{\mathcal{C}_1}$ and $\widetilde{\epsilon}_{\mathcal{C}_2}$ are occ-simple, we use the matrix equations in Corollary 6.4.3 and Lemma 6.4.2 to construct chain homotopies. In particular, for all MCS moves except move 6 and the Explosion move, the chain homotopy H between $\widetilde{\epsilon}_{\mathcal{C}_1}$ and $\widetilde{\epsilon}_{\mathcal{C}_2}$ is given in Table 6.1. The chain homotopy for MCS move 6 is as follows:

$$H(A_{j-1}) = \epsilon_1(B_{j-1}) + \epsilon_2(B_{j-1}) + \epsilon_1(B_{j-1})\epsilon_2(B_{j-1})$$

$$H(A_j) = H(A_{j-1}) + \epsilon_2(B_{j-1}) + H(A_{j-1})\epsilon_2(B_{j-1})$$

$H = 0$ on all other crossings.

The case of the Explosion move is slightly more complicated. In particular, just before the explosion, the chain complex (C_j, ∂_j) in $\mathcal{C}_1$ and $\mathcal{C}_2$ has a pair of generators $y_l < y_k$ such that $|y_l| = |y_k| + 1$. Let $y_{u_1} < y_{u_2} < \ldots < y_{u_s}$ denote the generators of C_j satisfying $\langle \partial y | y_k \rangle = 1$; see the left three arrows in Figure 3.8. Let $y_{v_r} < \ldots < y_{v_1} < y_i$ denote the generators of C_j appearing in $\partial_j y_l$; see the right two arrows in Figure 3.8. The explosion move introduces the handleslide marks $E_{k,v_r}, \ldots E_{k,v_1}, E_{u_1,l}, \ldots, E_{u_s,l}$. We assume that $\mathcal{C}_2$ includes these marks and $\mathcal{C}_1$ does not. Then we introduce $r + s$ dips to the right of D_j in $L_\Sigma^{d_1}$. As we add dips to $L_\Sigma^{d_1}$, we extend $\epsilon_{\mathcal{C}_1}$ by 0. By Corollary 5.4.1 we can keep track of the extensions of $\epsilon_{\mathcal{C}_1}$ after each dip. The chain homotopy between $\widetilde{\epsilon}_{\mathcal{C}_1}$ and $\epsilon_{\mathcal{C}_2}$ is given by:

$$\text{For all } 1 \leq i \leq r + s - 1,\ H(A_{j+i}) = \sum_{k=1}^{i} \epsilon_{\mathcal{C}_2}(B_{j+k})$$

$$H(B_{j+r+s}) = \delta_{k,l}$$

$H = 0$ on all other crossings.

Since each map H defined above has few non-zero entries, it is easy to check that H has support on generators with grading -1. Thus we need only check that the extension of H by linearity and the derivation product property satisfies $\widetilde{\epsilon}_{\mathcal{C}_1} - \widetilde{\epsilon}_{\mathcal{C}_2} = H \circ \partial$. In the case of MCS moves 1-21, this is equivalent to checking that H solves the matrix equations in Corollary 6.4.3. In the case of the Explosion move, we must check that H solves the matrix equations in Lemma 6.4.2. We leave it to the reader to check that the matrix equations in Corollary 6.4.3 and Lemma 6.4.2 hold for each MCS move.

The maps H given above and in Table 6.1 were constructed using the following process. The augmentations $\widetilde{\epsilon}_{\mathcal{C}_1}$ and $\widetilde{\epsilon}_{\mathcal{C}_2}$ are equal on dips outside of the region of the MCS move, thus $\widetilde{\epsilon}_{\mathcal{C}_1} - \widetilde{\epsilon}_{\mathcal{C}_2} = 0$ on these dips. Hence, $H = 0$ satisfies $\widetilde{\epsilon}_{\mathcal{C}_1} - \widetilde{\epsilon}_{\mathcal{C}_2} = H \circ \partial$ on the crossings of these dips. Within the region of the MCS moves we can write down explicit matrix equations relating $\widetilde{\epsilon}_{\mathcal{C}_1}$ and $\widetilde{\epsilon}_{\mathcal{C}_2}$. In particular, $\widetilde{\epsilon}_{\mathcal{C}_1} = \widetilde{\epsilon}_{\mathcal{C}_2}$ to the left of the MCS move and, within the region of the move, $\widetilde{\epsilon}_{\mathcal{C}_1}$ and $\widetilde{\epsilon}_{\mathcal{C}_2}$ are related by the matrix equations in Lemma 6.1.6. From these equations, we are able to define H.

We now show that $[\widetilde{\epsilon}_{\mathcal{C}_1}] = [\widetilde{\epsilon}_{\mathcal{C}_2}]$ implies $\Psi(\mathcal{C}_1) = \Psi(\mathcal{C}_2)$. This argument uses the dipping/undipping paths defined in Section 6.2.1. Let w_2 be a dipping/undipping path from $L_\Sigma^{d_2}$ to L_Σ. Let v denote the dipping/undipping path from L_Σ^{d} to L_Σ constructed by first undipping the extra dips added to $L_\Sigma^{d_2}$ and then following the dipping/undipping path w_2 from $L_\Sigma^{d_2}$ to L_Σ.

Let v_1 denote the dipping/undipping path from $L_\Sigma^{d_1}$ to L_Σ constructed by first adding the extra dips described above that take $L_\Sigma^{d_1}$ to L_Σ^d and then following the dipping/undipping path v from L_Σ^d to L_Σ. Let v_2 denote the dipping/undipping path from $L_\Sigma^{d_1}$ to L_Σ constructed by first adding the extra dips described above that take $L_\Sigma^{d_2}$ to L_Σ^d, and then following the dipping/undipping path v from L_Σ^d to L_Σ.

The dipping/undipping path v gives a map $\Psi_v : Aug^{ch}(L_\Sigma^d) \to Aug^{ch}(L_\Sigma)$. The dipping/undipping path v_1 gives a map $\Psi_{v_1} : Aug^{ch}(L_\Sigma^{d_1}) \to Aug^{ch}(L_\Sigma)$ which splits as the composition $\Psi_v \circ \Phi_1$ where $\Phi_1 : Aug^{ch}(L_\Sigma^{d_1}) \to Aug^{ch}(L_\Sigma^d)$ is the induced by the addition of dips to $Aug^{ch}(L_\Sigma^{d_1})$ defined above. Similarly, the map $\Psi_{v_2} : Aug^{ch}(L_\Sigma^{d_1}) \to Aug^{ch}(L_\Sigma)$ splits as the composition $\Psi_v \circ \Phi_2$ where $\Phi_2 : Aug^{ch}(L_\Sigma^{d_2}) \to Aug^{ch}(L_\Sigma^d)$. By construction, $\Phi_1([\epsilon_{\mathcal{C}_1}]) = [\widetilde{\epsilon}_{\mathcal{C}_1}]$ and $\Phi_2([\epsilon_{\mathcal{C}_1}]) = [\widetilde{\epsilon}_{\mathcal{C}_2}]$. Thus, $[\widetilde{\epsilon}_{\mathcal{C}_1}] = [\widetilde{\epsilon}_{\mathcal{C}_2}]$ implies:

$$\begin{aligned}
\Psi_{v_1}([\epsilon_{\mathcal{C}_1}]) &= \Psi_v \circ \Phi_1([\epsilon_{\mathcal{C}_1}]) \\
&= \Psi_v([\widetilde{\epsilon}_{\mathcal{C}_1}]) \\
&= \Psi_v([\widetilde{\epsilon}_{\mathcal{C}_2}]) \\
&= \Psi_v \circ \Phi_2([\epsilon_{\mathcal{C}_1}]) \\
&= \Psi_{v_2}([\epsilon_{\mathcal{C}_2}])
\end{aligned}$$

By Corollary 6.2.7, the definition of $\Psi : MCS(\Sigma) \to Aug^{ch}(L_\Sigma)$ is independent of dipping/undipping paths. Thus, we have:

$$\begin{aligned}\Psi(\mathcal{C}_1) &= \Psi_{v_1}([\epsilon_{\mathcal{C}_1}]) \\ &= \Psi_{v_2}([\epsilon_{\mathcal{C}_2}]) \\ &= \Psi(\mathcal{C}_1)\end{aligned}$$

□

Finally, note that Lemma 6.4.4 and Theorem 6.3.1 imply that the map $\widehat{\Psi} : \widehat{MCS}(\Sigma) \to Aug^{ch}(L_\Sigma)$ defined by $\widehat{\Psi}([\mathcal{C}]) = \Psi(\mathcal{C})$ is a well-defined, surjective map. Thus we have proven Theorem 6.4.1.

Chain Homotopy H between ϵ_1 and ϵ_2.		
Move	$H(A_j)$	$H(A_{j+1})$
(1)	$\epsilon_1(B_j)$	0
(2)	$\epsilon_1(B_j) + \epsilon_2(B_j)$	0
(3)	$\epsilon_1(B_j) + \epsilon_2(B_j)$	0
(4)	$\epsilon_1(B_j) + \epsilon_2(B_j)$	0
(5)	$\epsilon_1(B_j) + \epsilon_2(B_j)$	0
(7)	$\epsilon_1(B_j)$	$\epsilon_1(B_j)$
(8)	$\epsilon_1(B_j)$	$\epsilon_1(B_j)$
(9)	$\epsilon_1(B_j)$	$\epsilon_2(B_{j+2})$
(10)	$\epsilon_1(B_j)$	$\epsilon_2(B_{j+2})$
(11)	$\epsilon_1(B_j)$	$\epsilon_2(B_{j+2})$
(12)	$\epsilon_1(B_j)$	$\epsilon_2(B_{j+2})$
(13)	$\epsilon_1(B_j)$	$\epsilon_1(B_j)$
(14)	$\epsilon_1(B_j)$	$\epsilon_2(B_{j+2})$
(15)	$\epsilon_1(B_j)$	$\epsilon_2(B_{j+2})$
(16)	$\epsilon_1(B_j)$	$\epsilon_2(B_{j+2})$
(17)	$\epsilon_1(B_j)$	$\epsilon_2(B_{j+2})$
(18)	$\epsilon_1(B_j)$	$\epsilon_2(B_{j+2})$
(19)	$\epsilon_1(B_j)$	$\epsilon_2(B_{j+2})$
(20)	$\epsilon_1(B_j)$	0
(21)	$\epsilon_1(B_j)$	0

Table 6.1: Chain homotopies for each MCS move in Figures 6.7 and 6.8 except 6. In all cases, $H = 0$ on all other crossings.

Adding dips to $L_\Sigma^{d_1}$ and $L_\Sigma^{d_2}$.		
Move	$L_\Sigma^{d_1}$	$L_\Sigma^{d_2}$
1	$j, j+1$	–
6	$j+1$	–
7 - 19	$j+2$	j
20	–	j
21	–	j

Table 6.2: The table entries indicate which dotted lines in Figure 6.7 and Figure 6.8 refer to dips added to $L_\Sigma^{d_1}$ and $L_\Sigma^{d_2}$ to create L_Σ^{d}.

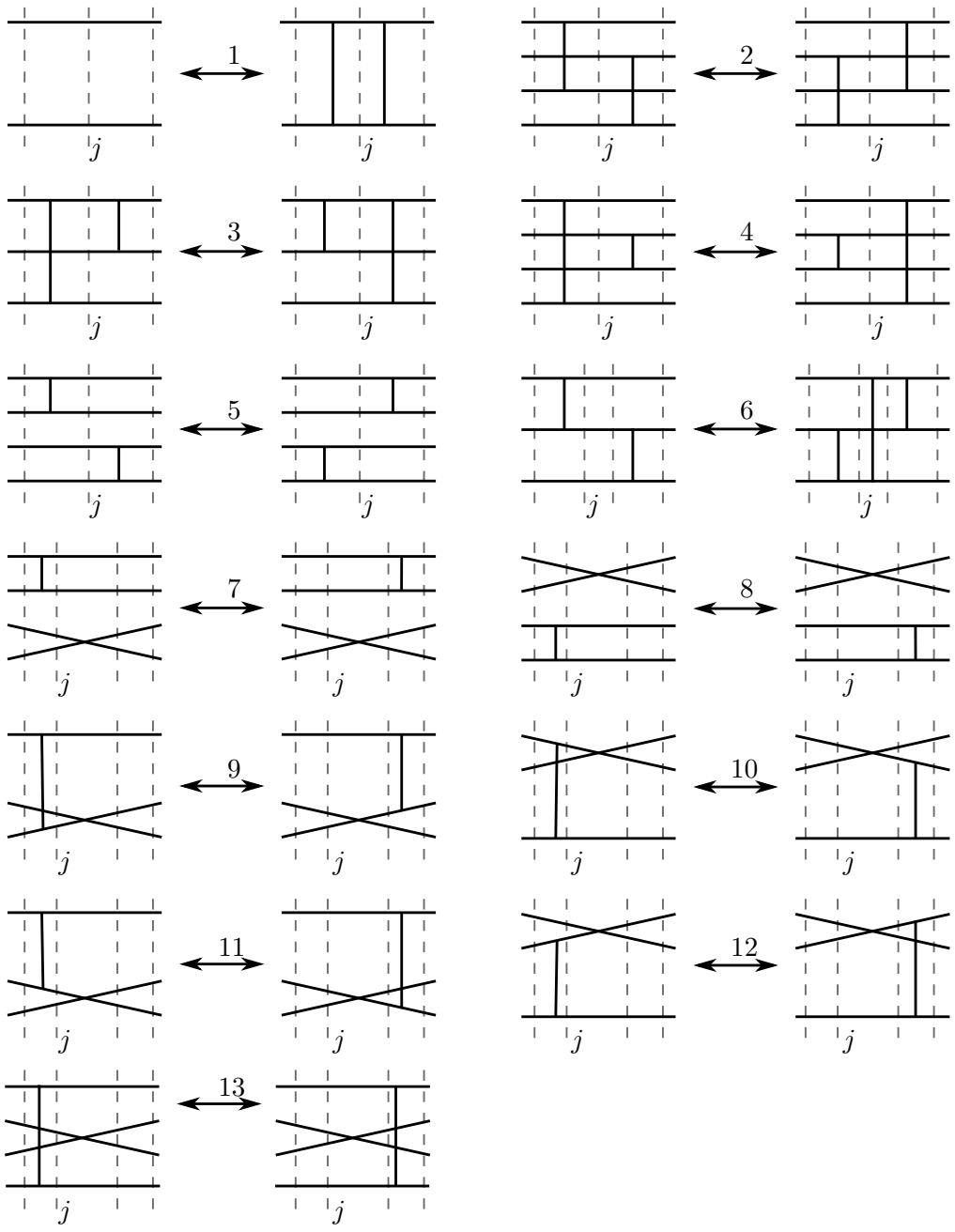

Figure 6.7: MCS equivalence moves 1 - 13. The dotted lines indicate the locations of dips in the resolved diagram. The location of dip D_j is indicated.

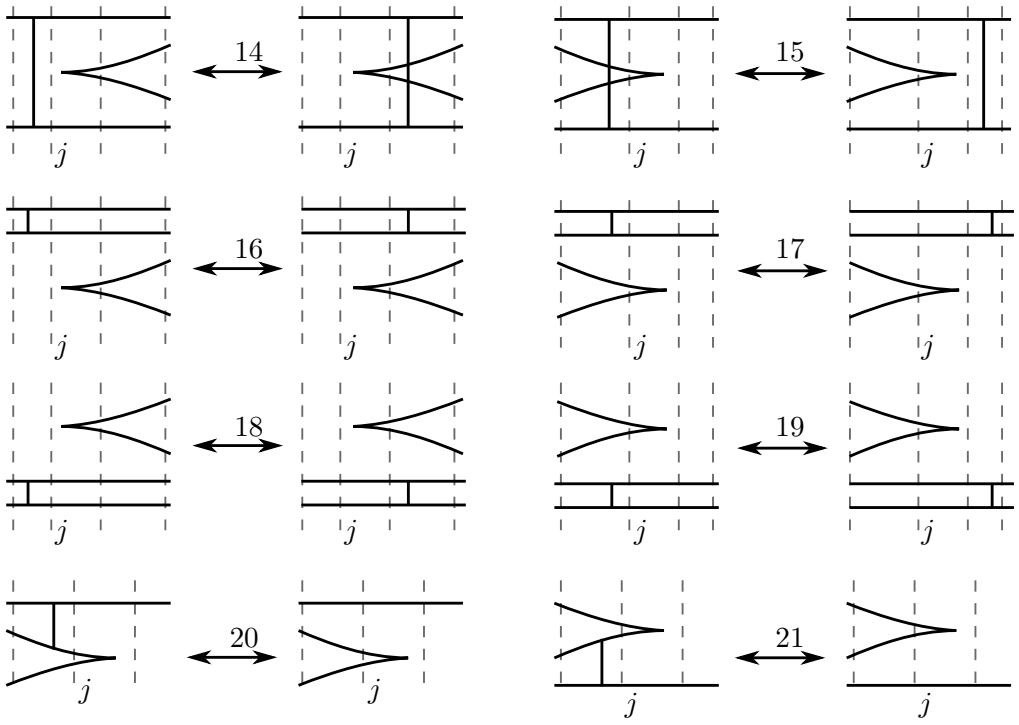

Figure 6.8: MCS equivalence moves 14 - 21. The dotted lines indicate the locations of dips in the resolved diagram. The location of dip D_j is indicated.

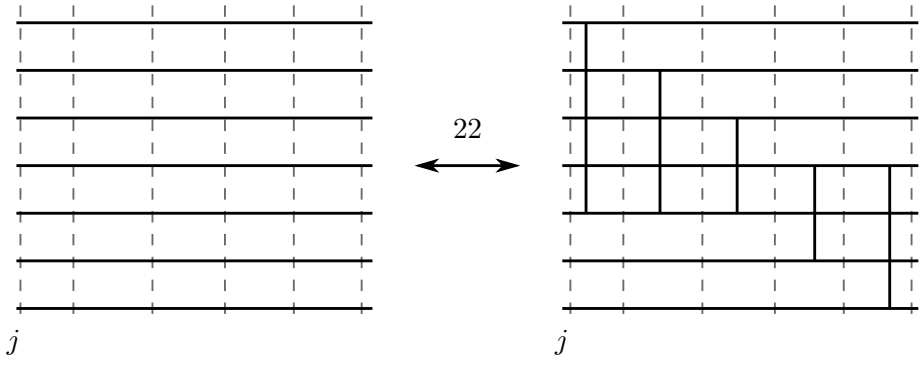

Figure 6.9: The Explosion move. The location of dip D_j is indicated.

6.5 Algorithm 2: Two standard forms for MCSs

As we have seen, an MCS $\mathcal{C}$ encodes both a graded normal ruling $N_{\mathcal{C}}$ on Σ and an augmentation $\epsilon_{\mathcal{C}}$ on L^d_Σ. In this section, we formulate two algorithms involving MCSs that highlight these connections. The first algorithm, called the *$S\bar{R}$-algorithm*, uses a sequence of MCS moves to place $\mathcal{C} \in MCS(\Sigma)$ in a form with handleslide marks that indicate the switches of $N_{\mathcal{C}}$. The resulting MCS, called the *$S\bar{R}$-form of $\mathcal{C}$*, has handleslide marks around the switches of $N_{\mathcal{C}}$ and possibly handleslide marks around graded returns. As a consequence, the $S\bar{R}$-algorithm implies that there are at most $2^{R(N)}$ MCS equivalence classes associated to a graded normal ruling N, where $R(N)$ is the number of graded returns of N. The $S\bar{R}$-form was motivated by discussions at the September 2008 AIM workshop[1], the work of Fuchs and Rutherford in [19], and the work of Ng and Sabloff in [29].

The second algorithm, called the *C-algorithm*, uses a sequence of MCS moves to turn an MCS $\mathcal{C}$ in $S\bar{R}$-form into a form that only has handleslides appearing immediately to the left of graded crossings; see Figure 6.12. We call the resulting MCS the *C-form of $\mathcal{C}$*. Using the process defined in Section 6.1.2 to assign $\epsilon_{\mathcal{C}} \in Aug(L^d_\Sigma)$ to an MCS $\mathcal{C}$, we are able to assign an explicit augmentation in $Aug(L_\Sigma)$ to an MCS in C-form.

When combined, these two algorithms provide an algorithm mapping $MCS(\Sigma)$ to $Aug(L_\Sigma)$. The upside is that this map does not require dipped

[1]See Section 1.4 for more details on the work accomplished at this workshop

diagrams or keeping track of chain homotopy classes of augmentations. In particular, given a graded normal ruling N, there are $2^{R(N)}$ MCSs in $S\bar{R}$-form for N. The C-algorithm maps these $2^{R(N)}$ MCSs to $2^{R(N)}$ different augmentations in $Aug(L_\Sigma)$. These last two comments are essentially restatements of results appearing in [29].

6.5.1 The $S\bar{R}$-form of an MCS

The goal of the $S\bar{R}$-algorithm is to make the sequence of ordered chain complexes that comprise an MCS as nice as possible. Recall that an ordered chain complex (C, ∂) in an MCS is in *simple form* if there is a fixed-point free involution $\tau : \{1, \ldots, n\} \to \{1, \ldots, n\}$ so that for all i either $\partial y_i = y_{\tau(i)}$ or $\partial y_{\tau(i)} = y_i$, where $y_1, \ldots, y_n$ are the generators of (C, ∂). Given an MCS $\mathcal{C}$ there is no sequence of equivalence moves that will put all of the ordered chain complexes of $\mathcal{C}$ in simple form. This is because the switches in the graded normal ruling associated to $\mathcal{C}$ require handleslides be present in the sequence of chain complexes. However, we are able to eliminate many of the handleslide marks in $\mathcal{C}$ so that handleslide marks only appear in a small neighborhood around switches and some graded returns and, away from these crossings, the chain complexes of $\mathcal{C}$ are in simple form.

Definition 6.5.1. We say a switch is *simple* if the MCS looks like one of the three possibilities listed in Figure 6.10. In particular, the MCS is in simple form before and after the switch.

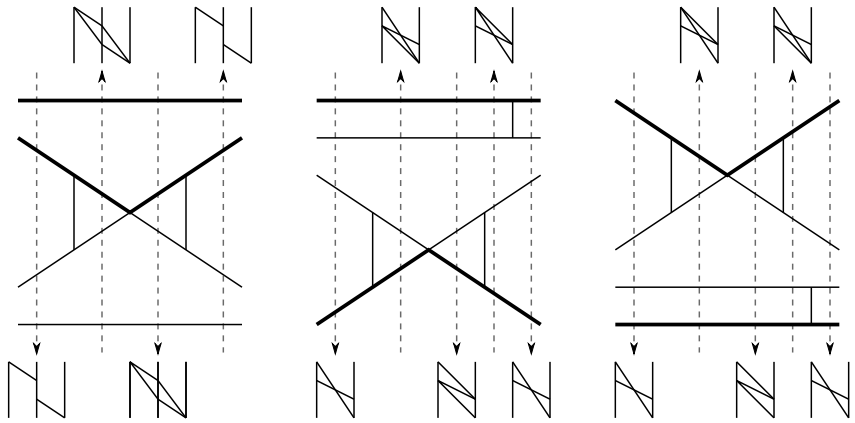

Figure 6.10: The three possible simple switches and their associated ordered chain complexes.

Definition 6.5.2. We say a return is *simple* if the MCS looks like one of the six possibilities listed in Figure 6.11. In particular, the MCS is in simple form before and after the return. We say that a simple return is *marked* if it is one of the three possibilities in the top row of Figure 6.11.

Definition 6.5.3. An MCS is in $S\bar{R}$-form if:

1. All of the switched crossings are simple;
2. All of the graded returns are simple; and
3. Besides the handleslide marks near simple switches and returns, no other handleslide marks appear in $\mathcal{C}$.

Theorem 6.5.4. Every $\mathcal{C} \in MCS(\Sigma)$ is equivalent to an MCS in $S\bar{R}$-form.

Proof. We will prove this theorem using the following algorithm which sweeps handleslide marks from left to right in the front projection.

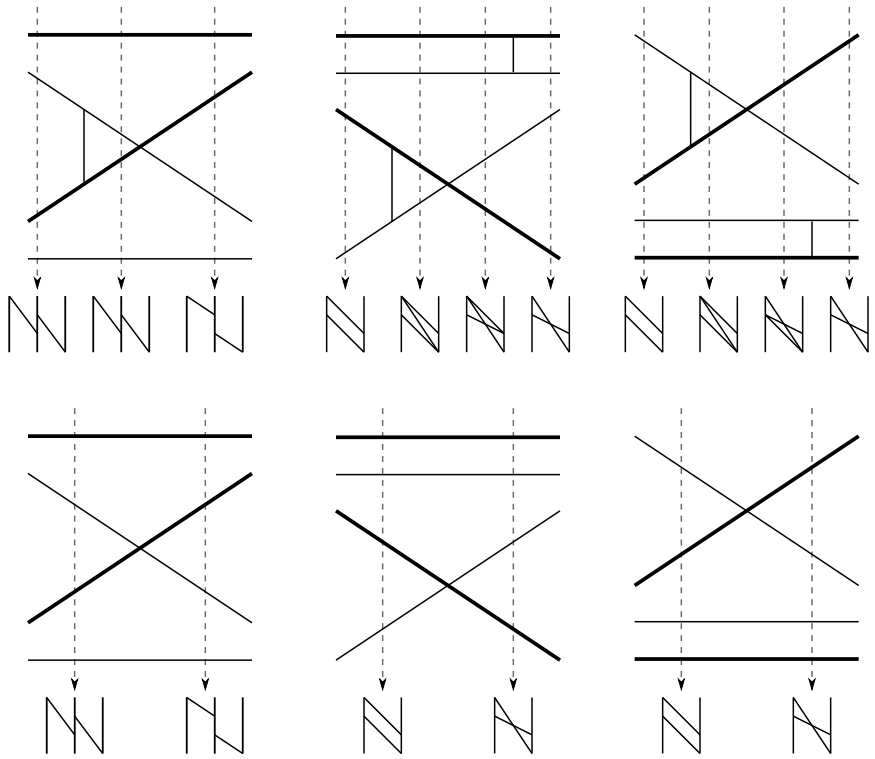

Figure 6.11: The six possible simple returns and their associated ordered chain complexes.

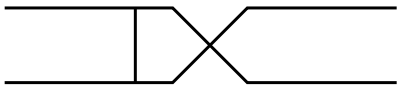

Figure 6.12: A handleslide mark that can not be swept to the right.

The $S\bar{R}$-algorithm on $\mathcal{C}$ proceeds as follows. We begin at the left most cusp of Σ. Our mental image is of a broom that tries to sweep all of the handleslide marks to the right. As we sweep, we want to make sure that the MCS we leave behind is in $S\bar{R}$-form. The MCS moves allow us to sweep handleslides past a crossing except when a handleslide occurs between the strands of the crossing; see Figure 6.12. In that case, we must decide if the crossing is a switch or return and then make the appropriate changes to the MCS so that as we continue sweeping to the right the crossing we leave behind is simple. We also have to deal with handleslides accumulating on right cusps. At a right cusp, we are able to use a series of MCS moves to remove the accumulated handleslides. Once our sweeping is finished we are left with an MCS in $S\bar{R}$-form.

We begin by forming a matrix V to keep track of the handleslide marks during the sweeping process. In a slight abuse of notation, we will also let V denote the actual collection of handleslide marks in Σ. Let t denote a point on the x-axis away from the crossings and cusps of Σ. Suppose we have swept the collection V into a small neighborhood N of $\{t\} \times \mathbb{R}$ in the (x, z)-plane. Label the strands of $N \cap \Sigma$ from bottom to top with the integers $1, \ldots, n$. Then, as a matrix, V is the strictly lower triangular $n \times n$ matrix with $\mathbb{Z}_2$ entries $v_{k,l}$ defined by $v_{k,l} = 1$ if and only if the collection of handleslides V

includes a mark between strand k and strand l where $k > l$. We denote this handleslide mark by $v_{k,l}$ as well and say $v_{k,l}$ *begins on* k and *ends on* l.

We keep the collection of handleslide marks in V nicely ordered as we sweep. If $k' < k$ and $v_{k,l} = v_{k',l'} = 1$ in the matrix V, then $v_{k',l'}$ appears to the left of $v_{k,l}$ in the collection of handleslides. If $l' < l$ and $v_{k,l} = v_{k,l'} = 1$ in the matrix V, then $v_{k,l'}$ appears to the left of $v_{k,l}$ in the collection of handleslides; see Figure 6.13.

We begin the sweeping process at the left most cusp of $\mathcal{C}$. As we sweep V from left to right, we may encounter four types of obstructions; a handleslide mark, a left cusp, a right cusp, or a crossing. In another abuse of notation, we will let V denote the collection of handleslide marks both before and after an obstruction. In the case of a handleslide mark, we incorporate the mark into V using the SR move 1 defined below and keep sweeping right. In the case of a left cusp, we can sweep V past the cusp using MCS moves 14, 16, and 18 without changing the handleslides. In these two cases, Condition 1 is satisfied. Sweeping V past a crossing or right cusp requires more care. In both cases, the algorithm defined below ensures Condition 1 is satisfied after we sweep V past a crossing or right cusp.

Condition 1. If the MCS is in in $S\bar{R}$-form to the left of V before the obstruction, then the MCS is in $S\bar{R}$-form to the left of V after V passes through the obstruction.

By definition, the first chain complex of $\mathcal{C}$ is in simple form and the matrix

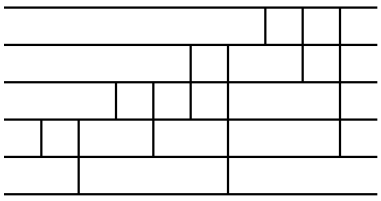

Figure 6.13: An example of the ordering of V.

V occurring just after the first left cusp is the 0 matrix. Thus we may use an induction argument, along with Condition 1, to sweep V past all of the obstructions and, hence, put $\mathcal{C}$ in $S\bar{R}$-form.

We now define a series of moves that either sweep handleslides into or out of V or sweep V past cusps and crossings. We call these *SR moves*. These moves provide the tools we need to ensure that Condition 1 is satisfied as we sweep V past the four types of obstructions.

SR moves

1. Sweeping a handleslide to the right of V into/out of V; see Figure 6.14.

   (a) Suppose the handleslide mark h sitting to the left of V is between strands k and l, with $k > l$. We use MCS moves 2 - 6 to commute h past the handleslides in V. We are able to commute h past the handleslides in V without creating new handleslides until we arrive at handleslides that begin on strand l. Suppose $v_{l,i}$ is a handleslide in V that begins on strand l. In order to commute h past $v_{l,i}$, we must use MCS move 6 and, thus, create a new handleslide mark h' between strands k and i. By the ordering of V

we can commute h' to the right so that it becomes properly ordered with the other marks in V. There may already exist a handleslide between strands k and i. If so, h' cancels this handleslide by MCS move 1. We continue this process of commuting h past each of the strands that begin on strand l. Once we have done so, the ordering of V allows us to commute h past the other marks in V, without introducing new marks, until it becomes properly ordered in V; see Figure 6.15.

(b) Since each of the MCS moves 1 - 6 is reversible, we are able to sweep an existing handleslide mark $v_{k,l}$ of V out of V to the left. As we commute $v_{k,l}$ past the marks that begin on strand l, we create other handleslides. These are incorporated into our ordering as in the case above.

2. Sweeping a handleslide to the left of V into/out of V; see Figure 6.14.

(a) The process of sweeping a handleslide into (out of) V from the left is equivalent to performing SR move 1 after a 180 degree rotation of the front projection.

3. Sweeping V past a crossing q between strands $i+1$ and i assuming $v_{i+1,i} = 0$; see Figure 6.17.

(a) We may sweep all of the handleslides of V past q using MCS moves 7 - 13. After pushing V past q, the handleslides may be unordered.

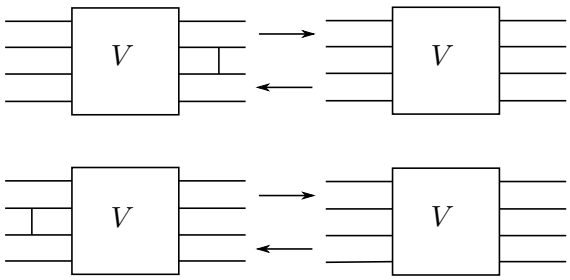

Figure 6.14: Sweeping a handleslide into/out of V.

However, we may put them back in order without introducing new handleslides.

4. Sweeping V past a right cusp between strands $i+1$ and i assuming columns and rows $i+1$ and i of V are all zero; see Figure 6.16.

   (a) All of the handleslides in V sweep past the right cusp using MCS moves 15, 17, and 19 and the ordering of the handleslides is maintained as they do. The assumption that columns and rows $i+1$ and i of V are all zero ensures that no handleslides accumulate on the right cusp.

SR moves 3. and 4. ensure that given specific conditions on V we may sweep V past a crossing or right cusp so that Condition 1 is satisfied. The next two sections describe what to do when these conditions are not satisfied. In particular, we see that Condition 1 is satisfied in all cases.

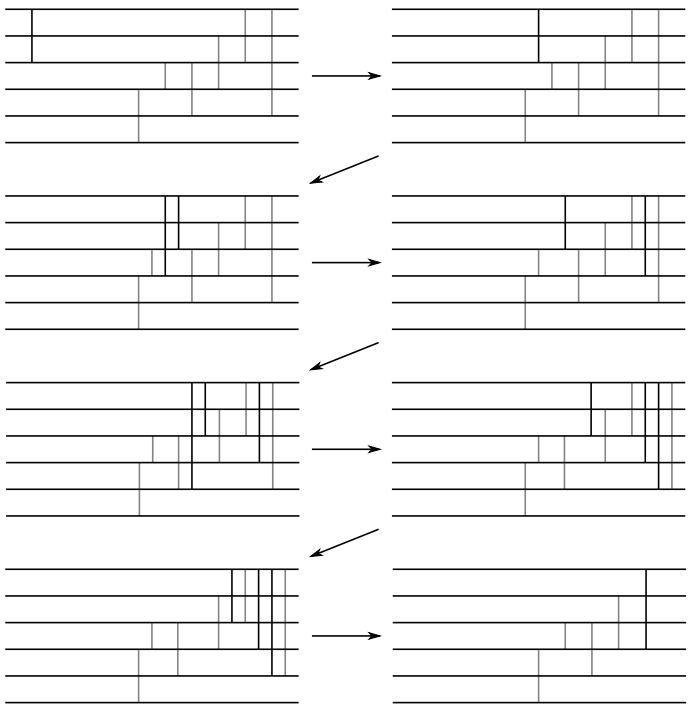

Figure 6.15: Sweeping a handleslide mark into V from the left. The grey marks are those contained in the original V.

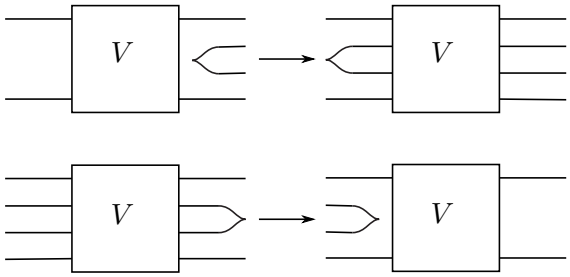

Figure 6.16: Sweeping V past cusps.

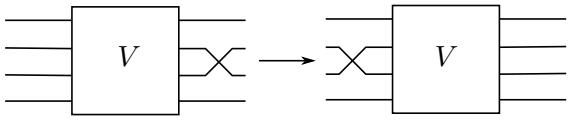

Figure 6.17: Sweeping V past a crossing.

Sweeping past a crossing with $v_{i+1,i} = 1$.

Suppose that while sweeping V to the right, we arrive at a crossing q between strands $i+1$ and i and $v_{i+1,i} = 1$. In this case, we use the following algorithm to ensure that q is a simple switch or simple return after we push V past q.

1. Use SR move 1 to sweep the handleslide $v_{i+1,i}$ to the left of V, so now $v_{i+1,i} = 0$ in the matrix V. We let h denote the handleslide we have just swept to the left of V.

2. Use SR move 3 to sweep V past q.

3. Suppose the ordered chain complex of $\mathcal{C}$ is in simple form just before h. So just before and after h, $\mathcal{C}$ looks like one of the 6 cases in Figure 6.18. The top three cases indicate that q is a switch and the bottom three cases indicate that q is a return. The next set of moves will add handleslides to the right of q so that the switches look like those in Figures 6.10 and the returns look like those in the top row of Figure 6.11.

   (a) If q is a switch of type (1), use MCS move 1 to introduce two handleslides just to the right of the crossing between strands $i+1$ and i. Use SR move 1 to sweep the right handleslide into V. The resulting MCS now has a simple switch at q.

   (b) If the crossing is a switch of type (2) or (3), use MCS move 1 to introduce two handleslides just to the right of the crossing between

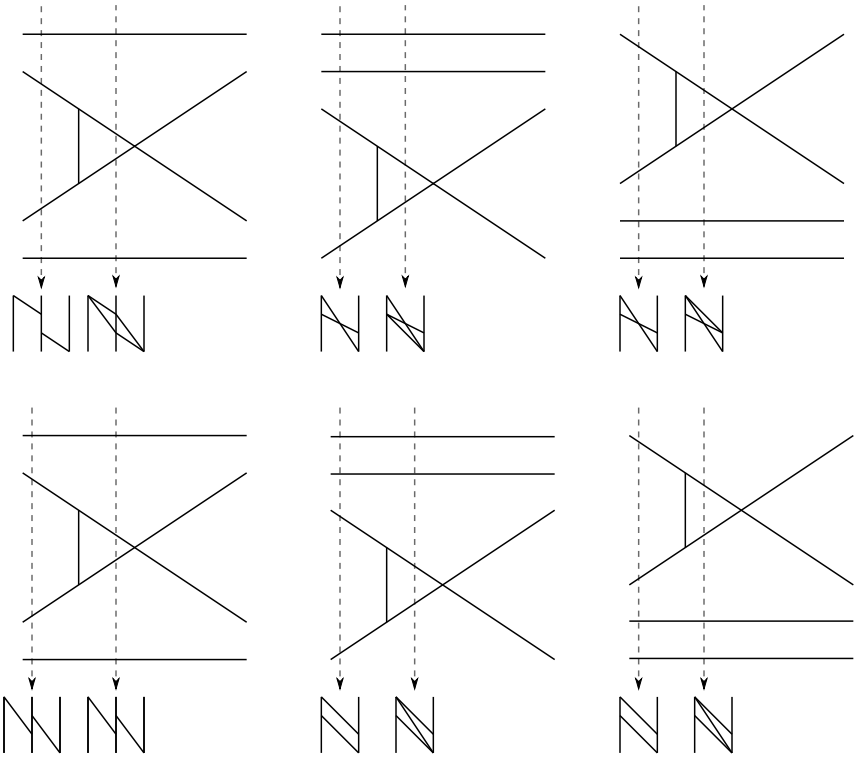

Figure 6.18: Sweeping V past a crossing with a handleslide immediately to the left. The top row will be switches and the bottom will be marked returns. In each row, we label the cases (1), (2), (3) from left to right.

strands $i+1$ and i. Use SR move 1 to sweep the right handleslide into V. Use MCS move 1 again to introduce two handleslides just to the right of q between the companion strands k and l of the strands $i+1$ and i. Lastly, use SR move 1 to sweep the right handleslide of this new pair of handleslides into V. The resulting MCS now has a simple switch at q.

(c) If q is a return of type (1), then q is a simple return and so we introduce no other handleslide marks.

(d) If the crossing is a return of type (2) or (3), use MCS move 1 to introduce two handleslides just to the right of the crossing between the companion strands k and l. Use SR move 1 to sweep the right handleslide into V. The resulting MCS now has a simple return at q.

Sweeping past a right cusp with accumulated handleslides.

Suppose V arrives at a right cusp q between strands $i+1$ and i and there are non-zero entries in rows and columns $i+1$ and i of V. Suppose also that the MCS is in $S\bar{R}$-form to the left of V. In this case, the $S\bar{R}$-algorithm does the following. Figure 6.19 walks through these steps with an example.

1. The Maslov potentials on strands $i+1$ and i differ by one, thus V does not include a handleslide between strands $i+1$ and i. As a consequence, each of the following moves pushes handleslides out of V without in-

troducing new handleslides either ending or beginning on $i+1$ or i. In the next four steps, we move handleslides out of V one at a time, beginning with the left most handleslide.

(a) Use SR move 1. to sweep all of the handleslides that end on strand i to the left of V.

(b) Use SR move 1. to sweep all of the handleslides that begin on strand $i+1$ to the left of V.

(c) Use SR move 1. to sweep all of the handleslides that begin on strand i to the left of V.

(d) Use SR move 1. to sweep all of the handleslides that end on strand $i+1$ to the left of V.

2. The result of these moves is that rows and columns $i+1$ and i of V are now full of zeros. Use SR move 4 to sweep V past the right cusp.

3. Use MCS move 20 and 21 to remove all of the handleslides ending on $i+1$ and beginning on i.

Now we need to eliminate the handleslides that end on strand i or begin on strand $i+1$. Let $h_1, \ldots, h_n$ denote the handleslides ending on strand i, ordered from left to right, and let $g_1, \ldots, g_m$ denote the handleslides beginning on strand $i+1$. By assumption, the MCS is simple just to the left of h_1. Thus just before and after h_1 the pairing and MCS must look like one

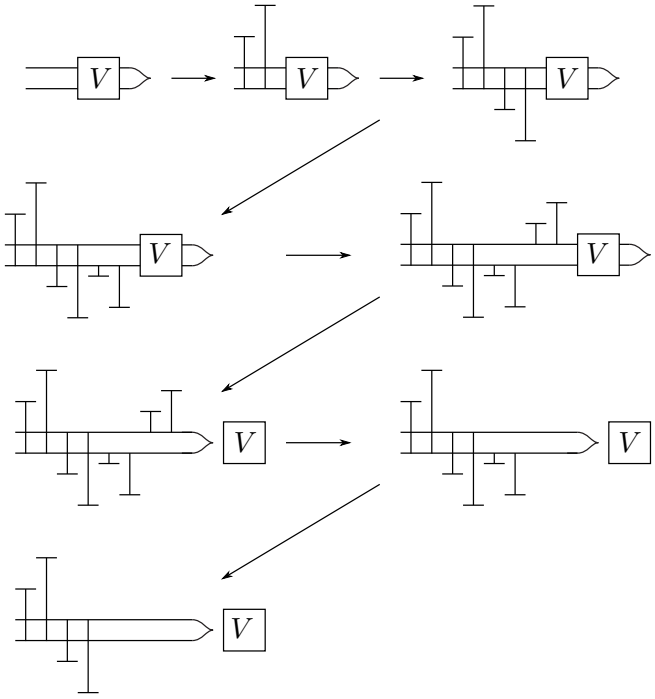

Figure 6.19: SR-Algorithm: The figure indicates the first half (parts 1. - 3.) of the process by which we sweep V past a right cusp when there are accumulated handleslides.

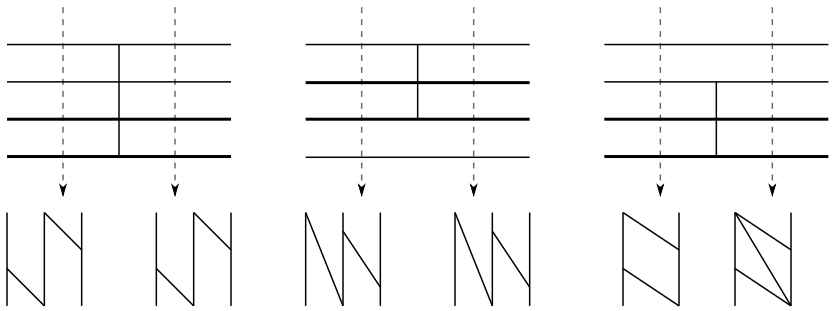

Figure 6.20: The possible local neighborhoods of the handleslide h_1. The two dark lines correspond to the strands entering the right cusp.

of the three cases in Figure 6.20. If h_1 is of type 1 or 2, we can eliminate it using the Explosion Move. If h_1 is of type 3, we do the following.

1. Suppose h_1 begins on strand l and in the ordered chain complex just before h, generator l is paired with generator k. Use MCS move 20 to introduce a new handleslide, denoted h', between strands k and $i+1$.

2. Use MCS move 6 to move h_1' past each of $g_1, \ldots, g_m$. Each time we do such a move, we will create a new handleslide which we will slide to the right past the cusp using MCS move 15 and incorporate into V using SR move 1.

3. Use MCS moves 2 - 4, to move h_1' past $h_2, \ldots, h_m$ so that it sits just to the right of h_1. Now h_1 and h_1' look like Figure 6.21.

4. Use the Explosion Move to remove h_1 and h_1'.

Using this procedure, we eliminate all of $h_1, \ldots, h_n$. The argument to eliminate the $g_1, \ldots, g_m$ is essentially identical. Either we can eliminate g_1

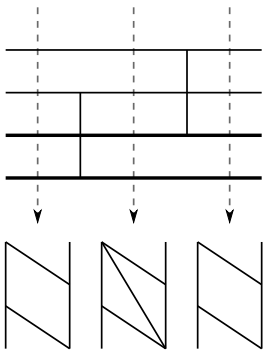

Figure 6.21: An explosion move at a right cusp after introducing a new handleslide mark. The two dark lines correspond to the strands entering the right cusp.

using the Explosion Move or we can push on a handleslide using MCS move 20 and then eliminate the pair with the Explosion Move. After eliminating $h_1, \ldots, h_n$ and $g_1, \ldots, g_m$, the MCS is in simple form just before and just after the right cusp. Hence, the resulting MCS is in $S\bar{R}$-form to the left of V.

As we carry out this algorithm from left to right, each time we encounter a handleslide, crossing or cusp we are able to sweep V past this obstruction so that the MCS we leave behind is in $S\bar{R}$-form.

□

As a corollary, we have the following:

Corollary 6.5.5. Let N be a graded normal ruling on Σ with switched crossings $q_1, \ldots, q_n$ and graded returns $p_1, \ldots, p_m$. Then N is the graded normal ruling of 2^m MCSs in $S\bar{R}$-form. Hence, N is the graded normal ruling of at most 2^m MCS classes in $\widehat{MCS}(\Sigma)$.

Proof. By Lemmata 3.4.5 and 3.4.6, each MCS equivalence class has an associated graded normal ruling and, by Theorem 6.5.4, each MCS equivalence class has at least one representative in $S\bar{R}$-form. Thus, it is sufficient to show there are exactly 2^m MCS's in $S\bar{R}$-form with graded normal ruling N.

It is easy to read off the graded normal ruling associated to an MCS in $S\bar{R}$-form. The switched crossings are those with handleslide marks corresponding to Figure 6.10. The other handleslide marks occur around graded returns.

Let $V \subset \{p_1, \ldots, p_m\}$. We construct an MCS $\mathcal{C}_V$ in $S\bar{R}$-form as follows. Around each switch q_i place handleslide marks as indicated in Figure 6.10. Around each graded return $p \in V$ place handleslide marks as indicated by the figures in the bottom row of Figure 6.11. Thus the set of crossings in V become marked returns in the MCS. The resulting marked front projection is an MCS in $S\bar{R}$-form. There are 2^m ways to choose V and every $S\bar{R}$-form with graded normal ruling N must correspond to one of these choices. □

6.5.2 The C-form of an MCS.

The C-algorithm uses the sweeping idea from the $S\bar{R}$-algorithm. Our mental image is of a broom sweeping the handleslide marks to the right. However, now we do not make modifications at crossings to ensure that they are simple once we move past. We still have to address the issue of handleslides accumulating on a right cusp. If we assume that the MCS we start with is in $S\bar{R}$-form, then this is easy to do.

Definition 6.5.6. An MCS $\mathcal{C} \in MCS(\Sigma)$ is in C-form if:

1. Outside a small neighborhood of the crossings of Σ, $\mathcal{C}$ has no handleslide marks.

2. Within a small neighborhood of a crossings q, either $\mathcal{C}$ has no handleslide marks or it has a single handleslide mark to the left of q between the strands crossings at q.

Theorem 6.5.7. Every $\mathcal{C} \in MCS(\Sigma)$ is equivalent to an MCS in C-form.

Proof. We will prove this theorem using the following algorithm which sweeps handleslide marks from left to right in the front projection.

Let $\mathcal{C} \in MCS(\Sigma)$. Apply the $S\bar{R}$-algorithm and let $\mathcal{C}$ also denote the resulting MCS in $S\bar{R}$-form. The C-algorithm uses the idea of sweeping a collection of handleslide marks from left to right in Σ. As in the $S\bar{R}$-algorithm, we will use the same matrix V to keep track of handleslide marks and use the SR moves to sweep V past handleslides, crossings and cusps. The C-algorithm differs from the $S\bar{R}$-algorithm in two respects. The first is that the C-algorithm does not introduce new handleslides at switches and marked graded returns. Thus, as we sweep V to the right, we do not have explicit control over the the chain complex immediately to the left of V. In the $S\bar{R}$-algorithm, we knew this chain complex was simple. The other difference is how the C-algorithm eliminates handleslides accumulating on a right cusp. In the case of the $S\bar{R}$-algorithm, we relied heavily on the fact that the chain complex immediately to the left of V is simple. This allowed us to eliminate

the handleslide moves accumulating on the right cusp one-by-one from left to right. In C-algorithm, we first put $\mathcal{C}$ in $S\bar{R}$-form. Thus, at all times, the chain complex to the immediate right of V is simple. This will allow us to eliminate handleslides moves accumulating on a right cusp.

In the next two sections, we describe how the C-algorithm pushes V past crossings and right cusps. In the case of handleslides and left cusps, the C-algorithm works the same as the $S\bar{R}$-algorithm.

Sweeping V past a crossing q.

Suppose that while we are sweeping V to the right, we arrive at a crossing q between strands $i+1$ and i. If $v_{i+1,i} = 0$, then we sweep V past q as described in SR move 3. If $v_{i+1,i} = 1$, then we use the following algorithm.

1. Use SR move 1 to sweep the handleslide $v_{i+1,i}$ to the left of V, so now $v_{i+1,i} = 0$ in the matrix V. We let h denote the handleslide we have just swept to the left of V.

2. Use SR move 3 to sweep V past q.

3. Slide h to the right so that it is within a small neighborhood of q.

Sweeping past a right cusp with accumulated handleslides.

Suppose that while we are sweeping V to the right, we arrive at a right cusp q between strands $i+1$ and i. If columns and rows $i+1$ and i in V are all 0, then we sweep V past the right cusp using SR move 4. If there are non-zero

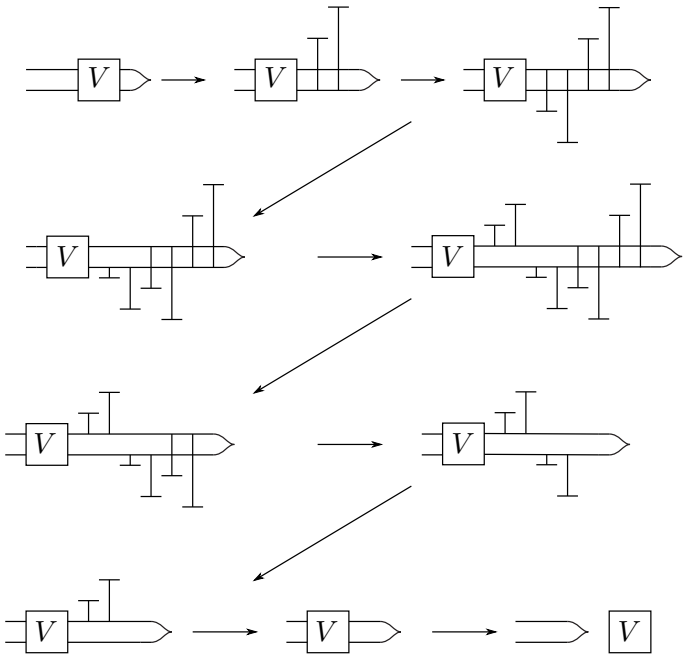

Figure 6.22: C-Algorithm: Sweeping V past a right cusp with accumulated handleslides.

entries in rows and columns $i+1$ and i of V, then the C-algorithm works as follows. Figure 6.22 walks through these steps with an example.

In the next four steps, we move the handleslides out of V one at a time, beginning with the right most handleslide.

1. Use SR move 1. to sweep all of the handleslides that end on strand i to the right of V.

2. Use SR move 1. to sweep all of the handleslides that begin on strand $i+1$ to the right of V.

3. Use SR move 1. to sweep all of the handleslides that begin on strand

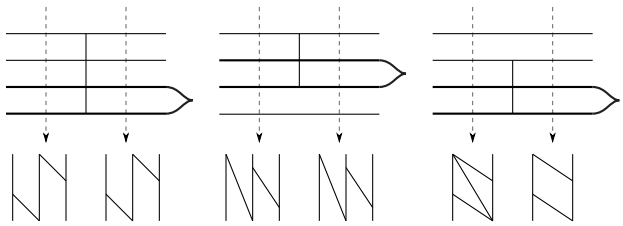

Figure 6.23: The possible local neighborhoods of the handleslide h_1. The two dark lines correspond to the strands entering the right cusp.

i to the right of V.

4. Use SR move 1. to sweep all of the handleslides that end on strand $i+1$ to the right of V.

Now we eliminate the handleslides that end on strand i, followed by the handleslides that begin on strand $i+1$. Let $h_1, \ldots, h_n$ denote the handleslides ending on strand i, ordered from right to left, and let $g_1, \ldots, g_m$ denote the handleslides beginning on strand $i+1$, also ordered from right to left. Since the MCS is in $S\bar{R}$-form to the right of h_1, we know that the chain complex between h_1 and the right cusp is simple. Thus, just before and after h_1 the pairing and MCS must look like one of the three cases in Figure 6.23. If h_1 is of type 1 or 2, we can eliminate it using the Explosion Move.

If h_1 is of type 3, we do the following. Suppose h_1 begins on strand l and in the ordered chain complex just after h, generator l is paired with generator k. Use the Explosion Move to introduce two new handleslides to the left of h_1; See Figure 6.24. One new handleslide is between strands l and i. We remove h_1 and this new handleslide using MCS move 1. The

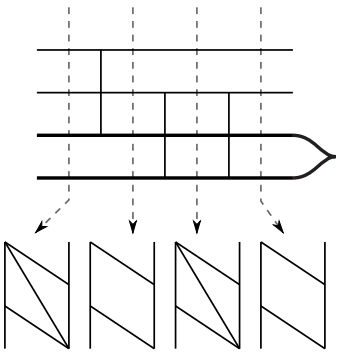

Figure 6.24: An explosion move at a right cusp introducing two new handleslides. The two dark lines correspond to the strands entering the right cusp.

second handleslide is between strands k and $i+1$ and can be slid off the right cusp using MCS move 20. Using this procedure, we eliminate all of $h_1, \ldots, h_n$. The argument to eliminate the $g_1, \ldots, g_m$ is essentially identical. After eliminating $h_1, \ldots, h_n$ and $g_1, \ldots, g_m$, we use MCS move 20. and 21. to remove all of the handleslides ending on $i+1$ and beginning on i.

The result of these moves is that rows and columns $i+1$ and i of V are now full of zeros. Use SR move 4 to sweep V past the right cusp and continue the C-algorithm. The moves in the C-algorithm that sweep V past handleslides, crossings and cusps only leave handleslides to the immediate left of crossings. Hence, after pushing V past the right most cusp, we are are left with and MCS in C-form.

As we carry out this algorithm from left to right, each time we encounter a handleslide, crossing or cusp we are able to sweep V past this obstruction so that the MCS we leave behind is in C-form.

□

In Section 6.3, we described an algorithm that assigns to an augmentation $\epsilon \in Aug(L_\Sigma)$ an MCS $\mathcal{C}_\epsilon$. By construction, $\mathcal{C}_\epsilon$ is in C-form. In fact, the crossings of $\mathcal{C}_\epsilon$ with handleslide marks to their immediate left correspond to the resolved crossings in L_Σ that are augmented by ϵ. This process is reversible. Suppose $\mathcal{C}$ is in C-form with handleslide marks to the immediate left of crossings $p_1, \ldots, p_k$. From Section 6.1.2, we have an associated augmentation $\epsilon_\mathcal{C}$ in a sufficiently dipped diagram with dips $D_1, \ldots, D_m$. We may undip $D_1, \ldots, D_m$, beginning with D_m and working to the left, so that the resulting augmentation on L_Σ only augments the crossings corresponding to $p_1, \ldots, p_k$. As a result, we have the following corollary.

Corollary 6.5.8. Let N be a graded normal ruling on Σ with switched crossings $q_1, \ldots, q_n$ and graded returns $p_1, \ldots, p_m$. Then the 2^m MCSs in $S\bar{R}$-form with graded normal ruling N correspond to 2^m different augmentations on L_Σ.

Proof. By Corollary 6.5.5, N corresponds to 2^m MCSs in $S\bar{R}$-form. In fact, two MCSs in $S\bar{R}$-form corresponding to N differ only by handleslide marks around graded returns. Suppose $\mathcal{C}_1, \mathcal{C}_2 \in MCS(\Sigma)$ are in $S\bar{R}$-form and $N = N_{\mathcal{C}_1} = N_{\mathcal{C}_2}$. Then, as marked front projections, $\mathcal{C}_1$ and $\mathcal{C}_2$ only differ at graded returns. Let p denote the left most crossing of Σ that is a graded return in N such that p is marked in $\mathcal{C}_1$ and unmarked in $\mathcal{C}_2$. Apply the C-algorithm to $\mathcal{C}_1$ and $\mathcal{C}_2$ and label the resulting MCSs $\mathcal{C}_1'$ and $\mathcal{C}_2'$. Then

$\mathcal{C}_1'$ has a handleslide mark to the immediate left of p if and only if $\mathcal{C}_2'$ does not. Thus the augmentations on L_Σ corresponding to $\mathcal{C}_1$ and $\mathcal{C}_2$ will differ on the resolved crossing corresponding to p. Thus the 2^m MCSs in $S\bar{R}$-form with graded normal ruling N correspond to 2^m different augmentations on L_Σ. □

This corollary is a special case of a more general result in [29].

Chapter 7

Two-Bridge Legendrian Knots

In this chapter, we prove that in certain situations the map $\widehat{\Psi} : \widehat{MCS}(\Sigma) \rightarrow Aug^{ch}(L_\Sigma)$ is bijective.

7.1 Two-Bridge Front Projections

Definition 7.1.1. A knot projection is *n-bridge* if it has exactly n local maxima. The *bridge number* of smooth knot K is the smallest number n such that K has an n-bridge projection.

All smooth prime knots with fewer than 10 crossings are 2-bridge except: $8_5, 8_{10}, 8_{15}$ - $8_{21}, 9_{16}, 9_{22}, 9_{24}, 9_{25}, 9_{28}, 9_{29}, 9_{30}$, and 9_{32} - 9_{49} [26]. Given a front projection Σ with n left cusps, the Ng resolution L_Σ is an n-bridge projection of the Legendrian knot K, and hence an n-bridge projection of the smooth knot K. We concentrate our attention on front projections with exactly 2

left cusps.

Definition 7.1.2. A front Σ of a Legendrian knot K with exactly 2 left cusps is called a 2-*bridge front projection*.

Lemma 7.1.3. [26] A smooth knot admitting a 2-bridge knot projection is smoothly isotopic to a Legendrian knot admitting a front projection with exactly 2 left cusps.

It is possible to completely understand the relationship between the sets $\widehat{MCS}(\Sigma)$ and $Aug^{ch}(L_\Sigma)$ when Σ is a 2-bridge projection.

7.2 Injectivity of $\widehat{\Psi} : \widehat{MCS}(\Sigma) \to Aug^{ch}(L_\Sigma)$

Definition 7.2.1. Given a graded normal ruling N on a front Σ, we say two crossings $q_i < q_j$ of Σ, ordered by the x-axis, form a *departure-return pair* (q_i, q_j) if:

1. N has a departure at q_i and a return at q_j; and
2. The two ruling disks that depart at q_i are the same disks that return at q_j.

A *graded departure-return pair* (q_i, q_j) is a departure-return pair in which both crossings have grading 0. We let $\nu(N)$ denote the number of graded departure-return pairs of N.

Given a fixed graded normal ruling N on any front projection Σ, it is easy to check that each unswitched crossing is either a departure or a return and is part of a departure-return pair. In the special case of a 2-bridge front projection, we can say more.

Proposition 7.2.2. Suppose Σ is a 2-bridge front projection with graded normal ruling N. For each departure-return pair (q_i, q_j) of N, no crossings in Σ appear between q_i and q_j. In terms of the ordering of crossing by the x-axis, this says $j = i + 1$.

Proof. Since Σ is a 2-bridge front projection, there are only two ruling disks for N. After a departure, the two ruling disks overlap so that a normal switch or a right cusp can not occur between any of the four strands. This implies that a departure crossing must be immediately followed by a return crossing. □

Definition 7.2.3. $\mathcal{C} \in MCS(\Sigma)$ is in *$S\bar{R}_g$-form* if $\mathcal{C}$ is in $S\bar{R}$-form and each marked return is the return of a graded departure-return pair.

Lemma 7.2.4. If Σ is a 2-bridge front projection, every MCS class in $\widehat{MCS}(\Sigma)$ has a representative in $S\bar{R}_g$-form.

Proof. Let $[\mathcal{C}] \in MCS(\Sigma)$ and let $\mathcal{C}$ be a representative of $[\mathcal{C}]$ in $S\bar{R}$-form. We can find such a representative using the algorithm defined in Section 6.5.1. Let N be the graded normal ruling associated to $[\mathcal{C}]$ and (q_i, q_j) be a departure-return pair of N such that q_j is a marked graded return with

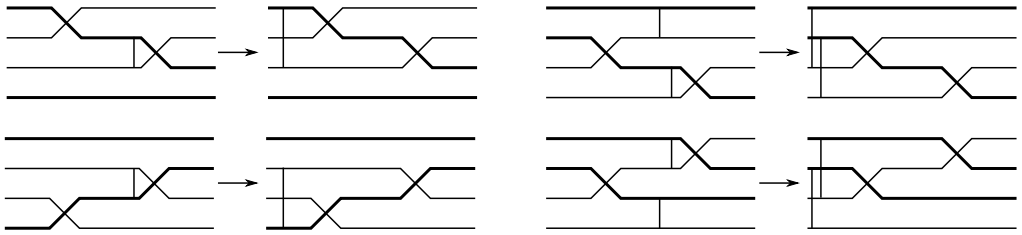

Figure 7.1: Unmarking graded returns that are paired with ungraded departures.

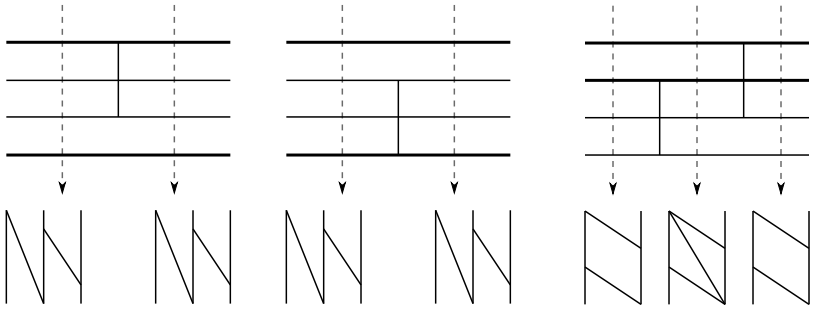

Figure 7.2: In each of these cases, we may use the Explosion move to remove the handleslide mark/marks.

an ungraded departure q_i. By Proposition 7.2.2, q_i and q_j are consecutive crossings in Σ. Thus, we can push the handleslide mark/marks at q_j to the left, past the ungraded departure q_i; see Figure 7.1. Since we assumed $\mathcal{C}$ is in $S\bar{R}$-form, the ordered chain complexes around the handleslide mark/marks looks like one of the three cases in Figure 7.2. Using the Explosion move, we may remove these handleslide mark/marks. In this manner, we can eliminate all of the handleslide marks near graded returns that are paired with ungraded departures. Thus, $\mathcal{C}$ is equivalent to an MCS in $S\bar{R}_g$-form.

□

In fact, the the $S\bar{R}_g$-form found in the previous proof is unique.

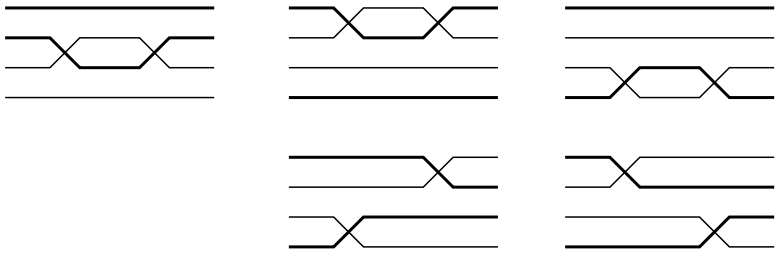

Figure 7.3: Graded departure-return pairs.

Lemma 7.2.5. If Σ is a 2-bridge front projection, every MCS class in $\widehat{MCS}(\Sigma)$ has a unique representative in $S\bar{R}_g$-form.

Proof. Let $\mathcal{C}_1$ and $\mathcal{C}_2$ be two representatives of $[\mathcal{C}]$ in $S\bar{R}_g$-form. Since $\mathcal{C}_1 \sim \mathcal{C}_2$, $\mathcal{C}_1$ and $\mathcal{C}_2$ induce the same graded normal ruling on Σ, which we will denote N. Thus, $\mathcal{C}_1$ and $\mathcal{C}_2$ have the same handleslide marks around switches and only differ on their marked returns. Suppose for contradiction that $\mathcal{C}_1$ and $\mathcal{C}_2$ differ at the graded departure-return pair (q_{i-1}, q_i). We assume $\mathcal{C}_1$ has a handleslide mark just to the left of the return q_i and $\mathcal{C}_2$ does not. The pair (q_{i-1}, q_i) looks like one of the five cases detailed in Figure 7.3. We will prove that $\Psi(\mathcal{C}_1) \neq \Psi(\mathcal{C}_2)$. Thus, by Lemma 6.4.4 we will have the desired contradiction.

Recall that $\Psi(\mathcal{C}_1)$ and $\Psi(\mathcal{C}_2)$ are computed by mapping the augmentations $\epsilon_{\mathcal{C}_1}$ and $\epsilon_{\mathcal{C}_2}$ constructed in Lemma 6.1.7 to augmentations in $Aug(L_\Sigma)$ using a dipping/undipping path. The augmentations $\epsilon_{\mathcal{C}_1}$ and $\epsilon_{\mathcal{C}_2}$ occur on sufficiently dipped diagrams $L_\Sigma^{d_1}$ and $L_\Sigma^{d_2}$. The dipped diagrams $L_\Sigma^{d_1}$ and $L_\Sigma^{d_2}$ differ by one or two dips between the resolved crossings q_{i-1} and q_i. Add these dip to $L_\Sigma^{d_2}$ and extend $\epsilon_{\mathcal{C}_2}$ by 0 using Lemma 5.4.1. We let $\widetilde{\epsilon}_{\mathcal{C}_2}$ denote the resulting

augmentation on $L_\Sigma^{d_1}$.

From Lemma 6.2.6, the definition of Ψ is independent of dipping/undipping paths. Let w be a dipping/undipping path from $L_\Sigma^{d_1}$ to L_Σ and let v denote the dipping/undipping path from $L_\Sigma^{d_2}$ to L_Σ that first travels to $L_\Sigma^{d_1}$ by adding dips as above and then travels from $L_\Sigma^{d_1}$ to L_Σ along the path v. Note that $[\widetilde{\epsilon}_{\mathcal{C}_2}]$ is the image of $[\epsilon_{\mathcal{C}_2}]$ after the first part of this path. Thus $\Psi(\mathcal{C}_1) = \Psi(\mathcal{C}_2)$ if and only if $\epsilon_{\mathcal{C}_1}$ and $\widetilde{\epsilon}_{\mathcal{C}_2}$ are chain homotopic as augmentations on $L_\Sigma^{d_1}$. We will show that they are not, in fact, chain homotopic.

Suppose for contradiction that $H : (\mathcal{A}(L_\Sigma^{d_1}), \partial) \to \mathbb{Z}_2$ is a chain homotopy between $\epsilon_{\mathcal{C}_1}$ and $\widetilde{\epsilon}_{\mathcal{C}_2}$. We will prove a contradiction exists for two of the five cases in Figure 7.3. A contradiction for each of the remaining three cases may be constructed using arguments essentially identical to the arguments in Case 1 and 2.

Case 1: Suppose the graded departure-return pair looks like the left-most picture in Figure 7.3. The dotted lines in Figure 7.4 indicate the location of the dips in $L_\Sigma^{d_1}$. Let $k+1$ and k denote the strands crossing at q_i. The following calculations use the the formulae for ∂ from Lemma 5.2.1 and the fact that all of the chain complexes involved are simple in the sense of Definition 3.4.1 or are only one handleslide away from being simple.

Then the chain homotopy H must satisfy:

$$\begin{aligned} 0 &= \epsilon_{\mathcal{C}_1} - \widetilde{\epsilon}_{\mathcal{C}_2}(q_i) \\ &= H \circ \partial(q_i) \\ &= H(a_j^{k+1,k}) \end{aligned}$$

So $H(a_j^{k+1,k}) = 0$. And:

$$\begin{aligned} 1 &= \epsilon_{\mathcal{C}_1} - \widetilde{\epsilon}_{\mathcal{C}_2}(b_j^{k+1,k}) \\ &= H \circ \partial(b_j^{k+1,k}) \\ &= H(a_j^{k+1,k}) + H(a_{j-1}^{k+1,k}) \end{aligned}$$

Thus, $H(a_j^{k+1,k}) = 0$ implies $H(a_{j-1}^{k+1,k}) = 1$. But we also have:

$$\begin{aligned} 0 &= \epsilon_{\mathcal{C}_1} - \widetilde{\epsilon}_{\mathcal{C}_2}(b_{j-1}^{k+1,k}) \\ &= H \circ \partial(b_{j-1}^{k+1,k}) \\ &= H(a_{j-1}^{k+1,k}) \end{aligned}$$

So $H(a_{j-1}^{k+1,k}) = 0$. This contradicts the calculation above giving $H(a_{j-1}^{k+1,k}) = 1$. Thus $\epsilon_{\mathcal{C}_1}$ and $\widetilde{\epsilon}_{\mathcal{C}_2}$ are not chain homotopic.

Case 2: Suppose the graded departure-return pair looks like the bottom picture in the third column of Figure 7.3. The dotted lines in Figure 7.4

indicate the location of the dips in $L_{\Sigma}^{d_1}$. Let $k+1$ and k denote the strands crossing at q_{i-1} and let $l+1$ and l denote the strands crossing at q_i. The following calculations use the the formulae for ∂ from Lemma 5.2.1 and the fact that all of the chain complexes involved are simple in the sense of Definition 3.4.1 or are only one handleslide away from being simple.

Then the chain homotopy H must satisfy:

$$\begin{aligned} 0 &= \epsilon_{\mathcal{C}_1} - \widetilde{\epsilon}_{\mathcal{C}_2}(q_i) \\ &= H \circ \partial(q_i) \\ &= H(a_j^{l+1,l}) \end{aligned}$$

So $H(a_j^{l+1,l}) = 0$. Using Lemma 5.2.1, we can write out the terms in $\partial a_j^{k+1,l}$ and compute:

$$0 = H \circ \partial(a_j^{k+1,l}) = H(a_j^{k+1,k})$$

So $H(a_j^{k+1,k}) = 0$. And:

$$\begin{aligned} 0 &= \epsilon_{\mathcal{C}_1} - \widetilde{\epsilon}_{\mathcal{C}_2}(b_j^{k+1,k}) \\ &= H \circ \partial(b_j^{k+1,k}) \\ &= H(a_j^{k+1,k}) + H(a_{j-1}^{k+1,k}) \end{aligned}$$

Thus, $H(a_j^{k+1,k}) = 0$ implies $H(a_{j-1}^{k+1,k}) = 0$. We also have:

$$\begin{aligned} 1 &= \epsilon_{\mathcal{C}_1} - \widetilde{\epsilon}_{\mathcal{C}_2}(b_{j-1}^{k+1,k}) \\ &= H \circ \partial(b_{j-1}^{k+1,k}) \\ &= H(a_{j-1}^{k+1,k}) + H(a_{j-2}^{k+1,k}) \end{aligned}$$

Thus, $H(a_{j-1}^{k+1,k}) = 0$ implies $H(a_{j-2}^{k+1,k}) = 1$. Lastly, we note:

$$\begin{aligned} 0 &= \epsilon_{\mathcal{C}_1} - \widetilde{\epsilon}_{\mathcal{C}_2}(b_{j-2}^{k+1,k}) \\ &= H \circ \partial(b_{j-2}^{k+1,k}) \\ &= H(a_{j-2}^{k+1,k}) \end{aligned}$$

So $H(a_{j-2}^{k+1,k}) = 0$. This contradicts the calculation above giving $H(a_{j-2}^{k+1,k}) = 1$. Thus $\epsilon_{\mathcal{C}_1}$ and $\widetilde{\epsilon}_{\mathcal{C}_2}$ are not chain homotopic. This implies $\Psi(\mathcal{C}_1) \neq \Psi(\mathcal{C}_2)$ and so by Lemma 6.4.4, $\mathcal{C}_1 \nsim \mathcal{C}_2$, which is a contradiction. □

Using these two lemmata, we prove Theorem 1.2.6 from Chapter 1.

Theorem 7.2.6. If Σ is a 2-bridge front projection, then $\widehat{\Psi} : \widehat{MCS}(\Sigma) \to Aug^{ch}(L_\Sigma)$ is a bijection.

Proof. The surjectivity of $\widehat{\Psi}$ is the content of Theorem 6.4.1. Thus, we need only show injectivity. Suppose $\widehat{\Psi}([\mathcal{C}_1]) = \widehat{\Psi}([\mathcal{C}_2])$ and let $\mathcal{C}_1$ and $\mathcal{C}_2$ be representative of $[\mathcal{C}_1]$ and $[\mathcal{C}_1]$ in $S\bar{R}_g$-form. Suppose for contradiction, that

$[\mathcal{C}_1] \neq [\mathcal{C}_2]$. Then either $\mathcal{C}_1$ and $\mathcal{C}_2$ induce different graded normal rulings on Σ or they induce the same ruling, but have different marks on their graded departure-return pairs. We will show that both of these cases imply that $\widehat{\Psi}([\mathcal{C}_1]) \neq \widehat{\Psi}([\mathcal{C}_2])$, which is a contradiction.

Recall that $\Psi(\mathcal{C}_1)$ and $\Psi(\mathcal{C}_2)$ are computed by mapping the augmentations $\epsilon_{\mathcal{C}_1}$ and $\epsilon_{\mathcal{C}_2}$ constructed in Lemma 6.1.7 to augmentations in $Aug(L_\Sigma)$ using a dipping/undipping path. The augmentations $\epsilon_{\mathcal{C}_1}$ and $\epsilon_{\mathcal{C}_2}$ occur on sufficiently dipped diagrams $L_\Sigma^{d_1}$ and $L_\Sigma^{d_2}$. We may add dips to $L_\Sigma^{d_1}$ and $L_\Sigma^{d_2}$ and extend by 0 using Lemma 5.4.1 so that the resulting augmentations $\widetilde{\epsilon}_{\mathcal{C}_1}$ and $\widetilde{\epsilon}_{\mathcal{C}_2}$ occur on the same sufficiently dipped diagram L_Σ^d. This gives two dipping/undipping paths w_1 and w_2, where w_1 is a path from $L_\Sigma^{d_1}$ to L_Σ^d and w_2 is a path from $L_\Sigma^{d_2}$ to L_Σ^d.

From Lemma 6.2.6, the definition of Ψ is independent of dipping/undipping paths. Let v be a dipping/undipping path from L_Σ^d to L_Σ. Thus, the concatenations $w_1 v$ and $w_2 v$ give dipping/undipping paths defining $\Psi(\mathcal{C}_1)$ and $\Psi(\mathcal{C}_2)$. Thus $\Psi(\mathcal{C}_1) = \Psi(\mathcal{C}_2)$ if and only if $\widetilde{\epsilon}_{\mathcal{C}_1}$ and $\widetilde{\epsilon}_{\mathcal{C}_2}$ are chain homotopic as augmentations on L_Σ^d. We will show that they are not, in fact, chain homotopic.

Suppose for contradiction that H is a chain homotopy between $\widetilde{\epsilon}_{\mathcal{C}_1}$ and $\widetilde{\epsilon}_{\mathcal{C}_2}$. Since $\widetilde{\epsilon}_{\mathcal{C}_1}$ and $\widetilde{\epsilon}_{\mathcal{C}_2}$ are occ-simple, part 2 of Corollary 6.4.3 implies that $\widetilde{\epsilon}_{\mathcal{C}_1}(A_j) = (I + H(A_j))\widetilde{\epsilon}_{\mathcal{C}_2}(I + H(A_j))^{-1}$ for all j. Recall that $\widetilde{\epsilon}_{\mathcal{C}_1}(A_j)$ and $\widetilde{\epsilon}_{\mathcal{C}_2}(A_j)$ encode the differential of a corresponding chain complex in $\mathcal{C}_1$ and $\mathcal{C}_2$. Since they are chain isomorphic by a lower triangular matrix, the pairing

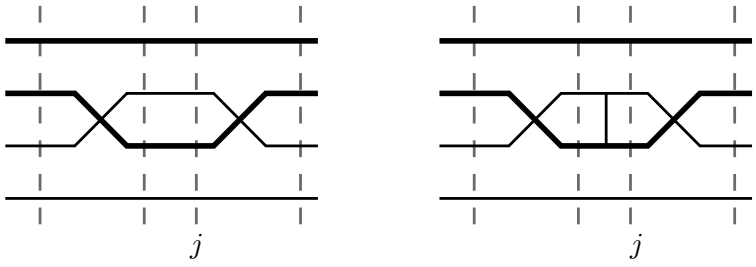

Figure 7.4: A graded departure-return pair with a middle departure and middle return. The MCS $\mathcal{C}_1$ is on the left and $\mathcal{C}_2$ is on the right. The dotted lines indicate the locations of dips. The location of dip D_j is indicated.

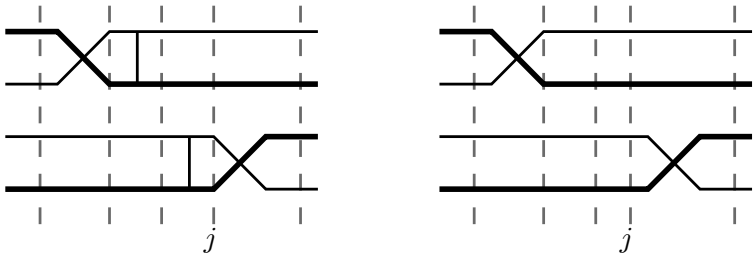

Figure 7.5: A graded departure-return pair with a top departure and bottom return. The MCS $\mathcal{C}_1$ is on the left and $\mathcal{C}_2$ is on the right. The dotted lines indicate the locations of dips. The location of dip D_j is indicated.

of the strands of Σ determined by $\widetilde{\epsilon}_{\mathcal{C}_1}(A_j)$ and $\widetilde{\epsilon}_{\mathcal{C}_2}(A_j)$ agree. Thus, $\mathcal{C}_1$ and $\mathcal{C}_2$ determine the same graded normal ruling on Σ.

Thus, as MCSs in $S\bar{R}_g$-form, $\mathcal{C}_1$ and $\mathcal{C}_2$ must have different marks on their graded departure-return pairs. In this situation, we proved in Lemma 7.2.5 that $\widetilde{\epsilon}_{\mathcal{C}_1}$ and $\widetilde{\epsilon}_{\mathcal{C}_2}$ are not chain homotopic. This implies $\Psi(\mathcal{C}_1) \neq \Psi(\mathcal{C}_2)$ and so $\widehat{\Psi}([\mathcal{C}_1]) \neq \widehat{\Psi}([\mathcal{C}_2])$, which is a contradiction. □

As an immediate corollary, we have:

Corollary 7.2.7. $|Aug^{ch}(L_\Sigma)| = |\widehat{MCS}(\Sigma)| = \sum_{N \in N(\Sigma)} 2^{\nu(N)}$ where $\nu(N)$ denotes the number of graded departure-return pairs of N.

Corollary 7.2.7 corresponds to Corollary 1.2.7 in Chapter 1.

Bibliography

[1] V. I. Arnol'd, S. M. Gusein-Zade, and A. N. Varchenko, *Singularities of differentiable maps.*, vol. 1, Monographs in Mathematics, no. 82, Birkhauser, Boston, 1985.

[2] S. A. Barannikov, *The framed Morse complex and its invariants*, Adv. Soviet Math. **21** (1994), 93–115.

[3] D. Bennequin, *Entrelacements et equations de Pfaff*, Asterisque **107-108** (1983), 87–161.

[4] J. Cerf, *Stratification naturelle des espaces de fonctions différentiables réeles et le théorème de la pseudo-isotopie*, Inst. Hautes Etudes Sci. Publ. Math. **39** (1970), 5–173.

[5] Y. V. Chekanov, *Critical points of quasifunctions and generating families of Legendrian manifolds*, Funct. Anal. Appl. **30** (1996), no. 2, 118–128.

[6] ———, *Differential algebra of Legendrian links*, Invent. Math. (2002), no. 150, 441–483.

[7] ———, *Invariants of Legendrian knots*, Proceedings of the International Congress of Mathematicians (Beijing), vol. II, Higher Ed. Press, 2002, pp. 385–394.

[8] Y. V. Chekanov and P. E. Pushkar, *Combinatorics of fronts of Legendrian links and Arnol'd's 4-conjectures*, Uspekhi Mat. Nauk **60** (2005), 99–154.

[9] S. Chmutov and V. Goryunov, *Polynomial invariants of legendrian links and wave fronts*, Topics in Singularity Theory. V.I.Arnold's 60th Anniversary Collection. (A. Khovanskii, A. Varchenko, and V. Vassiliev, eds.), vol. 180, Amer. Math. Soc. Translations, no. 2, AMS, Providence, RI, 1997, pp. 25–44.

[10] Ya. Eliashberg, *The structure of* 1*-dimensional wave fronts, nonstandard Legendrian loops and Bennequin's theorem*, Topology and geometry—Rohlin Seminar, Lecture Notes in Math., vol. 1346, Springer, Berlin, 1988, pp. 7–12.

[11] ———, *Invariants in contact topology*, Proceedings of the International Congress of Mathematicians, Vol. II (Berlin 1998), vol. Extra Vol. II, 1998, (electronic), pp. 327–338.

[12] Ya. Eliashberg, A. Givental, and H. Hofer, *Introduction to Symplectic Field Theory*, Geom. Funct. Analysis **10** (2000), no. 3, 560–673.

[13] J. Etnyre, *Legendrian and transversal knots*, Handbook of knot theory, Elsevier B. V., 2005, pp. 105–185.

[14] J. Etnyre, L. Ng, and J. Sabloff, *Invariants of Legendrian knots and coherent orientations*, J. Symplectic Geom. **1** (2002), no. 2, 321–367.

[15] Y. Felix, S. Halperin, and J-C Thomas, *Handbook of Algebraic Topology*, ch. Differential Graded Algebras in Topology, pp. 829–865, North-Holland, Amsterdam, 1995.

[16] E. Ferrand, *On Legendrian knots and polynomial invariants*, Proc. Amer. Math. Soc. **130** (2002), no. 4, 1169–1176.

[17] D. Fuchs, *Chekanov-Eliashberg invariant of Legendrian knots: existence of augmentations*, J. Geom. Phys. **47** (2003), no. 1, 43–65.

[18] D. Fuchs and T. Ishkhanov, *Invariants of Legendrian knots and decompositions of front diagrams*, Mosc. Math. J. **4** (2004), no. 3, 707–717.

[19] D. Fuchs and D. Rutherford, *Generating families and Legendrian contact homology in the standard contact space*, arXiv:0807.4277v1 [math.SG] (2008).

[20] A. Hatcher and J. Wagoner, *Pseudo-isotopies of compact manifolds*, Asterisque, no. 6, Société Mathématique de France, 1973.

[21] J. Jordan and L. Traynor, *Generating family invariants for Legendrian links of unknots*, Alg. Geom. Top. **6** (2006), 895–933.

[22] T. Kalman, *Contact homology and one-parameter families of Legendrian knots*, Geom. and Top. **9** (2005), 2013–2078.

[23] ———, *Braid-positive Legendrian links*, Int. Math. Res. Not. (2006), Art. ID 14874.

[24] F. Laudenbach, *On the Thom-Smale complex*, appendix to J-M Bismut and W. Zhang, An extension of a theorem by Cheeger and Muller, Asterique, vol. 205, 1992.

[25] K. Mishachev, *The N-copy of a topologically trivial Legendrian knot*, J. Symplectic Geom. **1** (2003), no. 4, 659–682.

[26] L. Ng, *Maximal Thurston-Bennequin number of two-bridge links*, Algebr. Geom. Topol. **1** (2001), 427–434.

[27] ———, *Computable Legendrian invariants*, Topology **42** (2003), 55–82.

[28] ———, *A Legendrian Thurston-Bennequin bound from Khovanov homology.*, Algebr. Geom. Topol. **5** (2005), 1637–1653.

[29] L. Ng and J. Sabloff, *The correspondence between augmentations and rulings for Legendrian knots*, Pacific J. Math. **224** (2006), no. 1, 141–150.

[30] L. Ng and L. Traynor, *Legendrian solid-torus links*, Journal of Symplectic Geom. **2** (2004), no. 3, 411–443.

[31] P. E. Pushkar, *Personal correspondence with D. Fuchs.*, (email), 2001.

[32] ———, *Notes from: Spring Morse theory for Legendrian links and surfaces in 1-jet spaces*, Transmitted via email by Sergei Chmutov, November 2008, CIRM Conference: Géométrie et topologie en petite dimension (dédiée au 60éme anniversaire d'Oleg Viro).

[33] ———, *Personal correspondence with D. Fuchs.*, (email), September 2008.

[34] D. Rutherford, *Thurston-Bennequin number, Kauffman polynomials, and ruling invariants of a Legendrian link: the Fuchs conjecture and beyond*, Int. Math. Res. Not. **Art. ID 78591** (2006), 15.

[35] J. Sabloff, *Invariants for Legendrian knots from contact homology*, (unpublished).

[36] ———, *Augmentations and rulings of Legendrian knots*, Int. Math. Res. Not. **19** (2005), 1157–1180.

[37] J. Swiatkowski, *On the isotopy of Legendrian knots*, Ann. Global Anal. Geom. **10** (1992), no. 3, 195–207.

[38] S. Tabachnikov, *Estimates for the Bennequin number of Legendrian links from state models for knot polynomials*, Math. Research Lett. **4** (1997), 143–156.

[39] D. Theret, *A complete proof of Viterbo's uniqueness theorem on generating functions*, Topology Appl. **96** (1999), 249–266.

[40] L. Traynor, *Legendrian circular helix links*, Math. Proc. Cambridge Philos. Soc. (1997), no. 122, 301–314.

[41] ———, *Generating function polynomials for Legendrian links*, Geom. Topol. **5** (2001), 719–760.

[42] C. Viterbo, *Symplectic topology as the geometry of generating functions*, Math. Ann. **292** (1992), 685–710.